An Investigation of the Cardiovascular Effects of Apelin

Katherine M Hamilton-Smith

Submitted for the degree of Doctor of Philosophy

University of Edinburgh 2010

Table of Contents

Declaration ..... ***vii***
Acknowledgements ..... ***ix***
Abstract ..... ***x***
Publications ..... ***xiii***
List of Figures ..... ***xiv***
List of Tables ..... ***xviii***
List of Abbreviations ..... ***xix***

Chapter 1 Introduction ***1***
1.1 Apelin and the APJ receptor ***2***
1.1.1 Apelin 2
1.1.1.2 Distribution 4
1.1.2 APJ Receptor 5
1.1.2.1 Orphan receptor 5
1.1.2.2 APJ receptor distribution in rat and human tissues 5
1.1.2.3 Apelin receptor distribution by in-situ hybridisation studies in zebrafish embryos 6
1.1.2.4 Downstream signalling mechanisms 6
1.2 The cardiovascular effects of apelin ***9***
1.2.1 The effect of apelin on the heart 9
1.2.2 Vasoactive properties of apelin 9
1.2.3 Apelin and APJ knockout mice 10
1.2.4 Apelin and its potential role in cardiovascular disease 11
1.2.5 Metabolic effects of apelin 13
1.3 Hypoxia and Ischaemia ***16***
1.3.1 Hypoxia inducible factor-1α 16
1.3.1.1 The role of HIF-1α in apelin gene expression 16
1.3.1.2 Drugs modulating the HIF-1α pathway 17
1.3.2 Ischaemia 19
1.3.2.1 The reported cardioprotective effects of apelin 19
1.4 Zebrafish: a model organism for cardiovascular research 21
1.4.1 Development of zebrafish embryos 23
1.5 Hypothesis and Aims ***26***
1.5.1 Hypothesis 26
1.5.2 Models for the investigation of the cardiovascular effects of apelin 26
1.5.3 Aims 27

Chapter 2 Methods ***28***
2.1 Apelin in vivo in the rat ***29***
2.2 Papillary muscle and atrial strip preparations ***30***
2.3 Isolated, perfused rat heart (Langendorff) ***31***
2.4 Myography ***33***
2.4.1 Data analysis 34
2.5 Zebrafish Husbandry ***35***

2.5.1 Collection of fertilised eggs (Marbling) 35
2.5.2 Pair mating 35
2.6 Zebrafish Experiments ***36***
2.6.1 Video edge detection 36
2.6.1.1 Regional differences in ventricle wall motion in the zebrafish embryo 38
2.6.1.2 Zebrafish isolated embryonic hearts 41
2.6.2 Measurement of ejection fraction 43
2.6.3 Semi-quantitative scoring assessment: Hypoxia-Recovery Model 44
2.6.4 Morpholino 45
2.6.4.1 General applications of MO technology 45
2.6.4.2 Zebrafish microinjection of morpholinos 47
2.7 Molecular techniques ***48***
2.7.1 Western Blotting 48
2.7.1.1 Protein extraction and quantification 48
2.7.1.2 Blotting and Transfer 49
2.7.1.3 Probing with anti-rat APJ antibody 49
2.7.1.4 Membrane stripping and re-probing 50
2.7.2 Polymerase chain reaction (PCR) 50
2.7.2.1 RNA extraction and quantification 50
2.7.2.3 Reverse transcription PCR 52
2.7.2.4 Reverse Transcription Quantitative PCR 53
2.8 Statistical Analysis ***54***
2.8.1 Experimental unit in zebrafish experiments 55
2.9 Reagents ***55***

Chapter 3 The inotropic effects of apelin ***56***
3.1 Introduction ***57***
3.2 Methods ***60***
3.2.1 Western Blotting 60
3.2.2 Isolated right ventricular papillary muscles and right atrial strips 60
3.2.3 Langendorff 61
3.3 Results ***62***
3.3.1 APJ receptor expression in right ventricular papillary muscles and right atrial strips 62
3.3.2 In vitro functional studies 63
3.3.2.1 The effect of NA and calcium on rat RV papillary muscles and RA strips 63
3.3.2.2 The effect of pyr-apelin-13 on rat RV papillary muscles and RA strips 63
3.3.3 The effect of apelin-16 in the isolated perfused rat heart 70
3.4 Discussion ***71***

Chapter 4 The vasoactive effects of apelin 74
4.1 Introduction 75
4.2 Methods..... 78
4.2.1 Myography 78
4.2.2 In vivo blood pressure measurements 79
4.3 Results 80
4.3.1 In vitro vascular responses 80
4.3.2 In vivo effect on blood pressure and heart rate 85
4.4 Discussion 87
4.4.1 In vitro vessel responses..... 87
4.4.2 In vivo blood pressure measurements 88
4.4.3 Conclusion 91

Chapter 5 The apelin system in the zebrafish embryo and zebrafish adult heart 92
5.1 Introduction 93
5.1.3 The Apelin/APJ system in the zebrafish 93
5.1.4 Genetic manipulation of apelin and its receptors in zebrafish embryos... 95
5.1.4.1 Apelin 95
5.1.4.2 Agtrl1a receptor 95
5.1.4.3 Agtrl1b receptor 96
5.1.5 Aims of this chapter..... 98
5.2 Methods..... 99
5.2.1 qPCR 99
5.2.2 PCR to detect the presence or absence of mRNA of interest 100
5.2.3 Video edge detection 100
5.2.3.1 Embedded zebrafish embryos 3 dpf..... 100
5.2.3.2 Zebrafish isolated embryonic hearts 3 dpf and 4 dpf..... 101
5.2.4 Morpholino (MO)..... 102
5.2.4.1 Design of a morpholino targeting apelin 102
5.2.4.2 Determining the optimal injection quantity of the apelin morpholino 103
5.2.4.3 Morpholino microinjection in 1 - 4 cell zebrafish embryos..... 104
5.2.4.4 Calculation of ejection fraction of MO-apelin embryos 106
5.3 Results 107
5.3.1 The abundance of apelin, agtrl1a and agtrl1b mRNA transcripts during development..... 107
5.3.2 Apelin, agtrl1a and agtrl1b are present in the zebrafish adult heart 109
5.3.4 The effect of apelin on cardiac function in zebrafish embryos 110
5.3.5 The effect of calcium on isolated zebrafish embryonic hearts 112
5.3.6 The effect of pyr-apelin-13 on isolated zebrafish embryonic hearts..... 112
5.5.6 The effect of knockdown of apelin gene expression using a targeted morpholino 115
5.5.6.1 Survival in embryos with apelin knockdown..... 115
5.5.6.2 Phenotypic analysis of embryos with apelin knockdown 116
5.5.6.3 Ejection fraction in MO-apelin embryos..... 121
5.4 Discussion 122

5.4.1 mRNA studies of apelin and its receptors in zebrafish embryos and the adult zebrafish heart 122
5.4.2 The effect of exogenous apelin on cardiac function in zebrafish embryos 123
5.4.3 Knockdown of apelin mRNA using a targeted morpholino 126
5.4.4 Summary 129

Chapter 6 The development of an acute hypoxia-recovery model in zebrafish embryos 130
6.1 Introduction 131
6.1.1 Cardioprotection: a definition 131
6.1.2 Cardioprotective effects of apelin 131
6.1.1.2 The relationship between the apelin and HIF-1 pathways 132
6.1.2 Hypoxia studies in the zebrafish 133
6.2 Methods 135
6.2.1 Hypoxia-recovery model measured using a semi-quantitative scoring system 135
6.2.1.1 The effect of pharmacological agents on the hypoxia-recovery model 136
6.2.1.2 The effect of hypoxia on MO-apelin embryos 138
6.2.2 Hypoxia-recovery model measured using video edge detection 138
6.2.2.1 Apelin 138
6.2.2.2 Desferrioxamine 139
6.2.3 Quantitative PCR 139
6.6.1.2 Measuring mRNA of genes of interest in the hypoxia-recovery model 139
6.2.1.1 Measuring the abundance of HIF-1α mRNA during development .. 140
6.3 Results 142
6.3.1 The effect of hypoxia-recovery on the cardiovascular response in zebrafish embryos 142
6.3.1.1 Hypoxia-recovery response of embryos 3 dpf compared to embryos 5 dpf 142
6.3.1.2 Susceptibility to severe hypoxia by developmental stage: ventricle wall motion studies by video edge detection 145
6.3.1.3 mRNA abundance in the apelin and HIF systems in the hypoxia-recovery model 146
6.3.2 The effect of pharmacological agents on the hypoxia-recovery response in zebrafish embryos 155
6.3.2.1 Global circulatory hypoxia-recovery model 155
6.4 Discussion 164

Chapter 7 Summary and Conclusions 172
7.1 The effect of apelin on the heart 173
7.1.1 Rat 173
7.1.2 Zebrafish embryos 174
7.2 The vasoactive effect of apelin 175
7.2.1 Activity of apelin isoforms 176

7.3 The cardioprotective effects of apelin 177
7.4 Relevance of findings 178
7.5 Limitations and Future Directions 182
7.5.1 Is the cardioprotective effect of apelin dependent on developmental stage in zebrafish embryos? 183
7.5.2 Mechanism of cardioprotection 184
7.5.3 Further investigation of the role of apelin in development 187
7.6 Therapeutic potential of the apelin system in cardiovascular disease 190

References 192

Declaration

I hereby declare that the work described in this thesis was performed entirely by me with the following exceptions. Gill Brooker and Sarah Robertson performed the *in vivo* instrumentation of the animals used in the experiments described in section 2.1. Dr Carl Tucker performed the morpholino injections described in section 2.6.4.2. This work contains no material that has been previously submitted for any other degree or professional qualification.

Katherine M Hamilton-Smith

For my Grandparents

Acknowledgements

I would like to thank the following people who were instrumental in supporting me throughout my PhD research: my supervisor, Dr Martin Denvir, for his invaluable guidance, support and untiring enthusiasm; Professor David Newby for his support and for sharing his extensive knowledge of the apelin field; Dr Alan Japp for providing helpful comments throughout my studies.

I am especially grateful to Dr Carl Tucker who was generous with his time and knowledge. I am also grateful to Dr Chris Loughrey and Dr Elspeth Elliott (University of Glasgow) who welcomed me to their lab and generously shared their expertise in the Langendorff model. In addition, I would like to thank Gill Brooker and Sarah Robertson for assistance with *in vivo* studies and Dr Dawn Livingstone for advice with all aspects of qPCR.

I am indebted to the Medical Research Council for funding this project and grateful to past and present members of Lab E3.17 with whom it was a pleasure to work. I am also grateful to those who provided welcome distractions along the way, especially Craig, Mhairi and Louise.

I thank my Mum and Dad who took a genuine interest in my work and supported me wholeheartedly throughout. Thank you to Bill and Margaret for constant encouragement and helpful discussions. Finally, a huge thank you to Nicky for his good-humoured and loving support.

Abstract

Apelin was discovered in 1998 as the endogenous peptide ligand of the orphan APJ receptor. The apelin system is well conserved across vertebrate species and is reported to have cardiovascular effects including positive inotropy, vasodilation, vasoconstriction and cardioprotection during ischaemia. Recent studies in human healthy volunteers and in chronic heart failure patients have highlighted the apelin system as a potential target for drug development. However, the cellular and molecular pathways through which apelin acts remain poorly understood. This study aimed to confirm the inotropic and vasoactive actions of apelin and to further examine the proposed cardioprotective effects of apelin under ischaemic and hypoxic conditions. Cardioprotection is defined as a mechanism, for example induced by a drug, which reduces injury in response to ischaemia or hypoxia.

In vivo in the anaesthetised rat, apelin was administered as a bolus dose via the cannulated jugular vein and mean arterial pressure was measured by cannulation of the carotid artery. Pyr-apelin-13 had no effect on heart rate or mean arterial pressure. Apelin-13 decreased mean arterial pressure by approximately 20 mmHg, although the effect was highly variable among animals. Apelin-16 consistently lowered heart rate, but had no effect on mean arterial pressure. In rat isolated mesenteric arteries, studied using wire myography, apelin-13 and apelin-36 had no vasodilator or vasoconstrictor effect.

In rat isolated right ventricular papillary muscles and right atrial strips, no change in tension, time to peak or time to relax was observed in response to pyr-apelin-13

despite responding to standard pharmacological stimuli such as noradrenaline and increased calcium concentrations in the bathing medium. In isolated, perfused rat heart (Langendorff), infusion of apelin-16 for 15 minutes did not alter developed pressure, rate of rise or rate of fall detected by an intraventricular balloon positioned in the left ventricle throughout the infusion. As the isolated perfused hearts did not demonstrate an inotropic effect in response to apelin, no cardioprotective studies were carried out in this model.

Cardioprotective studies of apelin were performed in zebrafish embryos 3 – 5 days post fertilisation (dpf). I developed a hypoxia-recovery model in which we could test the effect of pharmacological agents, including apelin, on the hypoxia-recovery response. In zebrafish embryos 3 dpf, 2h hypoxia (1% oxygen) reduced heart rate and wall motion amplitude (to approximately 90% of control) and contraction velocity and relaxation velocity (to approximately 80% of control). All parameters recovered during a subsequent 2h in normoxia. Incubation in pyr-apelin-13 for 1h prior to and throughout hypoxia did not affect the depression in heart rate observed on exposure to hypoxia. However, apelin incubation resulted in an improvement in wall motion amplitude and relaxation velocity and a significant improvement in contraction velocity after hypoxia and throughout recovery. Pyr-apelin-13 had no inotropic or chronotropic effect on baseline heart function in embryos 3 dpf or in isolated hearts from embryos. However, apelin knockdown using a morpholino targeting the exon 2/intron 2 boundary of apelin pre-mRNA resulted in a high mortality rate and a severe total body and cardiovascular phenotype, suggesting that endogenous apelin is crucial during development in zebrafish embryos.

In order to test pharmacological agents more efficiently, I developed a semi-quantitative scoring method to screen a larger number of embryos in a reduced time period. Heart rate and circulation was defined as normal, reduced or absent after 2h and 4h in hypoxia and during recovery in normoxia. The abundance of apelin and HIF-1α mRNA was measured using quantitative RT-PCR. In zebrafish 5 dpf, a marked decrease in apelin mRNA expression was observed after 4h, but not 2h, hypoxia and this was not accompanied by a change in HIF-1α mRNA expression. In zebrafish 5 dpf, exogenous pyr-apelin-13 did not affect the proportion of embryos with normal heart rate and circulation at any timepoint in this model. However, desferrioxamine (iron chelator) and α-ketoglutarate (metabolite involved in aerobic respiration) significantly increased the proportion of embryos with normal heart rate and circulation during the recovery phase.

In summary, apelin-13 and apelin-16 were effective in lowering mean arterial pressure and heart rate, respectively, in the anaesthetised rat. However, apelin-13 did not vasodilate or vasoconstrict rat isolated mesenteric arteries. There was no effect of apelin on contractility parameters in rat isolated papillary muscles or in the isolated, perfused rat heart which made it difficult to pursue a cardioprotective effect in this model. In zebrafish, endogenous apelin appeared to be crucial in the development of the embryo, while exogenous apelin had no inotropic effect on cardiac function. In hypoxia-recovery, we demonstrate a cardioprotective effect of apelin in zebrafish 3 dpf, but not zebrafish 5 dpf.

Publications

Apelin has no vasoactive or inotropic action in the normal rat cardiovascular system.
Hamilton-Smith KM, Elliott E, Japp AG, Newby DE, Loughrey C, Denvir MA
Manuscript in preparation.

Apelin plays a key developmental role in zebrafish embryos.
Hamilton-Smith KM, Tucker CS, Livingstone DE, Japp AG, Newby DE, Denvir MA
Manuscript in preparation.

Circulatory responses to hypoxia and recovery in zebrafish embryos: a new approach for screening candidate pharmacological agents.
Hamilton-Smith KM, Tucker CS, Livingstone DE, Japp AG, Newby DE, Denvir MA
Manuscript in preparation.

Published abstracts

Hamilton-Smith KM, Tucker CS, Japp AG, Newby DE and Denvir MA (2009) Regional Cardiac Wall Motion in Zebrafish Embryos. *Mechanisms of Development*, 126 (suppl 1): S182

Hamilton-Smith KM, Kotwica A, Tucker CS, Japp AG, Newby DE, Denvir MA (2010) Hypoxia-Recovery of cardiovascular function in the zebrafish embryo. *Eur J Heart Fail*, 9 (suppl 1): S110 (abstract 601)

List of Figures

Figure 1.1: Apelin synthesis, post-translational processing and metabolism. 2
Figure 1.2: HIF-1α pathways and mechanism of action of HIF-1α modulators. 18
Figure 1.3: Adult zebrafish (i) and optically transparent embryonic zebrafish (3 days post fertilisation (dpf)) (ii). 21
Figure 1.4: Camera lucida sketches of the zebrafish embryo at selected developmental stages. 25
Figure 2.1: Isolated, perfused, rat heart (Langendorff). 32
Figure 2.2: Video edge detection. 37
Figure 2.3: Zebrafish embryo heart. 38
Figure 2.4: Representative traces and values showing regional differences in ventricular wall motion in a zebrafish embryo 3 dpf. 39
Figure 2.5: Regional differences in contraction and relaxation velocity in zebrafish embryos 3 dpf. 40
Figure 2.6: Regional differences in wall motion amplitude in zebrafish embryos 3 dpf. 41
Figure 2.7: Isolated heart from zebrafish 3 dpf. 42
Figure 2.8: Translation blocking morpholinos. 46
Figure 2.9: Morpholinos interfering with correct splicing of a pre-mRNA bind at an exon/intron boundary. 46
Figure 2.10: Morpholinos are injected into the cytoplasmic streaming area in 1 – 4 cell eggs. 47
Figure 2.11: RNA gel showing ribosomal subunits 28S and 18S in a 2:1 ratio confirming zebrafish RNA integrity. 51
Figure 2.12: Example standard curve calculated by LightCycler480™ software. 54
Figure 3.1: Western blotting shows APJ protein (42 kDa) and GAPDH (35 kDa) protein in right atrial strip (RA) and right ventricular papillary muscle (RVPM). 62
Figure 3.2: Concentration response curves in right ventricular papillary muscles and right atrial strip preparations in response to NA (i) and calcium (ii). 64
Figure 3.3: Effect of pyr-apelin-13 on RV papillary muscles (i and ii) and RA strips (iii) in presence of calcium 2 mM. 65

Figure 3.4: The effect of pyr-apelin-13 on time to peak and time to relaxation in RV papillary muscles in the presence of normal baseline calcium (2 mM). 66
Figure 3.5: Effect of pyr-apelin-13 on RV papillary muscles in the presence of NA 1 nM (i) and NA 100 nM (ii). 67
Figure 3.6: Effect of pyr-apelin-13 on RV papillary muscles in the presence of Ca^{2+} 5 mM (i) and ATII 100 nM (ii). 68
Figure 3.7: Apelin-16 had no effect on intraventricular pressure in the isolated perfused rat heart. 70
Figure 4.1: Constriction with PE (i) and relaxation of PE preconstricted vessels with ACh (ii) in rat second order mesenteric arteries. 81
Figure 4.2: Constriction with PE (i) and relaxation of PE preconstricted vessels with ACh (ii) in rat third order mesenteric arteries 82
Figure 4.3: Effect of apelin on isolated rat mesenteric arteries. 84
Figure 4.4: The effect of pyr-apelin-13, apelin-16 and apelin-13 on MAP (i) and HR (ii). 86
Figure 5.1: Apelin peptide sequence for human, rat, mouse, bovine, zebrafish and xenopus apelin-36. 93
Figure 5.2: Amino acid sequence of the apelin receptor orthologues, agtrl1a (Dr Agtrl1a) and agtrl1b (Dr Agtrl1b), in the zebrafish, and the human (Hs AGTRL1) and xenopus (Xl X-msr) sequences. 94
Figure 5.3: Morpholino targeting apelin. 102
Figure 5.4: Calculation of bolus size in morpholino experiments. 103
Figure 5.5: The abundance of apelin mRNA in zebrafish embryos during development from 8 hpf to 120 hpf. 107
Figure 5.6: The abundance of agtrl1a mRNA in zebrafish embryos during development from 8 hpf to 120 hpf. 108
Figure 5.7: The abundance of agtrl1b mRNA in zebrafish embryos during development from 8 hpf to 120 hpf. 108
Figure 5.8: Apelin, agtrl1a and agtrl1b mRNA was detected in the zebrafish adult heart. 109
Figure 5.9: The effect of pyr-apelin-13 (150 nM) on wall motion parameters in zebrafish 3 dpf. 111

Figure 5.10: The effect of calcium (5.5 mM) on wall motion parameters in isolated hearts of zebrafish 3 dpf. 113
Figure 5.11: The effect of pyr-apelin-13 (50 - 150 nM) on wall motion parameters in isolated hearts of zebrafish 3 dpf and 4 dpf. 114
Figure 5.12: Percentage survival at 24h in morpholino injected embryos..... 116
Figure 5.13: Apelin mRNA in MO-apelin injected embryos versus MO-mispair injected embryos 117
Figure 5.14: Kaplan-Meier survival curve of MO-apelin embryos compared to non-injected and MO-mispair controls. 117
Figure 5.15: Mean phenotypic score in non-injected control, MO-apelin and MO-mispair embryos. 118
Figure 5.16: MO-apelin and MO-mispair injected zebrafish embryos at 1 dpf. 119
Figure 5.17: MO-apelin and MO-mispair injected embryos at 3 dpf. 120
Figure 5.18: Ejection fractions in non-injected controls, MO-apelin and MO-mispair morpholino injected embryos. 121
Figure 6.1: Hypoxia-recovery model. 135
Figure 6.2: The effect of drugs on the hypoxia-recovery model. 137
Figure 6.3: The percentage of assessed zebrafish embryos with normal HR and circulation after exposure to 2h hypoxia and 4h normoxia. 144
Figure 6.4: The percentage of assessed zebrafish embryos with normal HR and circulation after exposure to 4h hypoxia and 4h normoxia. 144
Figure 6.5: Wall motion parameters in zebrafish 2 – 5 dpf exposed to 2h hypoxia. 145
Figure 6.6: The abundance of apelin mRNA transcript as determined by qPCR in zebrafish 3 dpf (i) and 5 dpf (ii) following 2h and 4h hypoxia and subsequent recovery in normoxia. 147
Figure 6.7: The abundance of agtrl1a mRNA transcript in zebrafish 3 dpf (i) and 5 dpf (ii) exposed to 2h and 4h hypoxia and subsequent recovery in normoxia. 149
Figure 6.8: The abundance of agtrl1b mRNA transcript in zebrafish 3 dpf (i) and 5 dpf (ii) exposed to 2h and 4h hypoxia and subsequent recovery in normoxia. 151
Figure 6.9: HIF-1α mRNA abundance in zebrafish embryos during development from 8 hpf to 120 hpf. 152

Figure 6.10: The abundance of HIF-1α mRNA transcript in zebrafish 3 dpf (i) and 5 dpf (ii) exposed to 2h and 4h hypoxia and subsequent recovery in normoxia..... 154
Figure 6.11: The effect of pharmacological agents on the global hypoxia-recovery response..... 158
Figure 6.12: The effect of pyr-apelin-13 (150 nM) incubation on wall motion parameters of the zebrafish (3 dpf) ventricle in the hypoxia-recovery model. 160
Figure 6.13: The effect of desferrioxamine (0.1 mM) incubation on wall motion parameters of the zebrafish (5 dpf) ventricle wall in the hypoxia-recovery model. 162
Figure 6.14: The response to hypoxia of MO-apelin, MO-mispair and non-injected controls (3 dpf)..... 163
Figure 7.1: Expression and physiological functions of the apelin–APJ system. 180
Figure 7.2: Comparison of apelin publication number to that of other named peptides. 181
Figure 7.3: Summary of processes which may produce a cardioprotective outcome. 185
Figure 7.4: Cardioprotective mechanisms documented in the literature..... 186
Figure 7.5: Morpholino rescue experiment involving coinjection of a rescue mRNA that does not contain the morpholino binding site. 188

List of Tables

Table 3.1: Effect of apelin-16 on contractility parameters measured in the isolated perfused rat heart. 70
Table 4.1: Apelin *in vitro* functional studies in rat and human vessels reported in the literature. 76
Table 4.2: Response of second and third order rat mesenteric arteries with intact endothelium to PE and ACh. 80
Table 4.3: Summary of apelin vasoactive studies *in vivo* in the rat. 90
Table 5.1: Summary of reported effects of overexpression and knockdown of apelin, agtrl1a and agtrl1b in zebrafish embryos. 97
Table 5.2: UPL probes and primer sequences for RT qPCR in the zebrafish. 99
Table 5.3: Primer sequences for RT-PCR in the zebrafish. 100
Table 5.4: Characterisation of morpholino phenotype. 105
Table 6.1: Criteria for categorising HR and global circulation in the hypoxia-recovery model. 135
Table 6.2: UPL probes and primer sequences for RT qPCR in the zebrafish. 141

List of Abbreviations

ACh	acetylcholine
ATP	adenosine triphosphate
ACTH	adrenocorticotropic hormone
Akt	protein kinase B
αKG	α-ketoglutarate
ANOVA	analysis of variance
ATII	angiotensin-II
agtrl1a	angiotensin receptor-like 1a
agtrl1b	angiotensin receptor-like 1b
ACE	angiotensin converting enzyme
AP	apelin
ApoE	apolipoprotein E
AVP	arginine vasopressin
Asc	ascorbate
ANP	atrial natriuretic peptide
bpm	beats per minute
BCA	bicinchoninic acid
BSA	bovine serum albumin
BA	bulbus arteriosus
cmlc2	cardiac myosin light chain 2
CHO	Chinese hamster ovary
CCK	cholecystokinin
CI	confidence interval

CV	contraction velocity
dpf	days post fertilisation
Dr	Danio rerio
DFO	desferrioxamine
DP	developed pressure
DAG	diacylglycerol
dP/dt min	rate of fall of pressure towards baseline
dP/dt max	rate of rise of pressure towards peak
DMSO	dimethyl sulfoxide
DTT	dithiothreitol
EF	ejection fraction
EF1a	elongation factor 1 alpha
ET-1	endothelin-1
eNOS	endothelial nitric oxide synthase
ECL	enhanced chemiluminescence
EVL	enveloping layer
EDTA	ethylenediaminetetraacetic acid
ERK	extracellular-regulated kinase
ENU	*N*-ethyl-*N*-nitrosourea
GAPDH	glyceraldehyde 3-phosphate dehydrogenase
G_i	inhibitory G-protein
GPCR	G-protein coupled receptor
GFP	green fluorescent protein
HR	heart rate

h	hour
hpf	hours post fertilisation
HEPES	4-(2-hydroxyethyl)-1-piperazineethanesulfonic acid
HIF-1α	hypoxia-inducible factor-1α
HRE	hypoxia-response element
IP_3	inositol-1,4,5-trisphosphate
ICV	intracerebroventricular
IV	intravenous
KH	Krebs-Henseleit
L-NAME	N-nitro-L-arginine methyl ester
LV	left ventricle
LVEDP	left ventricular end diastolic pressure
MAP	mean arterial pressure
MAPK	mitogen-activated protein kinase
MO	morpholino
NCX	Na+/Ca+ exchanger
NHE	Na+/H+ exchanger
NO	nitric oxide
NA	noradrenaline
P_{max}	maximum pressure
PM	papillary muscle
PE	phenylephrine
PLC	phopholipase C
PACAP	pituitary adenylate cyclase-activating peptide

PCR	polymerase chain reaction
PVDF	polyvinylidene fluoride
PHD	prolyl hydroxylase enzymes
PKC	protein kinase C
pyr-apelin-13	pyroglutamated apelin-13
qPCR	quantitative polymerase chain reaction
RV	relaxation velocity
RA	right atrium
RV	right ventricle
RISK	reperfusion injury salvage kinase
RT-PCR	reverse transcriptase polymerase chain reaction
RPL13a	ribosomal protein L13a
SV	sinus venosus
SM	smooth muscle
SDS	sodium dodecyl sulfate
SNP	sodium nitroprusside
sGC	soluble guanylate cyclase
TILLING	targeting induced local lesions in genomes
Ub	ubiquitin
UPL	Universal Probe Library
VHL	von Hippel-Lindau factor
WMA	wall motion amplitude
YSL	yolk syncytial layer
ZF	zebrafish

Chapter 1 Introduction

1.1 Apelin and the APJ receptor

1.1.1 Apelin

Apelin (named after APJ endogenous ligand) was first isolated from bovine stomach extracts in a screening experiment using Chinese hamster ovary (CHO) cells expressing the orphan receptor, APJ. A 17 amino acid peptide was isolated that was shown to arise from a 77 amino acid precursor, preproapelin (Tatemoto *et al.*, 1998). Several apelin isoforms have since been isolated, or synthesised, and have identical 13 amino acids at the C-terminal (Fig 1.1). Crucially, the 12 C-terminal amino acids appear to be those involved in agonist binding (De Mota *et al.*, 2000; Reaux *et al.*, 2001). Synthetic forms of apelin-13 (containing 13 amino acids) and apelin-36 (containing 36 amino acids) were also shown to increase the extracellular acidification rate in CHO cells expressing APJ (Tatemoto *et al*., 1998).

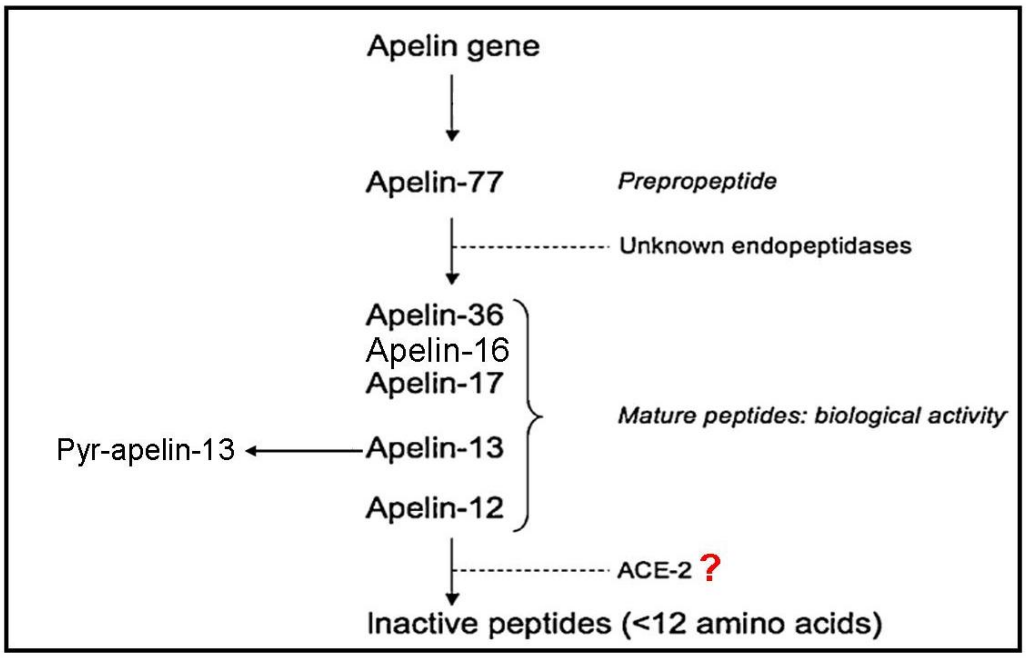

Figure 1.1: Apelin synthesis, post-translational processing and metabolism. Apelin isoforms arise from an apelin prepropeptide; the number following the apelin isoform denotes the number of amino acids. Figure adapted from Japp and Newby (2008).

Apelin-13 and apelin-36 are endogenous apelin isoforms expressed in humans (Tatemoto *et al.*, 1998) and rats (Lee *et al.*, 2000). Apelin expression has also been detected in the zebrafish early in development (Zeng *et al.*, 2007). The apelin gene has been identified in numerous species including horse, dog, pig, sheep, cow and chicken according to the Ensembl Genome Browser (www.ensembl.org). However, apelin expression has neither been identified in Drosophila nor does the apelin gene have a homologue in the Drosophila genome, suggesting apelin is only conserved among vertebrates.

Other forms of apelin (apelin-12, apelin-16) have been synthesised, although it is not clear if these forms are endogenous. Certainly, in humans, pyr-apelin-13 is the predominant form (Maguire *et al.*, 2009). Apelin-13 is the only form of apelin known to undergo post-translational pyroglutamation which is a modification known to render peptides more resistant to degradation by carboxypeptidases (Russo *et al.*, 2002).

Until recently, apelin was thought to be degraded by the carboxypeptidase, angiotensin-converting enzyme 2 (ACE-2) (Vickers *et al.*, 2002). However, recent data suggest that this may not be the case. It has been demonstrated that the action of ACE-2 on apelin-13 results in a cyclic peptide with similar efficacy and potency to apelin-13 (Davenport *et al.*, 2009). Therefore, the degradation pathway of apelin is, as yet, unclear.

1.1.1.2 Distribution

Plasma levels of apelin in rodents and humans are in the nanomolar range (Andersen et al., 2009; Chen et al., 2003). Apelin is thought to be produced in the right atrium where tissue levels of apelin are higher than in ventricular tissue (Foldes *et al.*, 2003). Apelin is produced by adipocytes in response to insulin and apelin levels in plasma of obese mice are increased compared to normal mice (Boucher *et al.*, 2005). A combination of these origins of the peptide is responsible for plasma apelin.

Within the cardiovascular system, apelin has been identified in the endothelium of the endocardium, in vascular endothelial cells of the heart and in the endothelium of large conduit vessels (Kleinz *et al.*, 2004). Within the cell, Kleinz *et al*. (2005) report that apelin is closely associated with the nuclear surface and is also found in vesicle-like structures in the cytoplasm.

In zebrafish, apelin expression was first detected by reverse transcription polymerase chain reaction (RT-PCR) at around 9 hours post fertilisation (hpf). By *in situ* hybridisation, apelin expression was observed in the notochord and developing heart as well as in specific regions in the head (Zeng *et al.*, 2007). The plasma concentration, cellular and spatial distribution of apelin in adult zebrafish is unclear as this has not yet been investigated.

1.1.2 APJ Receptor

1.1.2.1 Orphan receptor

The APJ receptor, a 7 transmembrane domain G-protein coupled receptor (GPCR), was first characterised by O'Dowd *et al*. (1993) and at the time was an orphan receptor. Five years later its ligand, apelin (named after APJ endogenous ligand), was identified using reverse pharmacology (Tatemoto *et al.*, 1998). Bovine stomach extracts were added to CHO cell cultures expressing the APJ receptor. Extracellular acidification rates were measured and apelin was isolated and identified from an extract which increased the extracellular acidification rate (Tatemoto *et al.*, 1998). This assay was based on the principle that the binding of a ligand to a receptor releases protons and thus increases the acidity of the extracellular space.

1.1.2.2 APJ receptor distribution in rat and human tissues

Apelin binding sites have been identified in the hearts of both rat and human and in human blood vessels, including the coronary artery and saphenous vein (Katugampola *et al.*, 2001). Immunocytochemistry of human and rat tissue identified the APJ receptor in endothelial cells of intramyocardial vessels, small coronary arteries, the endocardium and large conduit vessels (Kleinz *et al.*, 2005). These authors suggest that this distribution may indicate a paracrine role of the apelin/APJ system. Within rat ventricular myocytes, Farkasfalvi *et al*. (2007) demonstrated that the APJ receptor was found in T-tubules and at the intercalated disc region, providing evidence for a possible role in molecular signalling between myocytes.

1.1.2.3 Apelin receptor distribution by in-situ hybridisation studies in zebrafish embryos

In zebrafish, two genes encode apelin receptors with considerable sequence homology. As a result there are two closely related receptor subtypes: angiotensin receptor-like 1a (agtrl1a, sometimes known as aplnra) and angiotensin receptor-like 1b (agtrl1b, sometimes known as aplnrb). Agtrl1a receptor expression was first detected by *in situ* hybridisation at 3.7 hpf in a dorsal location in the embryo. At the two somite stage, agtrl1a expression was noted in areas which contribute to the heart and vasculature, among other tissues. However, expression in the dorsal aorta was not visualised at this early stage, leading the authors to suggest that agtrl1a expression may be confined to the venous circulation (Tucker *et al.*, 2007). Agtrl1b receptor expression can be detected in the blastoderm and mesodermal precursors by *in situ* hybridisation, as early as agtrl1a, at 4 hpf. Agtrl1b expression was detected in the developing heart as shown by expression patterns collocated with cardiac myosin light chain 2 (cmlc2). Agtr11b was also detected in the zebrafish dorsal aorta, caudal vein and intersomitic blood vessels at 24 hpf (Zeng *et al.*, 2007). Apelin expression patterns in the adult zebrafish have not been reported.

1.1.2.4 Downstream signalling mechanisms

The APJ receptor is thought to be coupled to both G_i and G_q. Pertussis toxin has been shown to abolish extracellular-regulated kinase (ERK) activation by apelin in CHO cells expressing the APJ receptor (Masri *et al.*, 2002); while G_q signal transduction pathway inhibitors have been shown to attenuate the inotropic response to apelin *ex vivo* in the isolated perfused rat heart (Szokodi *et al*., 2002).

A signalling mechanism for the APJ receptor has been proposed, based on inhibitor studies. Activation of the APJ receptor and G_q by apelin is thought to stimulate phospholipase C (PLC) which in turn triggers the formation of diacylglycerol (DAG) and inositol-1,4,5-trisphosphate (IP_3). DAG acts on protein kinase C (PKC) and potentiates the Na^+/H^+ exchanger (NHE) which carries H^+ ions out of the cell, therefore increasing the intracellular pH. In isolated perfused rat hearts, inhibitors of each stage of this pathway blocked the inotropic response to apelin to a similar degree (Szokodi *et al.*, 2002). Increasing intracellular pH has also been suggested to increase the sensitivity of myofilaments to calcium (Karmazyn *et al.*, 1999). IP_3 acts on the sarcoplasmic reticulum and triggers calcium release into the cytosol. This, in combination with the increase in calcium caused by the reverse action of the sodium calcium exchanger (NCX), potentiates the overall increase in calcium in the cell.

This signalling mechanism may account for both the vasoconstrictor and inotropic properties of apelin. However, there is still some debate as to whether the increase in cardiac contractility in response to apelin is ultimately due to an increase in calcium in the cell or an increase in myofilament sensitivity to calcium. Dai *et al*. (2006) measured Ca^{2+} transients in rat trabeculae and their findings suggest that increased intracellular Ca^{2+} concentration ($[Ca^{2+}]_i$) is responsible for the inotropic effect. In contrast, Farkasfalvi *et al*. (2007) report that they did not observe increased $[Ca^{2+}]_i$ in rat cardiomyocytes from both normal and failing hearts exposed to apelin-16. They hypothesise that the inotropic effect of apelin is due to increased myofilament sensitivity to Ca^{2+} and not increased $[Ca^{2+}]_i$.

The vasodilator actions of apelin are thought to be nitric oxide (NO) dependent in healthy individuals (Japp et al., 2008). It is proposed that the calcium increase that occurs after apelin activation of the APJ receptor, activates endothelial NO synthase (eNOS). The resultant NO acts on smooth muscle (SM) cells via soluble guanylate cyclase (sGC) to relax SM and thus vasodilate the vessel (see Japp and Newby, 2008).

1.2 The cardiovascular effects of apelin

1.2.1 The effect of apelin on the heart

Szokodi *et al*. (2002) demonstrated that apelin-16 produces a positive inotropic response in isolated perfused rat hearts with the effect more pronounced at increased preload. These authors also demonstrated that inhibitors of PLC, PKC, NCX and NHE suppressed this response, thereby beginning to elucidate a possible mechanism for the inotropic actions of apelin. *In vivo*, apelin-16 significantly increased maximum pressure development (Pmax) and the rate of rise of developed pressure towards the peak (dP/dt max) after 15 mins of intravenous infusion in control rats. In rats with heart failure induced by coronary artery ligation this effect on contractility was observed after a shorter period of infusion (5 mins) and maintained throughout the infusion period (Berry *et al.*, 2004). Berry *et al.* (2004) also reported that apelin-16 *in vivo* increased the rate of fall of developed pressure towards baseline (dP/dt min) after 15 mins infusion in both control and heart failure animals. In the mouse, Ashley *et al*. (2005) found an increase in cardiac contractility, measured by Doppler ultrasound, after chronic daily infusion for 2 weeks of pyroglutamated apelin-13 (pyr-apelin-13) *in vivo* using minipumps.

1.2.2 Vasoactive properties of apelin

Katumgampola *et al*. (2001) showed that pyr-apelin-13 caused constriction of human saphenous vein rings denuded of endothelium. This was the first report showing a functional influence of the apelin/APJ system on the cardiovascular system. Salcedo *et al*. (2007) later reported that human mesenteric arteries with intact endothelium relaxed in response to apelin. In the rat, apelin-17 has also been shown to cause

vasodilation of juxtamedullary afferent and efferent arterioles of the kidney (Hus-Citharel *et al.*, 2008). Therefore, the action of apelin on blood vessels, as a vasodilator or vasoconstrictor, appears to be dependent on the presence or absence of the endothelium. The first published non-peptidic apelin agonist (E339-3D6) is able to vasodilate preconstricted rat aorta, although the authors failed to report whether or not apelin itself had an effect on this preparation in their hands (Iturrioz *et al.*, 2009).

In vivo studies have also demonstrated the vasoactive properties of the apelin peptide. In sheep, intravenous bolus apelin-13 produced an initial decrease followed by an increase in mean arterial pressure (MAP) (Charles *et al.*, 2006). Bolus injection of apelin resulted in a decrease in MAP in anaesthetised rats (Tatemoto *et al.*, 2001), but an increase in MAP in conscious rats (Kagiyama *et al.*, 2005).

1.2.3 Apelin and APJ knockout mice

Apelin knockout mice exhibit a normal phenotype with normal body weight, food and water intake and heart rate (Kuba *et al.*, 2007). The hearts of these mice are structurally normal. Interestingly, aged apelin knockout mice display progressive heart failure and a more severe impairment in contractility in response to a model of pressure overload induced by aortic banding than wild-type controls (Kuba *et al.*, 2007). The development of the retinal vasculature has also been reportedly delayed in apelin knockout mice in the postnatal period (14 days), although the developmental delay was no longer detectable at the age of 84 days (Kasai *et al.*, 2008).

APJ knockout mice also exhibit a normal phenotype. When exposed to a high salt diet, APJ knockout mice produce a higher volume of urine compared to wild-type controls (Roberts *et al.*, 2009). Wild-type mice produce less urine in response to water deprivation, whereas APJ knockout mice continue to produce the same volume of urine as they did prior to water deprivation (Roberts *et al.*, 2009). An increased vasoconstrictor response to angiotensin-II (ATII) in apelin knockout mice has also been reported (Ishida *et al.*, 2004). These data indicate that the APJ receptor plays a key role in fluid homeostasis in mice.

In apolipoprotein E (ApoE) and APJ double-knockout mice, atherosclerotic lesions following high cholesterol feeding were decreased compared to ApoE knockout mice. Production of superoxide radicals in the vasculature were also decreased in these double-knockout mice suggesting a role for the apelin receptor in oxidative-stress induced atherosclerosis (Hashimoto *et al.*, 2007). However, in ApoE knockout mice, atherosclerosis induced by treatment with ATII, was attenuated by apelin delivered by osmotic minipump. Similarly, in ApoE and apelin double-knockout mice, atherosclerotic lesions induced by a high cholesterol diet were increased compared to ApoE knockout mice (Chun *et al.*, 2008).

1.2.4 Apelin and its potential role in cardiovascular disease

Current treatment of chronic heart failure includes use of β-blockers and ACE inhibitors. These slow HR and reduce blood pressure, thus alleviating the loading conditions on the failing heart (Havranek *et al.*, 1998; Swedberg *et al.*, 2005). In some cases of acute heart failure, inotropes, for example dobutamine (β-agonist), are

useful. This is especially true in cases where low blood pressure is a feature or where renal blood flow and consequently urine output falls. However, numerous studies have suggested that longer term therapy with inotropic drugs is associated with increased mortality (sudden death) (Schafer *et al.*, 2000; see Goldhaber and Hamilton *et al.*, 2010).

Continuous apelin infusion for 14 days using minipumps in mice did not result in cardiac hypertrophy (Ashley *et al.*, 2005). Longer term effects have not yet been studied, but at this stage an agonist of the apelin system is a promising therapeutic target as an agent that reduces MAP and is positively inotropic.

Dai *et al*. (2006) report that apelin-12 has a more profound inotropic effect in cardiac muscle from rats with heart failure induced by chronic hypoxia than in cardiac muscle from control rats. Conversely, Farkasfalvi *et al*. (2007) found no difference in the contractile response of failing and control isolated cardiomyocytes to apelin-16 in a coronary artery ligation heart failure model. These differences may be due to the underlying aetiology of the induced-heart failure and the type of preparation used to study the effects of apelin.

Sarzani *et al*. (2007) show that, in humans, plasma apelin levels are augmented in mild forms of heart failure, but are lower in more severe heart failure. This suggests that, as the disease progresses, plasma levels of the peptide are eventually down-regulated. Implantation of a left ventricular assist device was shown to reverse this

pattern (Chen *et al.*, 2003). Apelin may therefore be offering some protection initially, but this potential benefit may be lost in the longer term.

1.2.5 Metabolic effects of apelin

In obesity, a major risk factor for cardiovascular disease, apelin levels are increased (Heinonen *et al.*, 2005). Indeed, apelin has been shown to be produced in adipocytes (Boucher *et al.*, 2005). A single intracerebroventricular (ICV) injection of apelin-13 caused a decrease in food and water intake in obese rats eating normal chow, but had no effect on obese rats eating a high fat diet. Obese rats had higher hypothalamic APJ mRNA expression compared to controls. However, ICV apelin-13 administered to obese rats on a high fat diet caused downregulation of the APJ receptor (Clarke *et al.*, 2009).

Apelin may be associated with insulin resistance. In patients with established and treated type 2 diabetes mellitus, plasma apelin is increased (Li *et al.*, 2006). Conversely, in newly diagnosed and untreated type 2 diabetics, apelin levels are lower than normal controls (Erdem *et al.*, 2008). In a diabetic mouse model (db/db mouse), Zhong *et al*. (2007b) found an increased vasoconstrictor response to ATII and a decreased vasodilator response to acetylcholine (ACh) in aortic rings compared to those from control db/m+ mice. Preincubation of the db/db aortic rings with apelin, reduced the vasoconstrictor response to ATII and increased the vasodilator response to acetylcholine (ACh) to levels comparable with db/m+ control mice. These authors also identified a significant decrease in APJ protein expression in the aortas of db/db mice. In obese and insulin-resistant mice, intravenous apelin injection

lowered blood glucose and increased glucose utilisation in skeletal muscle (Dray *et al.*, 2008). Taken together, these studies suggest a role for apelin in maintaining sensitivity to insulin.

Hypertension, a condition which in 2005 was reported as affecting 26.4% of the global adult population (Kearney *et al.*, 2005), is another potential therapeutic target for an apelin agonist. Although NO is thought to be responsible for the vasodilatory properties of apelin in healthy individuals (Japp *et al.*, 2008); the effect appears to be prostanoid dependent in disease (Maguire *et al.*, 2009). Whatever the mechanism, a wide range of endothelium intact human vessels (mammary artery, mesenteric artery, hepatic artery) vasodilate in response to apelin *in vitro* (Maguire *et al.*, 2009; Salcedo *et al.*, 2007). Promisingly, human forearm blood flow is increased in response to apelin *in vivo* (Japp *et al.*, 2008) suggesting apelin as a potential antihypertensive.

Therefore, activation of the apelin system may be of benefit in heart failure, obesity, diabetes and hypertension. However, peptide drug delivery is not possible orally and this presents a challenge. Last year, Itturrioz *et al*. (2009) described their discovery of the first non-peptidic apelin agonist, E339-3D6. With optimisation of this agonist and the development of future non-peptidic agonists, the apelin system may yet be able to be exploited for therapeutic gain.

In addition to the potential therapeutic targets described above, apelin has also been termed “cardioprotective” in ischaemic heart models via pathways linked to the

hypoxia inducible factor-1α (HIF-1α) system which is involved in physiological and pathophysiological responses to hypoxia and ischaemia.

1.3 Hypoxia and Ischaemia

1.3.1 Hypoxia inducible factor-1α

Hypoxia inducible factors are transcription factors involved in oxygen sensing and signalling in response to changes in cellular oxygen. There are three hypoxia inducible factors (HIF 1-3) which each comprise α and β subunits (Wenger, 2000). HIF-1α is widely expressed and essential. Knockout of the HIF-1α gene results in embryonic lethality in mice. Regression of the vascular system was observed at embryonic day 9.0 as well as sparse endothelium and although cell death was widespread throughout HIF-1a -/- mice, the heart did not show any evidence of cell death (Kotch *et al.*, 1999).

HIF-1α is marked for degradation by hydroxylation. The enzymes responsible for this are the prolyl hydroxylase (PHD) enzymes. These enzymes form a complex with iron, α-ketoglutarate (αKG) and oxygen in the cytoplasm in order to hydroxylate HIF-1α. When oxygen is present this complex can be formed and HIF-1α is degraded. However, in hypoxia, the complex cannot be formed. Instead, HIF-1α translocates to the nucleus where it forms a heterodimer with HIF-1β. This heterodimer binds to the hypoxia-response element (RCGTG) of hypoxia responsive genes and can initiate transcription (Qutub *et al.*, 2006).

1.3.1.1 The role of HIF-1α in apelin gene expression

Apelin is up-regulated under hypoxic conditions by a HIF-dependent mechanism. Ronkainen *et al*. (2007) first described the link between apelin and HIF-1α by demonstrating that hypoxia increased apelin expression in rat myocardium and

cultured rat cardiomyocytes and that this effect could be abolished by the HIF inhibitory Per/Arnt/Sim protein. Furthermore, Eyries *et al*. (2008) identified the hypoxia-response element on the apelin gene and showed that cobalt chloride, by activation of the HIF pathway, promoted regeneration of the adult zebrafish caudal fin. By semiquantitative real-time PCR, this group also showed that apelin RNA expression was increased in regenerating fins treated with cobalt chloride. Chronic infusion of apelin-13 was also shown to attenuate the effects of pulmonary hypertension induced in rats exposed to hypoxia (Mao *et al.*, 2009).

1.3.1.2 Drugs modulating the HIF-1α pathway

Drugs can modulate the HIF-1α pathway by upregulating or downregulating the HIF-1α degradation pathway. Desferrioxamine (DFO) is an iron chelator and by this action stops the PHD complex being formed and consequently activates the HIF-1α pathway (Tang *et al.*, 2008). Conversely, αKG is a substrate for the PHD enzymes, therefore speeding up the degradation of HIF-1α and thus having an inhibitory affect on the HIF-1α pathway (Matsumoto *et al.*, 2006) (Fig 1.2).

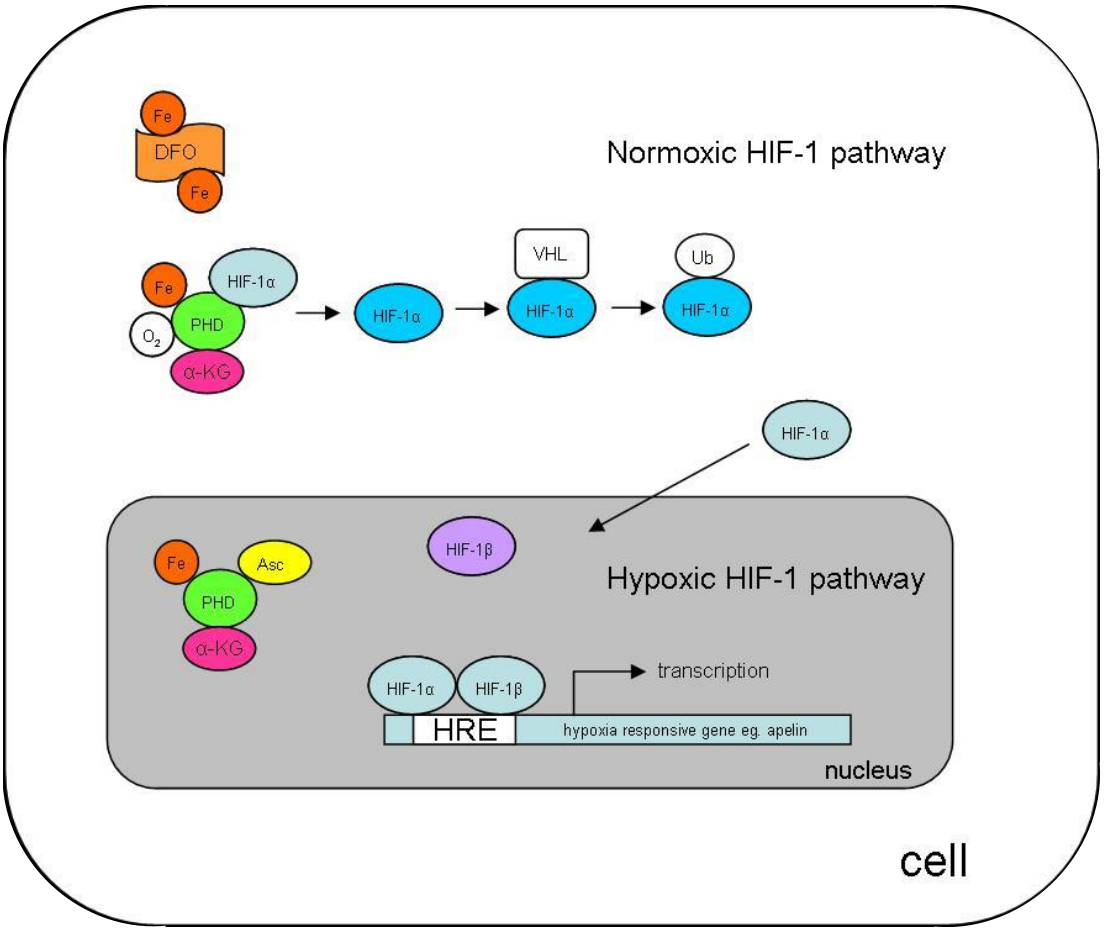

Figure 1.2: HIF-1α pathways and mechanism of action of HIF-1α modulators.
In normoxia, HIF-1α is hydroxylated by a prolyl hydroxylase enzyme (which requires iron, α-ketoglutarate and oxygen to bind HIF-1α), targetting HIF-1α for degradation via the ubiquitin pathway. DFO binds iron thereby disrupting the PHD complex, inhibiting degradation of HIF and potentiating the HIF pathway. In hypoxia, HIF-1α translocates to the nucleus as in the absence of oxygen the PHD complex cannot form. HIF-1α forms a heterodimer with HIF-1β and binds to the hypoxia response element on hypoxia sensitive genes and can upregulate or downregulate gene transcription.
DFO – desferrioxamine, α-KG - α-ketoglutarate, PHD – prolyl hydroxylase, VHL – von Hippel-Lindau factor, Asc – ascorbate, Ub – ubiquitin, HRE – hypoxia-response element. Adapted from Qutub *et al*. (2006).

1.3.2 Ischaemia

Ischaemia is characterised by reduced blood flow which fails to provide sufficient oxygenation to tissues. Ischaemia always results in hypoxia in the tissues in question and, therefore, the two conditions are inextricably linked. Ischaemic heart disease, in which there is a reduction in blood flow to the myocardium, is a global problem and was responsible for 12% of deaths worldwide in 2004 (World Health Organisation, 2004).

1.3.2.1 The reported cardioprotective effects of apelin

As apelin expression has been shown to be influenced by hypoxia, it is unsurprising that the effect of apelin in ischaemia has been studied. In a model of coronary artery ligation in isolated perfused mouse hearts, apelin-13 and apelin-36 were shown to be cardioprotective as reperfusion in the presence of exogenous apelin resulted in a smaller infarct size than reperfusion with saline alone (Simpkin *et al.*, 2007).

Similarly, Kleinz *et al*. (2008) demonstrated that pyr-apelin-13 reduces infarct size in a coronary artery ligation model in isolated perfused rat hearts when administered during reperfusion, but not when administered during the ischaemic period. In contrast to the work of Simpkin *et al*. (2007), Kleinz *et al*. (2008) found that the cardioprotective effect of apelin in the rat heart was not mediated via PI3K/Akt in the reperfusion injury salvage kinase (RISK) pathway.

In a rat model of isoproterenol-induced myocardial injury, apelin and APJ mRNA expression was decreased, while APJ receptor protein expression was increased.

Apelin treatment of these animals resulted in an improvement in left ventricular (LV) contractility parameters such as an increase in left ventricular developed pressure (LVDP), LV dP/dt max and LV dP/dt min. Furthermore, treatment with high or low dose apelin improved the observed features of histological damage (Jia *et al.*, 2006).

1.4 Zebrafish: a model organism for cardiovascular research

Zebrafish (*Danio rerio (Dr)*) (Fig 1.3) are an ideal model for research. In comparison to rodents, they are far cheaper to maintain and breed. Large numbers of offspring can be collected weekly from one tank of adult fish and this can be expected to be maintained for 12 - 18 months (see Rocke *et al.*, 2009). The large numbers of eggs collected mean that experimental studies can use high numbers of embryos; much higher than would be realistic in a rodent study. There is however arguably more variation among populations of zebrafish embryos, even among offspring collected from the same tank (Sun *et al.*, 2008).

(i)

(ii)

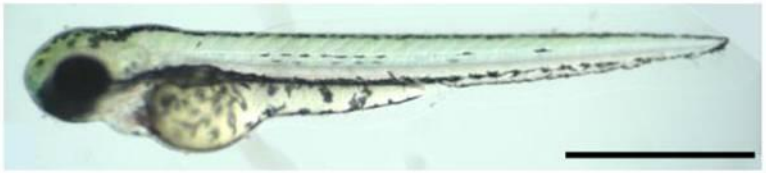

Figure 1.3: Adult zebrafish (i) and optically transparent embryonic zebrafish (3 days post fertilisation (dpf)) (ii).
(a) scale bar 0.5 cm, (b) scale bar 0.5 mm

In particular, zebrafish embryos are a key model in the cardiovascular field as their optical transparency allows the heart and vasculature to be visualised non-invasively by light microscopy. Embedding the zebrafish embryos in agar, which has been shown to have no detrimental effects on the embryo (Craig *et al.*, 2006; Denvir *et al.*, 2008), allows clear and reproducible images to be gathered as the fish are held still without anaesthesia. Although anaesthetic must be administered for the embedding process, this has minor effects on heart function and is fully reversible within 30 minutes (Denvir *et al.*, 2008). Once zebrafish are embedded detailed measurements of heart function may be carried out using techniques such as ultrasound (Sun *et al.*, 2008) and, as in this study, video edge detection of heart wall motion (Denvir *et al.*, 2008).

The effect of drugs can also be studied. Drugs can be injected into zebrafish embryos (Milan *et al.*, 2003), but are more commonly administered to embryos through the bathing water and this has been performed successfully in many studies (Denvir *et al.*, 2008; Milan *et al.*, 2003; Thirumalai *et al.*, 2008).

1.4.1 Development of zebrafish embryos

Development of the zebrafish embryo is a rapid process of which the key features can be observed by light microscopy and is summarised in Fig 1.4 (Kimmel *et al.*, 1995). Development begins with a cleavage period (0.75 – 2.25h) in which cells (blastomeres) divide at approximately 15 minute intervals. The blastula period (2.25 – 5.25h) encompasses the period in development where the blastomeres appear as a ball of cells, now termed the blastoderm. During the blastula period, the embryo enters midblastula transition in which zygotic gene transcription is activated and translation of maternally inherited mRNA ends (Kane and Kimmel, 1993). The yolk syncytial layer (YSL) is formed when the cytoplasm and nuclei of the blastomeres on the margin next to the yolk cell are released into the cytoplasm of the yolk cell immediately next to the blastoderm. Epiboly begins in the late blastula period and continues in the gastrula period (5.25 – 10h) (Kimmel *et al.*, 1995).

Epiboly is a process of thinning and spreading of cell layers and continues during the gastrula period (5.25 – 10h). The blastoderm moves towards the outermost layer of cells termed the enveloping layer (EVL). Both EVL and blastoderm cell layers now move around the border of the embryo, gradually enclosing more and more of the yolk cell (see Fig 5.1). At the end of the gastrula period the yolk cell is surrounded completely (Kimmel *et al.*, 1995). The segmentation period (10 – 24 h) follows, in which the number of somites increase as does the length of the embryo. The tail bud forms and the first organs develop, including the brain, otic vesicles and the pronephric kidney. The majority of cells within the somites become muscle cells and the first weak muscular contractions are visible at this stage of development. At the

end of the segmentation period, the blood island is clearly visible and contains dividing and differentiating blood cells (Herbomel *et al.*, 1999).

The pharyngula arches develop during the pharyngula stage (24 – 48 h). These arches will become the jaw, operculum and the gills. The heart is first visible at this stage below the brain. The heart begins to beat, at first with no direction, and later as a peristaltic wave. The vasculature is now also visible and blood cells circulate (Kimmel *et al.*, 1995). Other organs including the intestines are thought to be developing around this time, but cannot be visualised by light microscopy. During the hatching stage (48 – 72h), pectoral fins, jaw and gills develop and embryos hatch from their chorion. By 72 hpf, a protruding mouth is observed (Kimmel *et al.*, 1995).

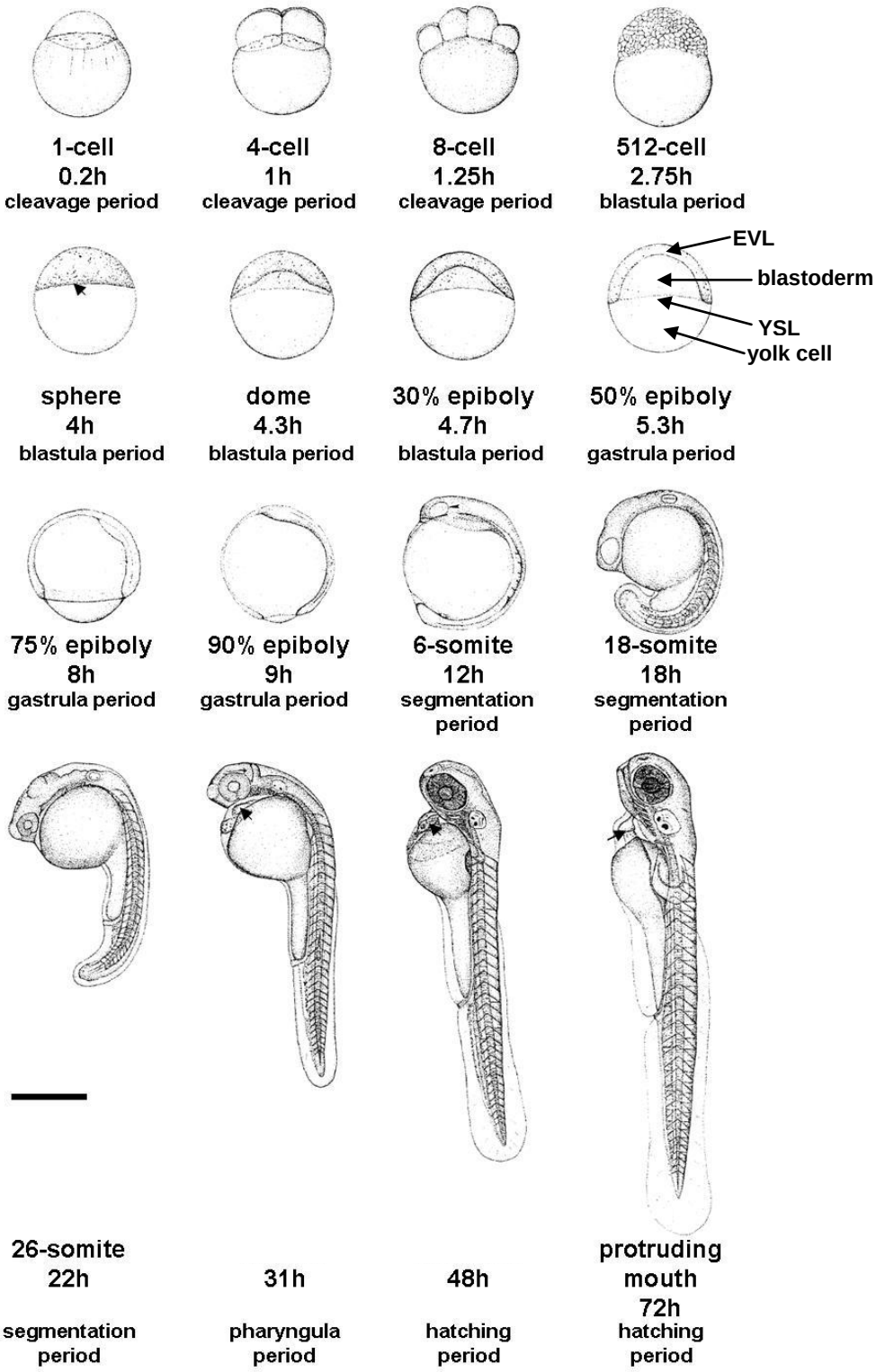

Figure 1.4: Camera lucida sketches of the zebrafish embryo at selected developmental stages.

Arrowheads indicate the smooth surface between blastoderm and yolk cell at the sphere stage (4h) (section 5.1.4.3) and the EVL, blastoderm, YSL and yolk cell involved in epiboly (section 5.1.2). Arrowheads also indicate the developing heart at 31h, 48h and 72h. The heart is first visible at 31h in these images, appears as a tube at 48h and heart looping has taken place by 72h. Scale bar 0.5 mm. Figure adapted from Kimmel *et al*. (1995).

1.5 Hypothesis and Aims

1.5.1 Hypothesis

This study hypothesises that the peptide apelin and its receptor are involved in a range of cardiovascular mechanisms including cardiac inotropy, vasodilatation and cardioprotection. These mechanisms are conserved across species.

1.5.2 Models for the investigation of the cardiovascular effects of apelin

In order to investigate the cardiovascular effects of apelin, rat and zebrafish models were used. The rat models (isolated perfused rat heart, isolated papillary muscles and myography) were chosen as these are well-characterised *in vitro* techniques for the study of potentially vasoactive and inotropic agents which were also well established in our laboratory. Indeed, in the discovery of the functional effects of the peptide endothelin, all three of these models have been used (Henriksson *et al.*, 2003; Qi *et al.*, 2001; Yamamoto *et al.*, 2004). The isolated perfused rat heart experiments were performed in this model as in addition to studying the inotropic effect of apelin, this model had the potential to perform a cardioprotection study.

The zebrafish was used as it allowed for rapid measurement of cardiovascular parameters *in vivo* and drugs could be administered easily via the bathing water. This model also allowed us to knockdown the apelin gene early in development using morpholino technology.

1.5.3 Aims

In order to investigate this hypothesis, the aims of the work were:

i. to study the inotropic effects of apelin *in vitro* in isolated papillary muscles and atrial strips and in the isolated, perfused rat heart (Langendorff)

ii. to determine whether apelin has vasoactive properties *in vivo* and in rat mesenteric resistance arteries *in vitro*

iii. to develop a hypoxia-recovery model in the zebrafish and to use this model to investigate the influence of the apelin system on the cardiovascular response to hypoxia

Chapter 2 Methods

2.1 Apelin in vivo in the rat

Animals were used in accordance with the Animals (Scientific Procedures) Act 1986 and with local ethical consent. All rats used in this study were housed in the Little France Biomedical Research Facility at the University of Edinburgh, except where clearly stated, on a 12h light: 12h dark cycle with free access to food and water.

A series of *in vivo* experiments were performed. Male Wistar rats (200 – 500 g, n = 16) were anaesthetised by inhalation of isoflurane. The rats were placed in an anaesthetising chamber and anaesthesia was induced by 5% isoflurane delivered in 100% oxygen. After induction, anaesthesia was maintained with 2 - 2.5% isoflurane in 100% oxygen via a nose cone. The rat was placed on a heat pad (27 °C) and the depth of anaesthesia was confirmed by the absence of a withdrawal reflex in response to a strong paw pinch. The jugular vein and carotid artery were cannulated by insertion of cannula tubing (outer diameter 0.96 mm, inner diameter 0.58 mm) (Jencons, Leicestershire, UK). Apelin was administered via the jugular vein. Data was recorded by a Powerlab™ recorder and analysed by Chart 5 software (ADInstruments, Oxfordshire, UK).

2.2 Papillary muscle and atrial strip preparations

Male Sprague Dawley rats (300 - 450 g) were sacrificed by cervical dislocation. The heart was rapidly excised and placed in chilled (4 °C) Krebs-Henseleit solution (KH) ((in mM) NaCl 119, KCl 4.7, $CaCl_2$ 2, $MgSO_4$ 1.17, $NaHCO_3$ 25, KH_2PO_4 1.18, ethylenediaminetetraacetic acid (EDTA) 0.026 and D-glucose 5.5) and allowed to beat to expel blood before being transferred to chilled KH (containing 2,3-butanedione 2-monoxime (30 mM)). Pinning the apex to hold the heart in place, the right ventricle was carefully opened and right ventricular papillary muscles were dissected free by first freeing the chordae and secondly freeing the base of the papillary muscle. Right atrial strips were dissected by cutting a strip free from the atria, allowing the muscle fibres to run down the length of the tissue strip. A loop was tightened around the chordae of the papillary muscle or one end of the atrial strip and the base of the muscle was held in place by a clip attached to a tissue holder. The tissue holder was mounted vertically in line with a micrometer via a wire rod connected to a force transducer (World Precision Instruments, Stevenage, UK). The tissue holder with papillary muscle or atrial strip was quickly placed in a tissue bath containing KH maintained at 35 °C and bubbled continuously with 95% O_2/5% CO_2.

The base of the tissue holder had embedded point electrodes permitting electrical stimulation at a voltage 30% above threshold. Papillary muscles were stimulated at a rate of 2 Hz (duration 2 ms); atrial strips were stimulated at a rate of 1 Hz (duration 5 ms) and allowed to equilibrate over a period of 30 minutes prior to any experimental protocol beginning. Any muscle preparation that demonstrated more than a 30% drop in peak developed force within this equilibration period was discarded. Data was

recorded continuously by a Powerlab™ recorder and analysed by Chart 5 software (ADInstruments, Oxfordshire, UK).

2.3 Isolated, perfused rat heart (Langendorff)

Rats were housed in the animal facility of the Glasgow Cardiovascular Research Centre at the University of Glasgow on a 12h light: 12h dark cycle with free access to food and water. Male Wistar rats (250 g) were killed by concussion followed by cervical dislocation. The heart and surrounding tissue was rapidly excised and placed in cold (4 °C) HEPES (4-(2-hydroxyethyl)-1-piperazineethanesulfonic acid) buffer ((in mM) NaCl 140, KCl 4, $MgCl_2$ 1, HEPES 5, glucose 11.1; pH 7.4) and washed gently to remove blood before transferring to another beaker of cold HEPES buffer. The heart and aorta were dissected free of adhering tissue. The aorta was held below the cannula for a few seconds to allow it to fill with solution before clipping and then securely tying the aorta onto the cannula. The heart was perfused with Tyrodes solution ((in mM) NaCl 116, $NaHCO_3$ 20, Na_2HPO_4 0.4, $MgSO_4$ 1, KCl 4, glucose 11, $CaCl_2$ 2.5) at 10 ml/min and maintained at 37 ± 1 °C for the duration of the experiment.

For measurement of left ventricular pressure, a latex balloon (size 5, Harvard Apparatus Ltd., Kent, UK) was attached to a cannula (Harvard Apparatus Ltd., Kent, UK) and connected to a syringe via a fluid filled tube (Fig 2.1). A pressure-volume catheter (Millar Instruments, Texas, USA) was inserted through the cannula and held in place using a connected haemostat valve. An incision was made in the left atrium and a hole was cut to allow the mitral valve to be seen. The balloon was deflated and

fed through the left atrium and mitral valve using forceps. Once positioned in the ventricle the balloon was inflated with distilled water using the attached syringe to achieve a diastolic pressure of 5 mmHg as recorded by Chart 5 software (ADInstruments, Oxfordshire, UK).

Pacing wires were attached to the right atrium and the heart was paced at 5 Hz (duration 2 ms) using a constant voltage isolated stimulator (Digitimer Ltd., Hertfordshire, UK) attached to a generator. The effect of apelin-16 on the isolated heart was then studied by adding apelin-16 to the perfusate.

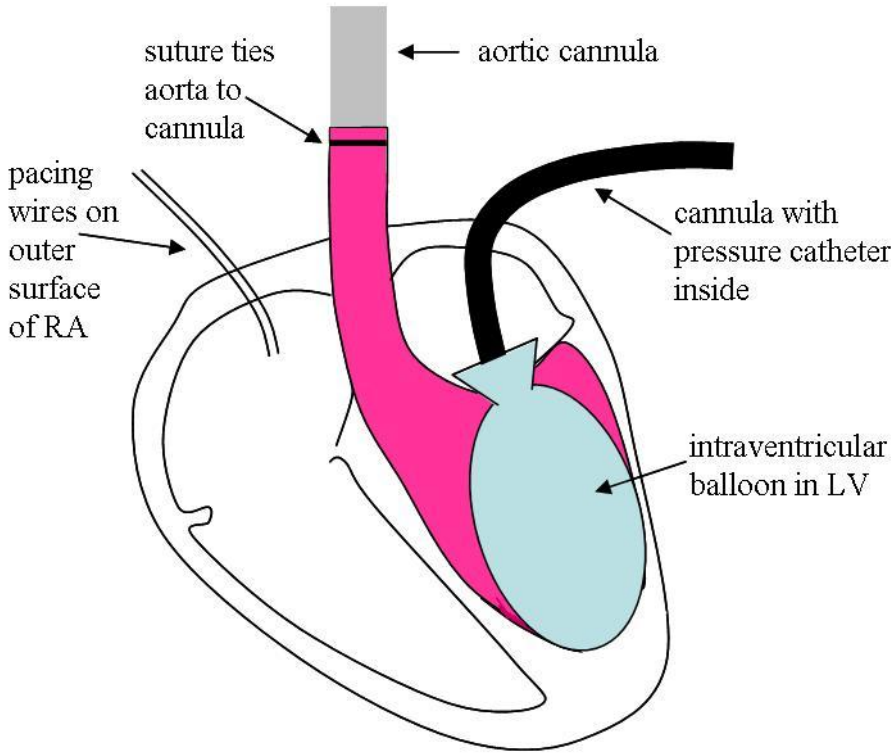

Figure 2.1: Isolated, perfused, rat heart (Langendorff).
The aorta is cannulated for retrograde perfusion of the heart. A balloon is inserted into the LV via the left atrium and pacing wires are attached to the RA.

2.4 Myography

Male Sprague Dawley rats (300 - 400 g) were sacrificed by cervical dislocation. The mesentery was removed from the animal and pinned out on a petri dish in chilled (4 °C) PSS. Adherent fat and the mesenteric vein were cut away. Second or third order mesenteric arteries were then cut free of the mesentery with a single cut at each end to give vessels approximately 2 mm in length.

A 40 µm tungsten wire was attached to the myograph chamber containing chilled KH solution. This wire was passed through the lumen of the vessel and secured to the myograph so that this wire secured the vessel to the transducer. A second wire was passed through the lumen and secured at both ends to a micromanipulator. The vessel length was then measured using a graticule eyepiece attached to the microscope. The myograph chamber was then placed back onto the myograph and the chilled KH was replaced with warm (37 °C) KH.

Resting tension was increased slowly to 6 mN in second order mesenteric arteries and 4 mN in third order mesenteric arteries. Vessels were allowed to equilibrate for 30 minutes at resting tension and were then re-tensioned after 15 minutes to correct for a drop-off in tension before beginning the experimental protocol described in chapter 4. Data was recorded by a Powerlab™ recorder and analysed by Chart 5 software (ADInstruments, Oxfordshire, UK).

2.4.1 Data analysis

PE concentration response curves were expressed as contraction in mN per mm of vessel length, calculated by the following:

$$response(mN/mm) = \frac{tension(mN)}{2 \times length(mm)}$$

Relaxation of vessels to ACh was expressed as the percentage relaxation of PE preconstriction. pD_2 (negative log of the EC_{50}) and slope of PE and ACh concentration response curves were determined by GraphPad Prism 5.0 (GraphPad Software Inc., California, USA) by nonlinear regression. Where a sigmoidal curve was not fitted by Prism 5.0 automatically, the slope was fixed to 1 or the top and bottom were fixed to 100 and 0 respectively to allow a sigmoidal curve to be fitted.

2.5 Zebrafish Husbandry

All zebrafish used for the studies presented in this thesis were kept in the Biomedical Research Resources Zebrafish Facility at the Queen's Medical Research Institute, University of Edinburgh in 10 L tanks (Aquatic Habitats, Florida, USA) on a 14 h light: 10 hour dark cycle. Water temperature (26 – 28 °C) and pH (6.8 – 7.5) were checked daily. Ammonia (< 0.25 mg/L), nitrate (< 200 mg/L) and nitrite (< 0.15 mg/L) levels as well as conductivity (180 – 350 µS) were measured weekly and maintained within levels appropriate to the maintenance of zebrafish stocks according to Brand *et al*. (2002). Zebrafish were fed twice daily.

2.5.1 Collection of fertilised eggs (Marbling)

Each tank was marbled as required to provide embryos for experiments. The evening before eggs were required, a tray of marbles on a wire mesh with a solid box underneath was placed into the tank. The following morning approximately an hour after the lights came on, the tray was removed from the tank and the water in the bottom of the box was passed through a tea strainer to collect eggs. Eggs were placed in a petri dish of dechlorinated system water containing methylene blue and placed in an incubator maintained at 28.5 °C. The water in the petri dishes was cleaned daily until the fish were prepared for an experiment.

2.5.2 Pair mating

In cases where large quantities of zebrafish eggs were required for experiments or when tanks of fish were not producing enough eggs regularly, pair mating was carried out. This involved putting one female and two males in a smaller tank and

separating the female from the male fish by a clear plastic barrier the evening before eggs were required. Marbles and plastic greenery were also placed in the tank. The barrier was removed from the tank as the lights came on the following morning and the fish were left for up to 2h before the water was strained and eggs collected and incubated as described above.

2.6 Zebrafish Experiments

2.6.1 Video edge detection

Video edge detection was used to measure zebrafish ventricular wall motion. Zebrafish embryos were anaesthetised in MS-222 (tricaine) (20 µM) which blocks sodium channels to inhibit the generation and conduction of action potentials (Hedrick *et al.*, 2003). The embryos were placed into molten agar, taking care to make sure it was not too hot, and orientated on their sides using forceps. Dechlorinated system water was added on top of the solidified agar. Embedded zebrafish were allowed to recover overnight in the incubator (28.5 °C) and could then be examined without anaesthesia. The system water in each dish was replaced before the start of each experiment.

A black and white high frame rate video camera (120 Hz) attached to a light microscope (Axioskop II MOT compound microscope) with a x 40 water dipper objective lens was used to visualise the hearts of the zebrafish. Video edge detection software (IonOptix Ltd., Dublin, Ireland) allows an image of the zebrafish ventricle to be observed continuously on a computer monitor. The IonOptix system is adapted from that used for tracking the motion of isolated cardiomyocytes. A cursor is placed

on the zebrafish ventricle wall to track its movement. The tracking of the wall can be controlled by adjusting settings on the software such as width and sensitivity of the signal and also by altering the light and focus on the microscope. The movement of the cursor as it tracks the ventricle wall is recorded as a continuous trace consisting of multiple movement transients (Fig 2.2). From these transients the following parameters of zebrafish ventricular wall motion can be determined: contraction velocity, relaxation velocity, magnitude of wall motion and heart rate. Each transient represents one cardiac cycle. Between 10 and 20 transients were analysed for each fish at each condition and time point, in no more than two groups of consecutive transients. This technique was used to study regional differences in the wall motion of the zebrafish embryo ventricle and to assess both the effect of drugs and hypoxia on ventricular wall motion. Further details of these experiments can be found in the relevant chapters.

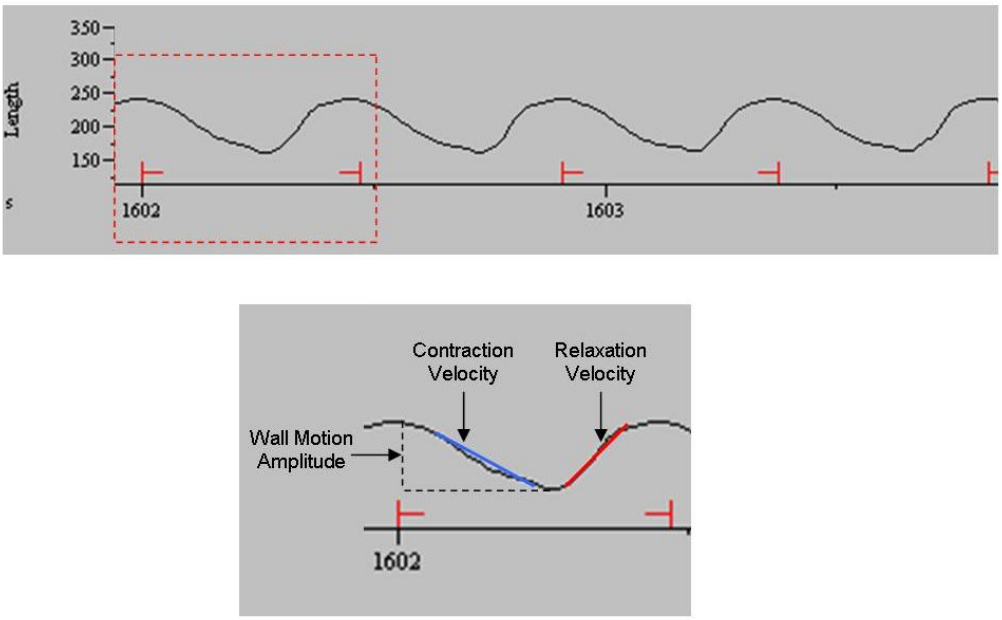

Figure 2.2: Video edge detection.
Video edge detection produces transients, each representing one cardiac cycle. Contraction velocity, relaxation velocity and wall motion amplitude are calculated from IonOptix software as shown. Contraction is downwards as length decreases. Enlargement is of boxed area.

2.6.1.1 Regional differences in ventricle wall motion in the zebrafish embryo

During preliminary experiments, we observed that wall motion varied depending on the region of the zebrafish embryo ventricle measured. Therefore, experiments were conducted to investigate the differences in wall motion at five regions of interest in order to determine the region that would be best suited to further experiments.

The zebrafish embryo ventricle was split into five regions of interest: inner wall, outer wall, inner near bulbus arteriosus, outer near bulbus arteriosus and the apical region (Fig 2.3). For each embryo in these experiments, as many as possible of these five regions of interest were tracked using the video edge detection system allowing the calculation of contraction velocity, relaxation velocity, amplitude of wall motion and HR.

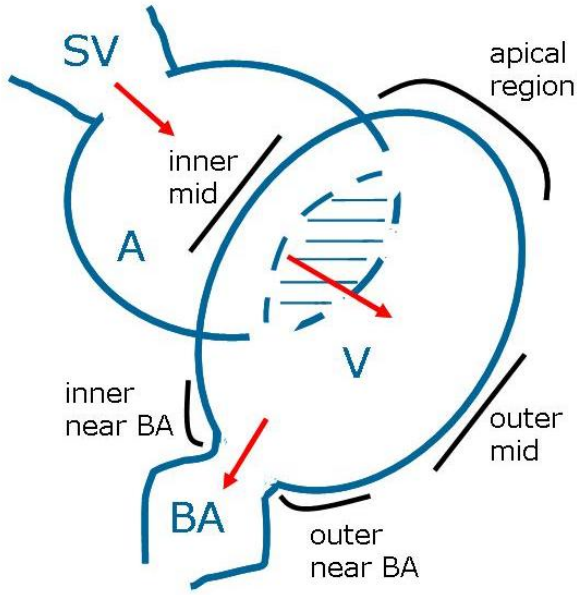

Figure 2.3: Zebrafish embryo heart.
Zebrafish embryo heart diagram with ventricular wall regions of interest: outer mid, inner mid, outer near bulbus arteriosus (BA), inner near BA and apical region. Shaded area represents atrioventricular valve. Arrows show direction of blood flow. SV – sinus venosus, A – atrium, V – ventricle.

Zebrafish (3 dpf) had a HR of 156.3 ± 6.4 bpm (n = 4, 4 - 6 embryos per experiment). Contraction velocity and relaxation velocity were significantly faster at the apical region than at all other regions measured ($P < 0.0001$ one-way ANOVA; Fig 2.5). Wall motion amplitude was greater at the apical region than all other regions ($P < 0.0001$ one-way ANOVA; Fig 2.6). No differences were found between other regions. Typical traces for an individual fish are shown in Figure 2.4.

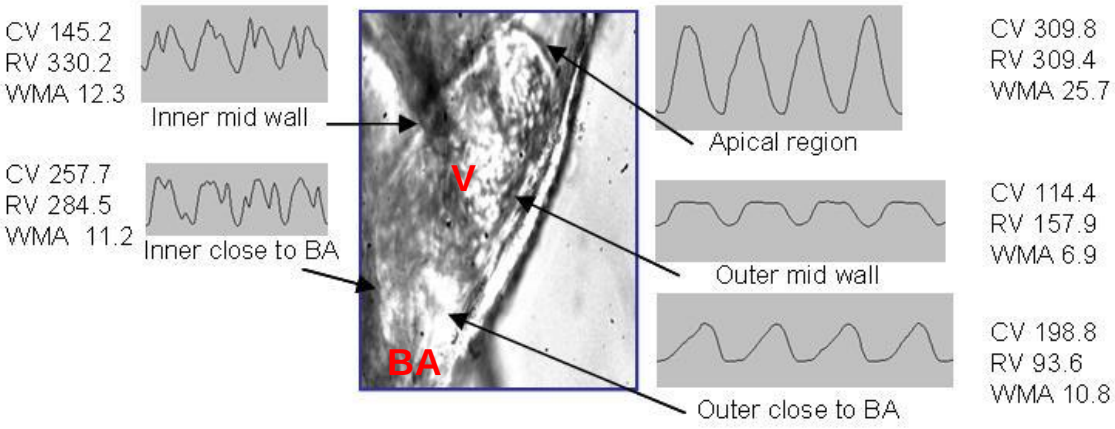

Figure 2.4: Representative traces and values showing regional differences in ventricular wall motion in a zebrafish embryo 3 dpf.
CV – contraction velocity (µm/s), RV – relaxation velocity (µm/s), WMA – wall motion amplitude (µm), V – ventricle, BA – bulbus arteriosus. Contraction is downwards; relaxation is upwards.

Throughout these experiments, we observed that the apical region was the region that could be captured most reproducibly. However, as this region had greater contraction velocity, relaxation velocity and wall motion amplitude, it was important to re-measure the same region in a given embryo in the case of experiments carried out over time. Therefore, for all experiments presented in this thesis, measurements have been made at the apical region where possible. If this was not possible, measurements were made at an alternative region and where the experiment was carried out over time, the same alternative region was re-measured at subsequent timepoints.

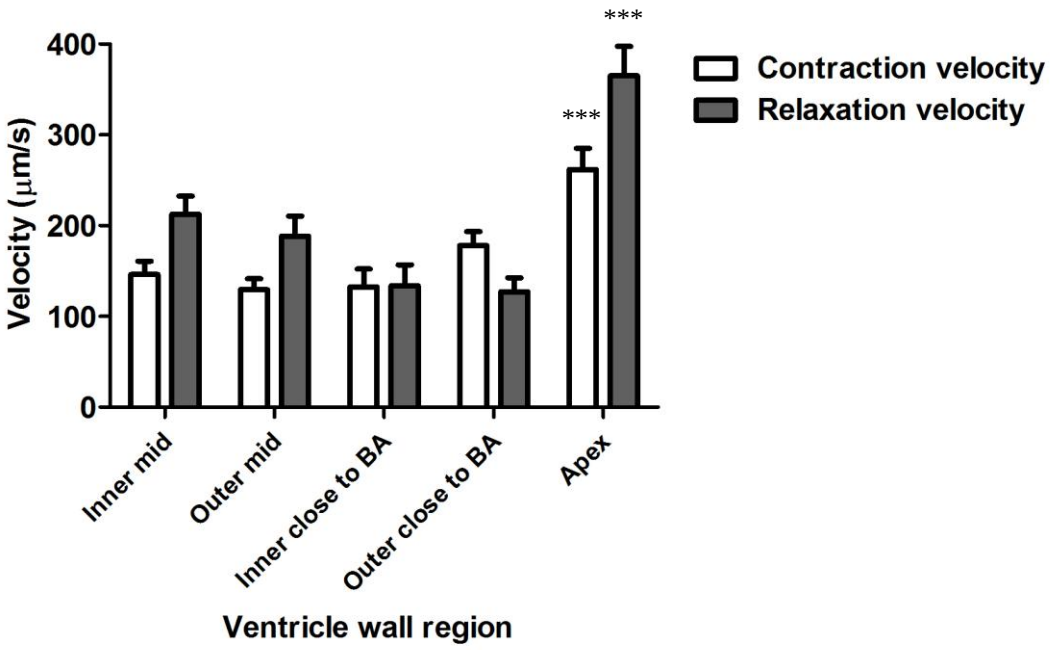

Figure 2.5: Regional differences in contraction and relaxation velocity in zebrafish embryos 3 dpf.
Contraction velocity: apical region vs. outer near BA * $P < 0.05$, apical region vs. all other regions *** $P < 0.001$ by one-way ANOVA; Relaxation velocity: apical region vs. all other regions *** $P < 0.001$ by one-way ANOVA. n = 4; 4 – 6 embryos per experiment.

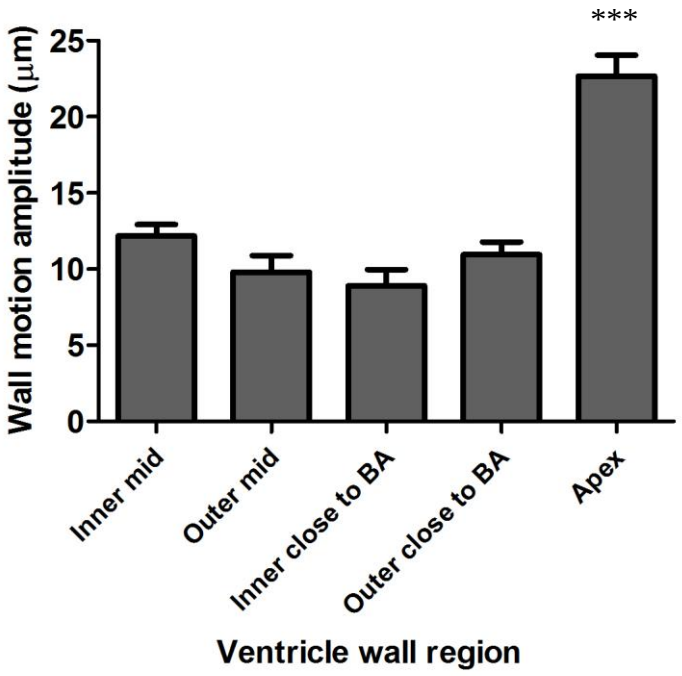

Figure 2.6: Regional differences in wall motion amplitude in zebrafish embryos 3 dpf.
Apical region vs all other regions *** $P < 0.001$ by one-way ANOVA. n = 4, 4 – 6 embryos per experiment.

2.6.1.2 Zebrafish isolated embryonic hearts

Transgenic zebrafish (cardiac myosin light chain 2: green fluorescent protein (cmlc2:GFP)) (Burns *et al.*, 2005) (3 dpf and 4 dpf) were anaesthetised with MS-222. HEPES buffer (pH 7.4) was prepared, which contained: (in mM) (HEPES 10, NaCl 136, KCl 5.4, $MgSO_4$ 1, Na_2HPO_4 0.3, glucose 10, $CaCl_2$ 2.5). Bovine serum albumin (BSA) (600 mg per 50 ml HEPES buffer) was added to the prepared buffer. Anaesthetised embryos were placed one at a time into the HEPES buffer plus BSA solution and their hearts were visualised using a dissection microscope with GFP filter. Hearts were isolated mechanically using one pair of forceps to hold the tail of

the embryo and the other to detach the heart by quickly and carefully freeing it from the surrounding tissue (Fig 2.7).

A 20 µl pipette was used to place the heart in a well in a prepared mould. HEPES buffer (without BSA) (3 ml) was added and an Axioskop II MOT compound microscope with a x 40 water dipper objective lens was used to locate the heart. Video edge detection, as described above, was used to measure isolated embryonic heart function with the addition of calcium and apelin as described in chapter 5.

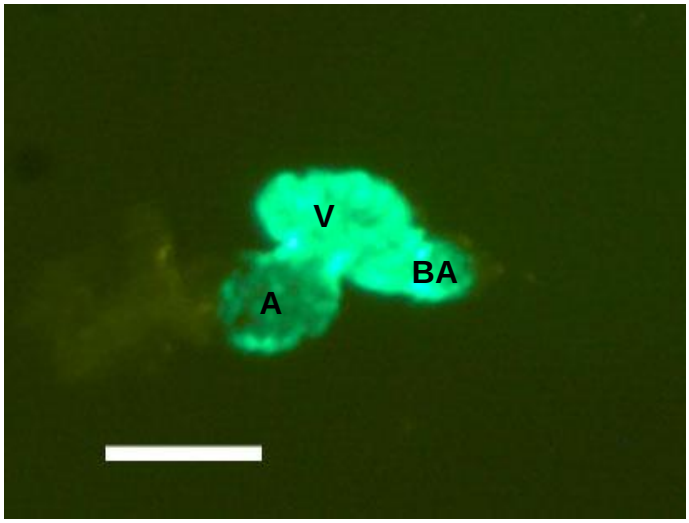

Figure 2.7: Isolated heart from zebrafish 3 dpf.
A – atrium, V – ventricle, BA – bulbus arteiosus. Scale bar represents 0.1 mm.

2.6.2 Measurement of ejection fraction

Ejection fraction was measured by anaesthetising embryos with minimal anaesthetic which inhibited swimming, but not heart function. A black and white high frame rate video camera attached to a light microscope (Axioskop II MOT compound microscope) with a x 40 water dipper objective lens was used to visualise the hearts of the zebrafish. The camera was attached to a Pinnacle Studio™ MovieBox (Avid Technology, S.L., Madrid, Spain) which allowed recording of a video of the heart using the Pinnacle Studio™ software. This video was processed using VirtualDub software (www.virtualdub.org) to convert the video file into a series of still images. Using ImageJ software (http://rsb.info.nih.gov/ij/), the area of the ventricle (in pixels) was measured in systole and diastole in three consecutive cardiac cycles. The ejection fraction (EF) was calculated for each cardiac cycle using the formula:

$$EF(\%) = \frac{systolic \quad area}{diastolic \quad area} \times 100$$

The mean ejection fraction from three cardiac cycles was used as the ejection fraction for each embryo.

2.6.3 Semi-quantitative scoring assessment: Hypoxia-Recovery Model

I developed a zebrafish embryo cardiac hypoxia-recovery model as part of the experimental work leading to this thesis. Zebrafish (3 dpf and 5 dpf) in dechlorinated system water were placed in the hypoxic chamber (1% oxygen, 94% nitrogen, 5% carbon dioxide; 26 °C) for 2h or 4h. After the assigned time in the hypoxic chamber, heart and circulatory function were assessed under a light microscope and each fish was described as having normal, reduced or absent heart rate (HR) and circulation compared to normoxic controls. A reduced HR was defined as less than 100 bpm. Circulatory assessments were also made 2h and 4h post-treatment recovery in normoxic conditions. Zebrafish embryos were euthanised in MS-222 and placed in RNAlater® (used according to manufacturer's instructions) (Applied Biosystems, Warrington, UK) for subsequent qualitative and quantitative assessment of abundance of mRNA of interest (see chapter 6).

Using this semi-quantitative assessment of global cardiovascular function, I was able to quite rapidly screen large numbers of embryos using a number of drugs that could potentially affect the hypoxic response. This emerged as a more efficient methodology for screening candidate drugs compared to the video edge detection system where we could use only small numbers of embryos and screen fewer drugs in a more time consuming approach. For example, using video edge detection, 4 embryos per group could be measured at a given timepoint, compared to screening of 10 embryos per group per timepoint using the global circulatory assessment.

A typical experimental protocol involved zebrafish embryos (5 dpf) incubated in a candidate drug or its vehicle for 1h before the embryos were exposed to hypoxia (1% oxygen) or normoxia for 2h. Qualitative assessments of cardiovascular function were made before, immediately after, and at 2h and 4h post-treatment recovery in normoxic conditions (see chapter 6).

2.6.4 Morpholino

2.6.4.1 General applications of MO technology

Morpholino technology is widely used in zebrafish research. Morpholinos are nucleic acid analogues which bind to mRNA and allow knockdown of expression of a gene of interest (Summerton, 1999). Morpholinos can be injected into embryos from the one cell stage until the 16 cell stage and knockdown expression of the gene of interest. Morpholinos act by blocking translation or appropriate splicing by binding near the start codon AUG or binding (Fig 2.8) at an exon/intron boundary, respectively (Fig 2.9). Successful knockdown of gene expression can be demonstrated by western blot or immunohistochemistry in the case of a translation blocking morpholino where an antibody is available. RT-PCR or qPCR is used to show successful knockdown of expression in experiments using splice blocking morpholinos (see Bill *et al.*, 2009).

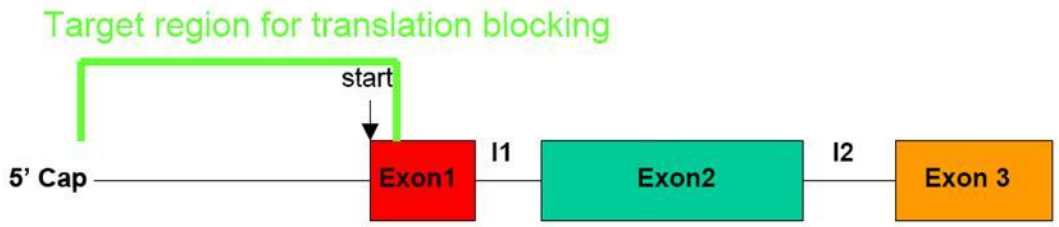

Figure 2.8: Translation blocking morpholinos.
Morpholinos blocking translation bind to or near to the start codon ATG to sterically inhibit binding of the translation complex (I1 – intron 1, I2 – intron 2; Figure from www.gene-tools.com).

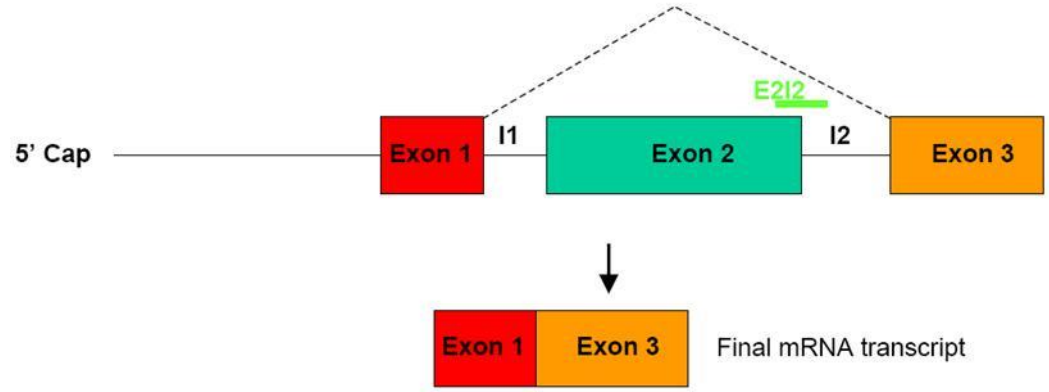

Figure 2.9: Morpholinos interfering with correct splicing of a pre-mRNA bind at an exon/intron boundary.
In this example, the morpholino binds at the boundary of exon 2/intron 2 sterically inhibiting binding of the spliceosome. This causes alternative splicing which results in deletion of exon 2 in the final mRNA transcript (I1 – intron 1, I2 – intron 2; Figure from www.gene-tools.com).

2.6.4.2 Zebrafish microinjection of morpholinos

Needles for morpholino injections were prepared from glass capillaries (outer diameter 1 mm, inner diameter 0.78 mm; Harvard Apparatus Ltd., Kent, UK) using a P-97 micropipette puller (Sutter Instrument Company, CA, USA). Morpholinos were diluted, as required, in potassium chloride (1 mM). Morpholinos were loaded into the prepared needles and attached to a micromanipulator (Narishige International Ltd., London, UK). The micromanipulator was connected to the IM-300 microinjector (Narishige International Ltd., London, UK). The system was balanced by air in a pressurised gas cylinder which was set to a pressure of approximately 15 psi throughout the morpholino injections. The quantity of each morpholino injected was calculated by injecting a bolus of morpholino into a drop of mineral oil on a graticule (see section 5.2.4.2). Then, eggs (1 – 4 cell) were lined up on a plastic mould with minimal water and the morpholino was injected into the cytoplasmic streaming area of the egg (Fig 2.10). After injection, eggs were transferred to system water containing methylene blue and stored in an incubator (28.5 °C).

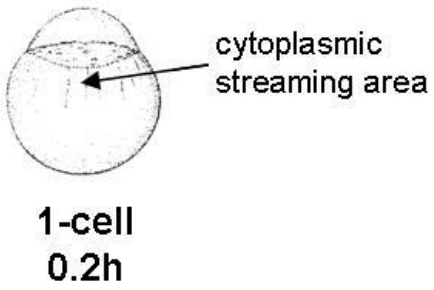

Figure 2.10: Morpholinos are injected into the cytoplasmic streaming area in 1 – 4 cell eggs.
Figure adapted from Kimmel *et al*., 1995.

2.7 Molecular techniques

2.7.1 Western Blotting

2.7.1.1 Protein extraction and quantification

Tissue for protein extraction was dissected on ice and kept in PBS until all samples were prepared. Tissue was weighed and protein was extracted by 5 minutes incubation in RIPA buffer on ice (300 µl per 100 mg tissue) containing phenylmethylsulfonyl fluoride (1 mM) and protease inhibitors (Sigma-Aldrich protease inhibitor cocktail P2714: AEBSF 2 mM, E-64 14µM, Bestatin 130 µM, Leupeptin 0.9 µM, Aprotinin 0.3 µM, EDTA 1 mM). Tissue was then homogenised with two metal beads in a mixer mill MM301 (60 – 120 s; 30 Hz) (Retsch, Leeds, UK). The beads were removed and each sample was centrifuged and the protein supernatant collected and stored (-20 °C).

Protein was quantified using a bicinchoninic acid (BCA) assay kit (Thermo Scientific UK Ltd., Loughborough, UK). Protein samples were diluted 1/10 and loaded in duplicate in a 96-well plate with protein standards (Thermo Scientific UK Ltd., Loughborough, UK). A colourimetric dye was added to the samples before incubation in the dark for 30 minutes. Absorbance at a wavelength of 562 nm was detected and measured by a MRX microplate plate reader (Dynex Laboratories Ltd., West Sussex, UK). Protein concentrations were calculated by comparison with the standard curve. Protein samples were diluted with a 1% sucrose solution and loading dye (dithiothreitol (DTT) 0.5 M, sodium dodecyl sulfate (SDS) 10%, sucrose 14%, bromophenol blue 0.01%) to a final protein content of 7.5 µg per sample.

2.7.1.2 Blotting and Transfer

Prepared protein samples were incubated at 95 °C with DTT (0.5 M) for 5 min and loaded (20 µl) on a protein gel (Thermo Scientific UK Ltd., Loughborough, UK). Samples were run using SDS/Tris/Hepes running buffer (x 1) (Thermo Scientific UK Ltd., Loughborough, UK) in a gel tank at 100 V for 45 min. Protein from the gel was then transferred to a polyvinylidene fluoride (PVDF) membrane by a wet transfer method (200 mA, 60 min) using transfer buffer (Tris base pH 8.3 25 mM, glycine 192 mM, methanol 20%).

2.7.1.3 Probing with anti-rat APJ antibody

Blocking was performed using 5% dried milk in TBST (NaCl 137 mM, Tris base pH 7.5 20 mM, Tween 20 0.1%) for 1h before overnight incubation in anti-rat APJ diluted in TBST with 5% dried milk (1:1250) (GeneTex, Inc., distributed by Patricell Ltd., Nottingham, UK; Cat no: GTX78179). After 3 x 5 min washes in TBST, the membrane was incubated in TBST containing secondary anti-rabbit IgG conjugated to horseradish peroxidise (1:10,000) (Santa Cruz Biotechnology, Heidelberg, Germany; Cat no: SC-2030) for 2h. Finally, 3 x 5 min TBST washes were performed. The membrane was placed on a shaker or roller for all blocking, washing and antibody incubation steps. With the exception of overnight incubation in primary antibody which was performed at 4 °C, all steps were carried out at room temperature. Enhanced chemiluminescence (ECL) (GE Healthcare, Buckinghamshire, UK) was applied to the membrane according to manufacturer's instructions. Photographic film was exposed to the ECL-loaded membrane for 40 minutes in a dark room to visualise the protein bands.

2.7.1.4 Membrane stripping and re-probing

To perform a loading control on the same PVDF membrane, the membrane was stripped by incubation (70 °C, 1h) in stripping buffer (SDS 2%, Tris base 62.5 mM pH 6.8, β-mercaptoethanol 0.8%), followed by washing in TBST (4 x 5 min). The membrane was blocked in 5% dried milk in TBST for 1h. Incubation in anti-rabbit GAPDH (1:10,000) (Sigma Aldrich, Dorset, UK; Cat no: G9545-2UL) was then carried out overnight. Following 3 x 5 min TBST washes, the membrane was incubated in TBST containing secondary anti-rabbit IgG conjugated to horseradish peroxidise (1:10,000) (Santa Cruz Biotechnology, Inc., Heidelberg, Germany; Cat no: SC-2030) for 2 h. Finally, 3 x 5 min TBST washes were performed before visualisation with ECL (exposure 20 minutes) as before.

2.7.2 Polymerase chain reaction (PCR)

2.7.2.1 RNA extraction and quantification

RNA from adult zebrafish heart was extracted using trizol (Invitrogen, Paisley, UK) by the following method. Adult zebrafish (n = 9) were killed by overdose with tricaine. Hearts were dissected free and placed in RNAlater® (Applied Biosystems, Warrington, UK). RNA extraction was performed by homogenising hearts in groups of 3 in trizol (500 µl) using a bead mixer mill (60 s; 30 Hz) proceeding according to the manufacturer's instructions. To eliminate potential DNA contamination, each RNA sample was treated with DNase I (Roche Diagnostics Ltd., West Sussex, UK).

RNA extraction from zebrafish embryos was performed using the RNeasy mini kit (Qiagen Ltd., West Sussex, UK) which allowed sufficient RNA to be extracted using

10 embryos per group. Embryos were stored in RNAlater® after experimental treatments and were homogenised in buffer RLT (provided in the kit) using a bead mixer mill (45 s; 30 Hz) immediately before RNA extraction. DNase treatment was performed at the time of RNA extraction using the DNase I kit (Qiagen Ltd., West Sussex, UK) according to manufacturer's instructions.

RNA was quantified using a NanoDrop® spectrophotometer ND-1000 (Thermo Scientific, Delaware, USA) which measured absorbance at a wavelength of 260 nm (extinction coefficient 40 ng/µl). RNA integrity was verified by: (i) a 260 nm/280 nm absorbance ratio close to 2 and (ii) by running RNA samples with cresol red loading dye at 100 V for 1 h on a 1% agarose gel (Promega, Southampton, UK). RNA samples were visualised with ethidium bromide (2 µM) as two bands corresponding to the 28S and 18S ribosomal subunits which are present in a 2:1 ratio in eukaryotic samples, including zebrafish (Peterson *et al.*, 2009) (Fig 2.11).

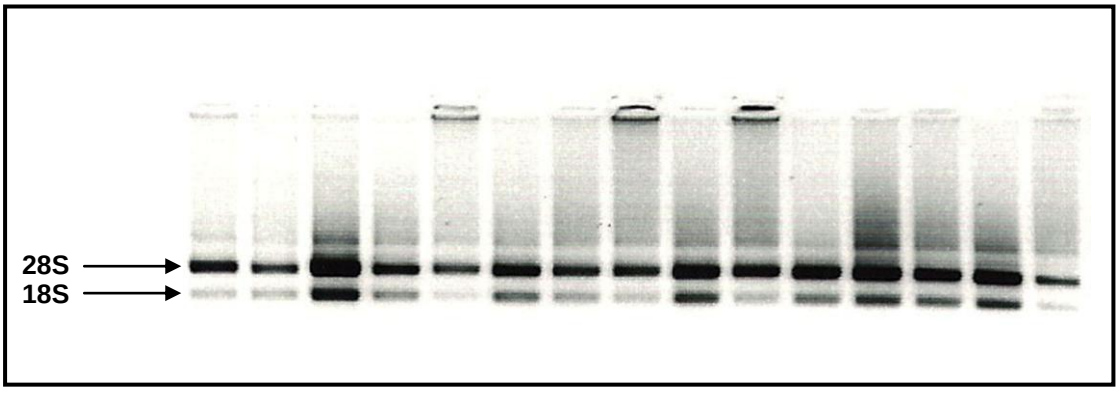

Figure 2.11: RNA gel showing ribosomal subunits 28S and 18S in a 2:1 ratio confirming zebrafish RNA integrity.

2.7.2.3 Reverse transcription PCR

RNA was transcribed to cDNA (0.5 – 1 µg) using a high capacity cDNA reverse transcription kit (Applied Biosystems, Warrington, UK) according to manufacturer's instructions. A water only negative control was included as were controls which omitted the reverse transcriptase enzyme. These negative controls demonstrate that there are no genomic DNA contaminants or other contaminants in the sample.

Detection of mRNA of interest was achieved by PCR (see relevant chapters for details). Primer pairs were designed using Primer 3 software followed by entering the amplicon in BLAST to ensure its specificity. PCR was performed using primer pairs (Eurofins MWG Operon) and PCR Master Mix (Promega UK Ltd., Southampton, UK). Each 25 µl PCR reaction volume contained cDNA (1 µg), forward and reverse primers (0.4 µM each), Taq DNA polymerase (0.625 units), dNTPs (200 µM each) and $MgCl_2$ (1.5 mM). The PCR program was as follows: 94 °C for 5 min, 30 cycles of 94 °C for 15 s, 55 °C for 30 s and 72 °C for 1 min, followed by 72 °C for 10 min. PCR products were separated by electrophoresis at 100 V on a 1% agarose gel (Promega UK Ltd., Southampton, UK) and visualised with ethidium bromide (2 µM).

2.7.2.4 Reverse Transcription Quantitative PCR

For reverse transcription quantitative PCR (qPCR) experiments, RNA was extracted from zebrafish embryos as described above. The universal probe library (UPL) (Roche Diagnostics Ltd., UK) was used. The *Assay Design Center* on the Roche website (http://www.roche-applied-science.com/sis/rtpcr/upl/ezhome.html) allowed qPCR assays to be designed for mRNA of interest in zebrafish.

PCR was performed using primer pairs (Eurofins MWG Operon) and LightCycler® 480 Probes Master Mix (Roche Diagnostics Ltd., UK). Each sample was assayed in triplicate. Each 10 µl qPCR reaction volume contained cDNA (0.0125 µg), 1 x LightCycler® 480 Probes Master Mix (containing FastStart Taq DNA Polymerase, reaction buffer, dNTP mix (with dUTP instead of dTTP) and $MgCl_2$ 6.4 mM), UPL probe (100 nM), forward and reverse primers (200 nM each). QPCR was performed using a LightCycler480® (Roche Diagnostics Ltd., UK) which detected the fluorophore FAM. The qPCR program was as follows: 95 °C for 5 min, 50 cycles of 95 °C for 10 s, 60 °C for 30 s and 72 °C for 1 s, followed by 40 °C for 30 s.

Standard curves (slope -3.3, efficiency 1.7 – 2.1, $R^2 > 0.9$; Fig 2.12) made by serial dilutions of pooled cDNA (0.5 µg) (1/4 – 1/1024) for each primer-probe set were performed to validate the qPCR assays. For each experiment, appropriate reference genes that did not change across experimental groups were selected. Transcripts were quantified by comparison with the standard curve and the mRNA of interest was then corrected by the mean of the appropriate reference genes.

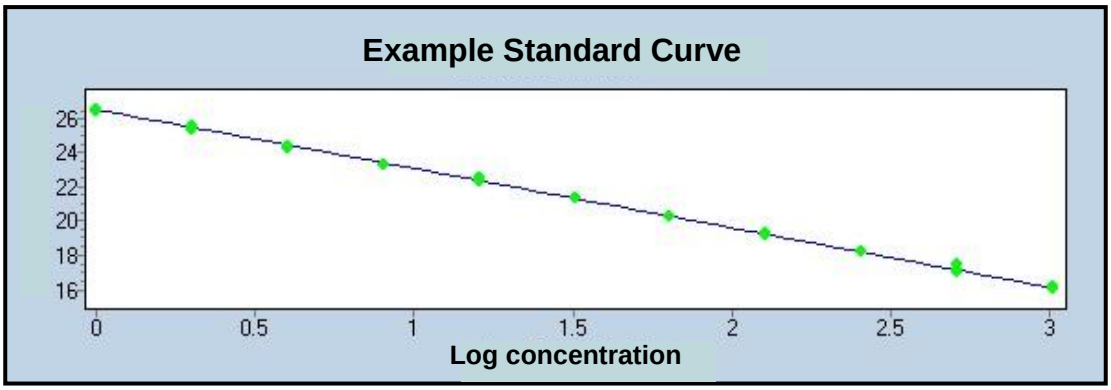

Figure 2.12: Example standard curve calculated by LightCycler480™ software.

2.8 Statistical Analysis

Data are presented as mean ± standard error of the mean (SEM). Comparison of two groups was made by unpaired t-tests (GraphPad Prism® 5.0). Comparison of three or more groups was made by one-way analysis of variance (ANOVA) followed by Tukey's post-hoc test (GraphPad Prism® 5.0) or repeated measures one-way ANOVA followed by post-hoc test for linear trend (GraphPad Prism® 5.0) in the case of time course experiments. Two-way ANOVA followed by Bonferroni post-hoc test was used to compare groups affected by two factors eg. drug and time. Comparison of Kaplan-Meier survival curves was made by the Log rank (Mantel-Cox) test (GraphPad Prism® 5.0). Significance was accepted at $P < 0.05$. For categorical data, comparison of proportions was carried out (MedCalc® Version 11.3.1.0) and to account for multiple comparisons in these cases, significance was accepted at $P < 0.01$.

2.8.1 Experimental unit in zebrafish experiments

For all zebrafish experiments, the definition of the experimental unit (or n) was important. The majority of experiments were performed in dishes of zebrafish embryos, where there may be unknown factors that influence all embryos in a given dish, but not in another dish. Therefore, the experimental unit is reported as the number of times the experiment was performed ie. the number of dishes of embryos rather than the actual number of embryos. However, the actual number of embryos used per experimental unit will be given after the n number. Where fish were kept in their own well, for example in the case of the ejection fraction experiment performed on morpholino injected embryos (chapter 5), the n number is the actual number of embryos measured.

2.9 Reagents

Pyr-apelin-13, apelin-13, apelin-16 and apelin-36 were purchased from Phoenix Europe GmbH (Karlsruhe, Germany). Purchased apelin was reconstituted with distilled water to make a stock solution (10 μM), aliquoted and stored at -20 °C. A fresh aliquot was diluted for each experiment. All other drugs and reagents are from Sigma-Aldrich Company Ltd. (Dorset, UK) unless otherwise stated in the text.

Chapter 3 The inotropic effects of apelin

3.1 Introduction

In 2002, apelin-16 was shown to be an inotrope (increase force of contraction) in the isolated perfused rat heart (Szokodi *et al.*, 2002). Apelin's inotropic effect was observed after 2 minutes of infusion and reached a maximum at 25 minutes. Apelin-16 increased dP/dt max significantly compared to vehicle infusion when preload was increased to 10 mmHg and 15 mmHg, but not at a left ventricular end diastolic pressure (LVEDP) of 5 mmHg (Szokodi *et al.*, 2002).

Apelin-16 is also inotropic *in vivo*. Apelin-16 significantly increased maximum pressure (Pmax) and rate of rise towards the peak (dP/dt max) after 5 minutes infusion in rats with heart failure induced by coronary artery ligation, but the effect was not observed in control animals until 15 minutes infusion via the femoral vein. Apelin-16 increased rate of fall towards baseline (dP/dt min) after 15 mins in both groups (Berry *et al.*, 2004). However, in the mouse, intravenous apelin-12 decreased Pmax and did not affect dP/dt max. Chronic administration of pyr-apelin-13, on the other hand, increased LV contractility as measured by Doppler ultrasound (Ashley *et al.*, 2005).

In right ventricular trabeculae in the rat, apelin-12 increased force and intracellular calcium concentration significantly in trabeculae from animals with heart failure, but not in control animals (Dai *et al.*, 2006). In rat ventricular myocytes, apelin-16 increased sarcomere shortening in both normal and failing myocytes, but had no effect on the intracellular calcium concentration (Farkasfalvi *et al.*, 2007), leading the authors to suggest that an increase in sensitivity of the myofilaments to calcium is

responsible for the effect. The maximum effect was observed after 1 min and lasted 1-2 mins (Farkasfalvi *et al.*, 2007). In human paced atrial strips from patients undergoing coronary bypass surgery, apelin-13, pyr-apelin-13 and apelin-36 all produced an increase in force (Maguire *et al.*, 2009).

In the first study assessing the inotropic effect of apelin in humans *in vivo*, apelin-36 decreased both maximum left ventricular pressure and end-diastolic pressure, while significantly increasing dP/dt max (Japp *et al.*, 2010). As these are load-dependent measures of cardiac contractility, it is difficult to determine if apelin is increasing contractility independent of load on the heart (Japp *et al.*, 2010). Vasodilation of coronary arteries also occurred with apelin administration which may contribute to the inotropic effect, as seen with some calcium antagonists (see Schwartz *et al.*, 1985).

The mechanism of apelin's inotropic action is not yet fully understood. However, it is thought that the APJ receptor couples to Gq, activating phospholipase C and protein kinase C (PKC) as demonstrated by inhibitors of these pathways attenuating the inotropic response in isolated rat hearts (Szokodi *et al.*, 2002). Furthermore, PKC may activate the Na^+/H^+ exchange leading to the NCX working in reverse and thereby increasing intracellular calcium. In isolated perfused rat hearts, inhibition of the NCX blunted apelin's inotropic response (Szokodi *et al.*, 2002).

Some groups argue that inotropy after apelin administration is due to an increase in intracellular calcium concentration (Dai *et al.*, 2006). However, others believe that

intracellular calcium concentration is unaffected and that an increase in sensitivity of the myofilaments to calcium is responsible for the effect (Farkasfalvi *et al.*, 2007).

From the published literature, it appears that apelin has its greatest inotropic effect in disease states such as heart failure. Indeed endogenous apelin appears to be crucial for cardiac contractility to be maintained in ageing and in the face of increased afterload as shown in studies with apelin knockout mice (Kuba *et al.*, 2007). In humans, apelin levels are increased in mild heart failure, but decrease to control levels in severe heart failure (Chen *et al.*, 2003; Foldes *et al.*, 2003).

In addition to the effect of disease state on the inotropic response to apelin, species, experimental preparation, administration period and the form of apelin investigated may all contribute to the variable responses demonstrated in the published studies.

This study aimed to further investigate the inotropic effects of apelin and the specific aims of this chapter were:

i. to demonstrate the presence of the APJ receptor on rat papillary muscles and right atrial strips
ii. to examine the inotropic effects of pyr-apelin-13, both alone and in combination with other pharmacological agents, in right ventricular papillary muscles and right atrial strips of the rat
iii. to investigate the inotropic effects of apelin-16 in the isolated perfused rat heart

3.2 Methods

3.2.1 Western Blotting

Western blotting was performed as described in section 2.7.1. Protein was extracted from rat right ventricular papillary muscle (n = 2) and right atrial strip (n = 2), run on a protein gel and transferred to a polyvinylidene fluoride (PVDF) membrane as described. The membrane was probed with anti-rabbit APJ antibody to detect APJ protein (42 kDa) and, following stripping of the membrane, re-probed with anti-rabbit GAPDH to detect GAPDH protein (35 kDa) as a positive control.

3.2.2 Isolated right ventricular papillary muscles and right atrial strips

Isolated rat right ventricular papillary muscles and rat right atrial strips were dissected from the heart and mounted in tissue baths for isometric tension recording as outlined (section 2.2).

Cumulative concentration response curves to noradrenaline (NA) (1 – 10,000 nM), calcium (2 - 10 mM) and pyr-apelin-13 (1 – 100 nM) were carried out. In papillary muscles, the effect of pyr-apelin-13 was also assessed in the presence of NA 1 and 100 nM, Ca^{2+} 5 mM and angiotensin II (ATII) 1 and 100 nM. The papillary muscles were pretreated with drugs for 3 minutes prior to pyr-apelin-13 application. At the end of each experiment either NA 100 nM or Ca^{2+} 10 mM was added to each preparation to confirm that the tissue was viable and had the potential to generate a positive inotropic response (increase in force of contraction) if this had not been carried out as part of the experimental protocol.

Time-matched controls were performed for all apelin experiments by the addition of an identical volume of vehicle (dH_2O) instead of apelin at the appropriate time points. For experiments which studied the effect of apelin after pre-treatment with another agent, the other drug was used as outlined in the experimental protocol, followed by vehicle instead of apelin additions. Decrease in force (termed drop-off) with time was also determined in the present study.

3.2.3 Langendorff

The procedure for successful mounting of the rat heart and retrograde perfusion of coronary arteries was carried out as described (section 2.3). A latex balloon was inserted into the left ventricle (section 2.3) for measurement of intraventricular pressure. Hearts were initially paced at 5 Hz by attachment of pacing wires to the right atrium; however breakthrough arrythmias were observed in some preparations and in these cases pacing was increased. No heart was paced above 6 Hz.

After 2 mins steady state, apelin-16 (10 nM) was delivered to the heart via the perfusate for 15 minutes. At the end of each experiment $CaCl_2$ 3.5 mM was perfused to confirm that all hearts were viable (and therefore the experiment was valid) and had the potential to generate an increase in force (positive inotropy).

3.3 Results

3.3.1 APJ receptor expression in right ventricular papillary muscles and right atrial strips

The APJ receptor was detected by western blotting in right ventricular papillary muscles and right atrial strips of the rat (Fig 3.1).

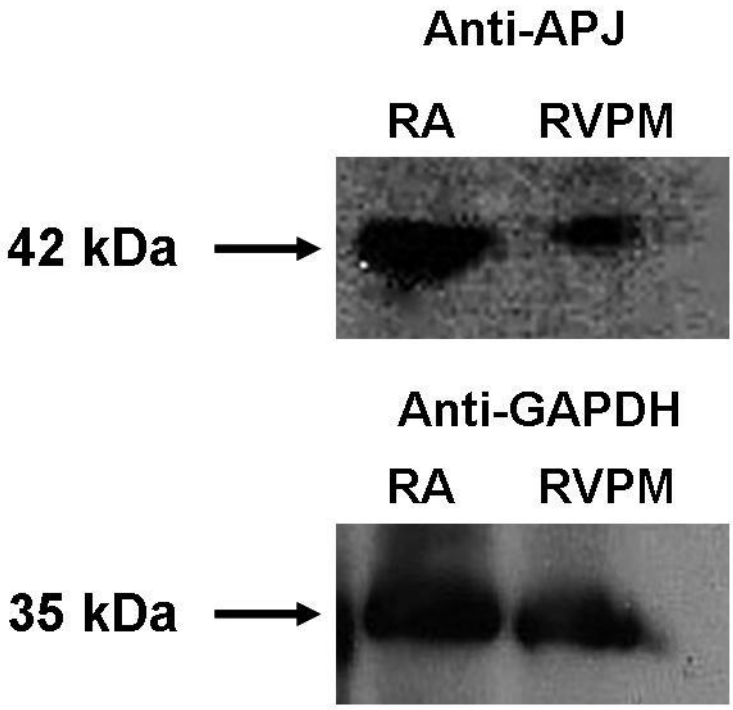

Figure 3.1: Western blotting shows APJ protein (42 kDa) and GAPDH (35 kDa) protein in right atrial strip (RA) and right ventricular papillary muscle (RVPM).

3.3.2 In vitro functional studies

3.3.2.1 The effect of NA and calcium on rat RV papillary muscles and RA strips

NA elicited a concentration dependent increase in the force generated by right ventricular (RV) papillary muscles (pD_2 6.09 ± 0.13, E_{max} 229.60 ± 82.55 mg, slope 0.88 ± 0.09, n = 6; Fig 3.2(i)) and right atrial (RA) strips (pD_2 6.01 ± 0.15, E_{max} 131.40 ± 40.79 mg, slope 1.17 ± 0.17, n = 5; Fig 32(i)). The response of the papillary muscles and atrial strips to NA did not differ significantly (P = 0.69 pD_2, P = 0.34 E_{max}, P = 0.15 slope, unpaired t-test). Ca^{2+} was also able to elicit a concentration dependent increase in force in both preparations (papillary muscles, pD_2 2.36 ± 0.04, E_{max} 334.30 ± 90.03 mg, slope 3.92 ± 0.45, n = 3; RA strips, pD_2 2.32 ± 0.03, E_{max} 304.70 ± 66.14 mg, slope 3.29 ± 0.39, n = 6; Fig 3.2(ii)). The response of the papillary muscles and atrial strips to Ca^{2+} did not differ significantly (P = 0.46 pD_2, P = 0.80 E_{max}, P = 0.36 slope, unpaired t-test).

3.3.2.2 The effect of pyr-apelin-13 on rat RV papillary muscles and RA strips

Pyr-apelin-13 failed to elicit a response in both RV ventricular papillary muscles and RA strips in the presence of 2 mM calcium when 1, 10 and 100 nM were added cumulatively at 3 min intervals (papillary muscles n = 4, P = 0.43 two-way ANOVA apelin vs vehicle; Fig 3.3(i)). In a larger number of animals, 100 nM had no effect on force of contraction in papillary muscles (P = 0.16 one-way ANOVA; n = 9; Fig 3.3(ii)). In right atrial strips, pyr-apelin-13 (100 nM) had no effect on force of contraction (n = 3; Fig 3.3(iii)). Pyr-apelin-13 had no effect on time to peak both in time course experiments (P = 0.18 one-way ANOVA; n = 3; Fig 3.4(i)) and in all experiments with all doses combined (P = 0.20 one-way ANOVA; n = 3 – 8; Fig

3.4(ii)). Pyr-apelin-13 had no effect on time to relaxation both in time course experiments (P = 0.38 one-way ANOVA; n = 3; Fig 3.4(iii)) and in all experiments with all doses combined (P = 0.87 one-way ANOVA; n = 3; Fig 3.4(iv)).

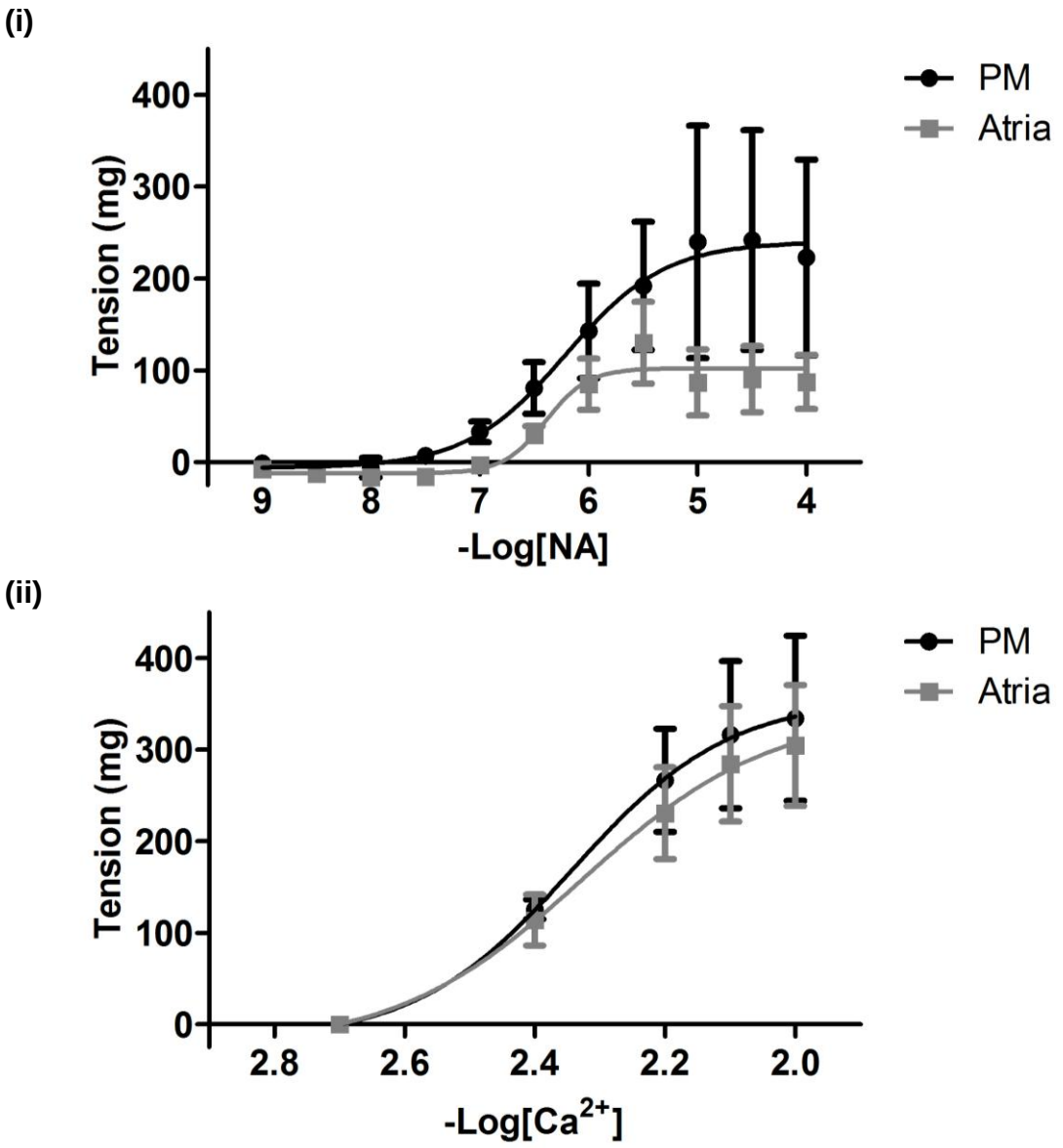

Figure 3.2: Concentration response curves in right ventricular papillary muscles and right atrial strip preparations in response to NA (i) and calcium (ii).
(i) n = 6 and n = 5, respectively (ii) n = 3 and n = 6, respectively.

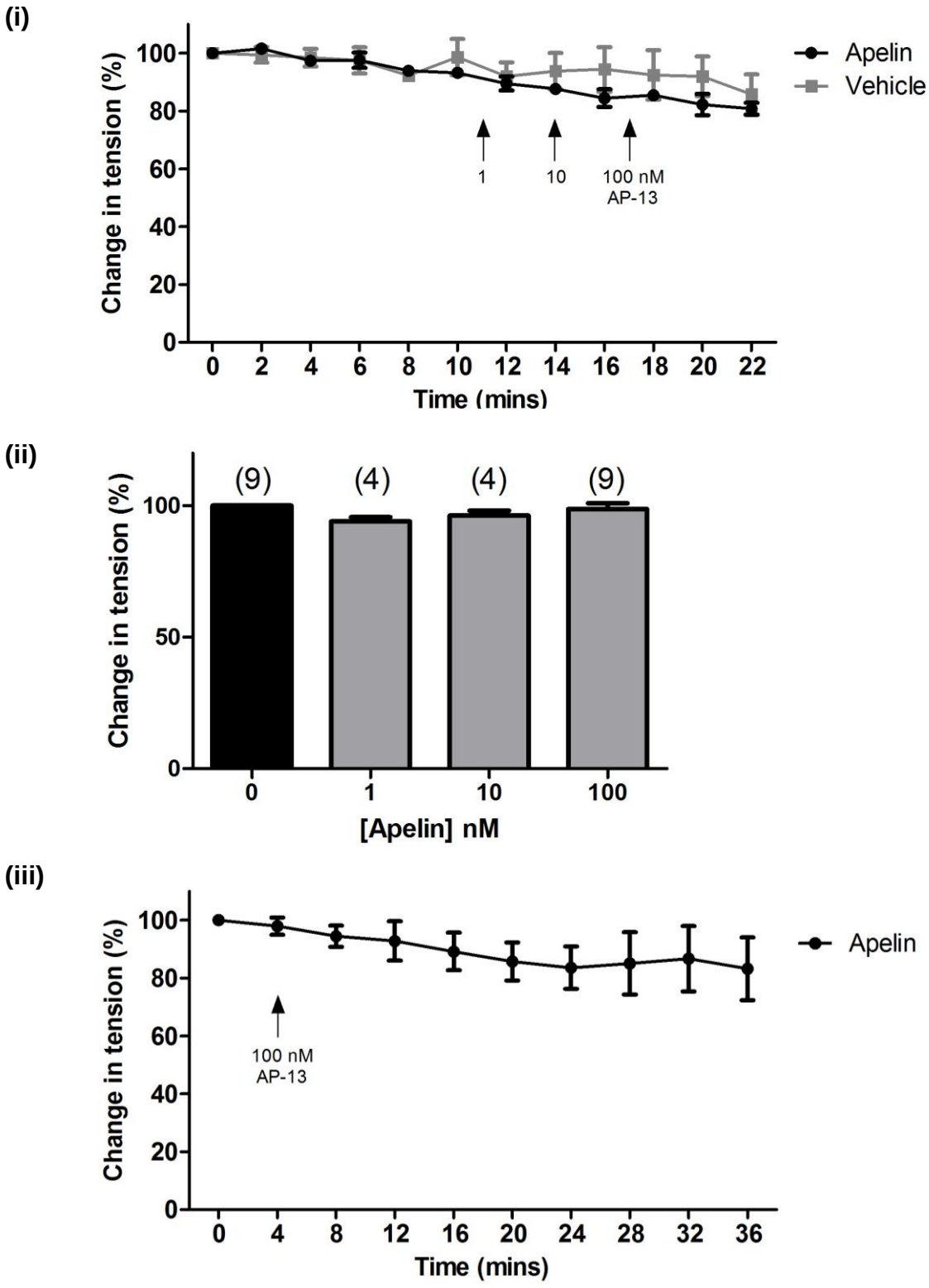

Figure 3.3: Effect of pyr-apelin-13 on RV papillary muscles (i and ii) and RA strips (iii) in presence of calcium 2 mM.
(i) $P = 0.42$ two-way ANOVA apelin (n = 4) vs vehicle (n = 3), (ii) $P = 0.16$, n = 4 – 9 (shown in brackets), (iii) n = 3.

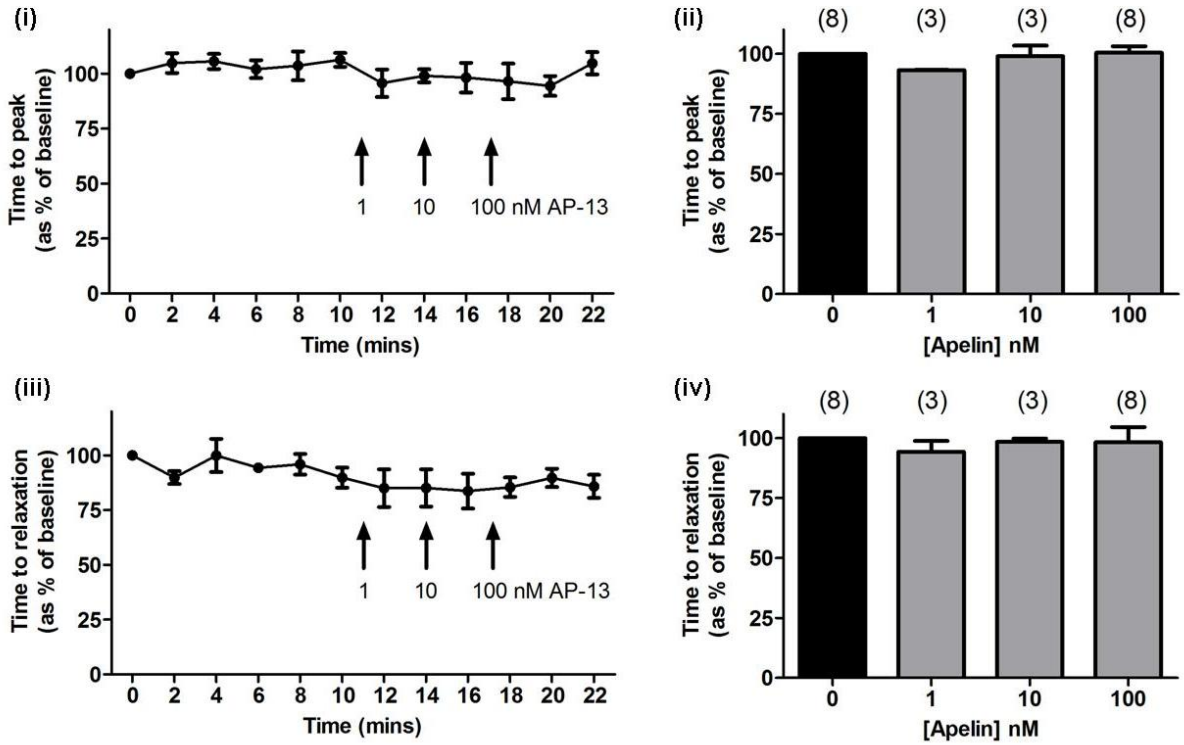

Figure 3.4: The effect of pyr-apelin-13 on time to peak and time to relaxation in RV papillary muscles in the presence of normal baseline calcium (2 mM).
Pyr-apelin-13 had no effect on time to peak both in time course experiments (*P* = 0.18 one-way ANOVA; n = 3) (i) and in all experiments with all doses combined (*P* = 0.20 one-way ANOVA; n = 3 – 8 shown in brackets) (ii). Pyr-apelin-13 had no effect on time to relaxation both in time course experiments (*P* = 0.38 one-way ANOVA; n = 3) (iii) and in all experiments with all doses combined (*P* = 0.87 one-way ANOVA; n = 3 – 8 shown in brackets) (iv).

In the presence of both low (1 nM) and high (100 nM) NA, pyr-apelin-13 had no effect in RV papillary muscles (n = 5 and n = 4, respectively, *P* = 0.68 and *P* = 0.26 two-way ANOVA apelin vs vehicle, respectively; Fig 3.5).

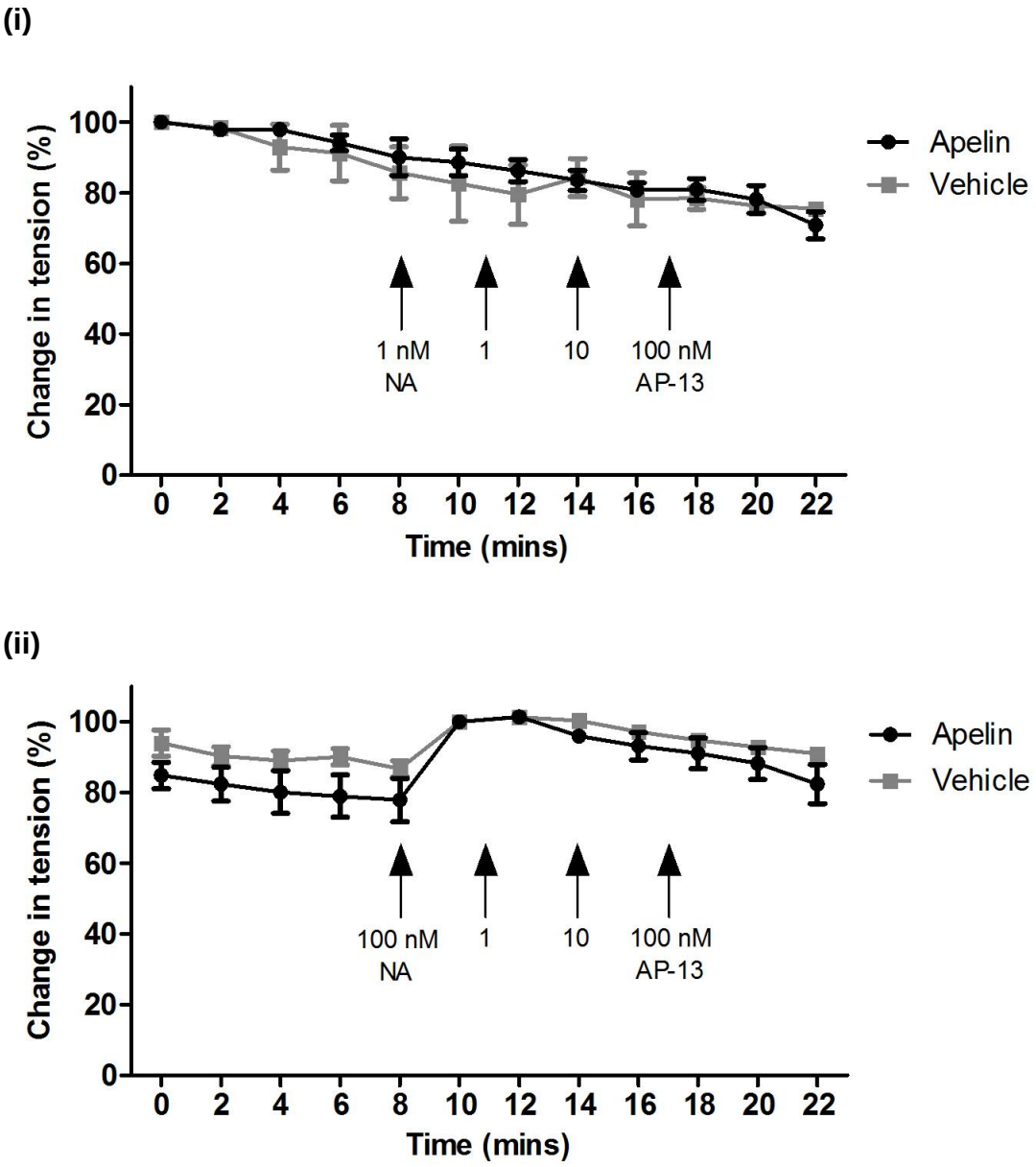

Figure 3.5: Effect of pyr-apelin-13 on RV papillary muscles in the presence of NA 1 nM (i) and NA 100 nM (ii).
(i) *P* = 0.68 two-way ANOVA apelin (n = 4) vs vehicle (n = 3) (ii) *P* = 0.26 two-way ANOVA apelin (n = 5) vs vehicle (n = 3).

Similarly, in the presence of high Ca^{2+} (5 mM) and high ATII (100 nM), pyr-apelin-13 had no effect on the force produced by right ventricular papillary muscles (n = 5 and n = 3, respectively, *P* = 0.41 and *P* = 0.97 two-way ANOVA apelin vs vehicle, respectively; Fig 3.6).

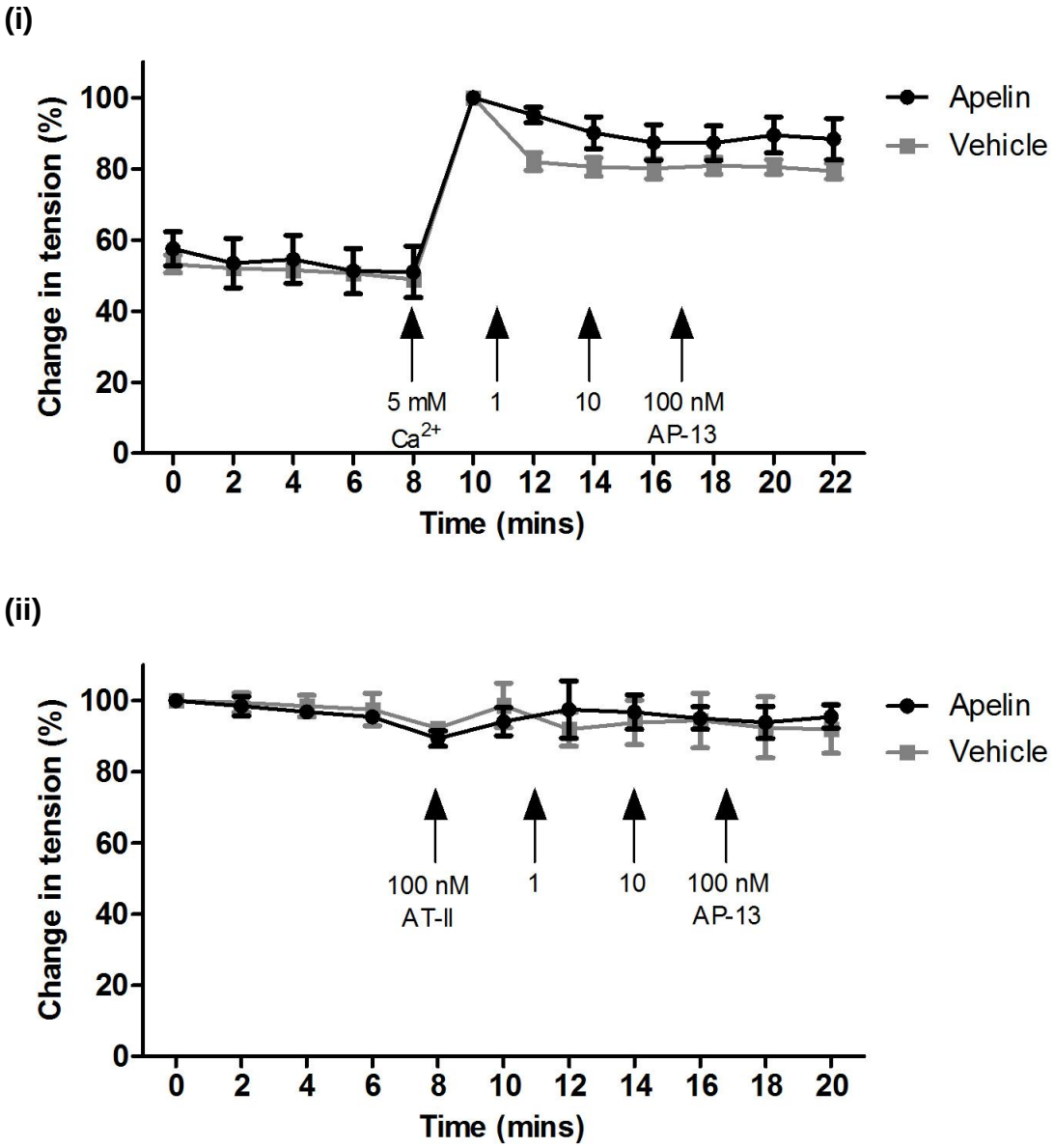

Figure 3.6: Effect of pyr-apelin-13 on RV papillary muscles in the presence of Ca^{2+} 5 mM (i) and ATII 100 nM (ii).
(i) *P* = 0.41 two-way ANOVA apelin (n = 5) vs vehicle (n = 3) (ii) *P* = 0.97 two-way ANOVA apelin (n = 3) vs vehicle (n = 3).

Drop-off in force of both papillary muscle and atrial strip preparations are unavoidable in this experimental set-up. It was found that the amplitude of the force generated in untreated PM preparations decreased by 2.6 ± 0.6 mg per minute across 2h (n = 4). In untreated RA strips, the amplitude of force generated decreased by 0.9 ± 0.3 mg (n = 3). Since all experimental protocols lasted approximately 1h 30 from equilibration of the preparation, we controlled for drop-off by performing time-matched controls for all papillary muscle experimental protocols.

3.3.3 The effect of apelin-16 in the isolated perfused rat heart

In the paced, isolated perfused rat heart, apelin-16 (10 nM) had no effect on any of the measured parameters of cardiac contractility in the 15 minute infusion period (Table 3.1; Fig 3.7).

Time after starting apelin-16 (10 nM) infusion	HR (bpm)	DP (mmHg)	dP/dt max	dP/dt min
-1	322.6 ± 13.4	84.5 ± 12.0	3223.7 ± 664.6	2349.7 ± 371.1
0	322.5 ± 13.4	84.4 ± 12.0	3234.8 ± 661.5	2339.2 ± 354.2
5	322.5 ± 13.4	81.2 ± 14.3	3226.7 ± 763.4	2278.6 ± 390.5
10	322.5 ± 13.4	84.1 ± 15.1	3373.8 ± 808.4	2328.6 ± 391.8
15	323.9 ± 12.8	83.6 ± 14.9	3407.5 ± 774.7	2329.5 ± 401.7
P	0.39	0.81	0.23	0.53

Table 3.1: Effect of apelin-16 on contractility parameters measured in the isolated perfused rat heart.
P value is the result of a repeated measures one-way ANOVA (n = 4).

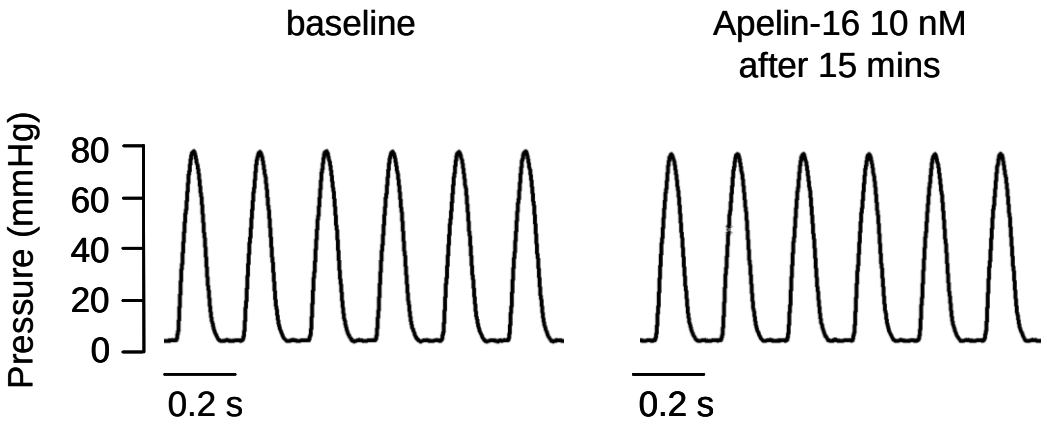

Figure 3.7: Apelin-16 had no effect on intraventricular pressure in the isolated perfused rat heart.
Trace is representative of n = 4.

3.4 Discussion

In these studies, no inotropic effects of apelin peptides were observed in the cardiac tissues of the normal rat. APJ protein is present in RV papillary muscle and RA strip tissue as determined by western blot. This is in agreement with other studies which found the APJ receptor to be widely expressed in rat heart tissue (Katugampola *et al.*, 2001; Kleinz *et al.*, 2005). However, this does not allow us to determine the cellular location of the receptor or whether or not the receptor is active and coupled to its G protein.

Using a widely utilised papillary muscle and atrial strip preparation (Skuladottir *et al.*, 1997; Sviglerova *et al.*, 2005; Wong *et al.*, 2010), we found no inotropic effect of apelin on isolated rat papillary muscles and atrial strips. This is in keeping with the results of Dai *et al*. (2006) who also failed to demonstrate any significant increase in force in response to apelin in normal trabeculae. However, they did observe an increase in force in response to apelin in trabeculae from rats with heart failure induced by chronic hypoxia. This is the only published study assessing the effect of apelin on rat cardiac tissue strips.

Dai *et al.* (2006) used a lower concentration (70 nM) than the highest concentration used in the present study, although they were in the same range. The authors measured force responses 15 minutes after adding apelin, whereas we measured force 3 minutes after each addition in papillary muscles. However, in atrial strip experiments, apelin incubation for 30 minutes had no effect so it is unlikely that the incubation time was a factor in this case, at least in atrial strips.

As there did not appear to be an inotropic effect in isolated papillary muscles and atrial strips, we used an isolated rat heart preparation as described by Langendorff (1895). The technique is used routinely by many groups over a century later (see Skrzypiec-Spring *et al.*, 2007). The isolated, perfused rat heart preparation allows for the study of cardiac contractility, isolated from any whole animal effects, for example nervous system activity. The preparation in the present study also isolated effects on cardiac contractility from the vasoactive effects of apelin as coronary flow was held constant. We used apelin-16 for these experiments as this form of apelin had previously been reported as an inotrope in a Langendorff preparation (Szokodi *et al.*, 2002).

Our intention was to confirm the inotropy of apelin-16 and follow up with a study investigating the potential cardioprotective effects of apelin-16 in an ischaemia-reperfusion model as the cardioprotective effects of apelin-13 and apelin-36 had previously been demonstrated using this model (Simpkin *et al.*, 2007).

However, in our study, we were unable to confirm the inotropic effect of apelin-16. There are several possible reasons for the discrepancy between the current study and that of Szokodi *et al*. (2002). Firstly, the present study used an intraventricular balloon which is a highly sensitive method of measuring cardiac contractions in the isolated heart. Szokodi *et al*. (2002) used a transducer attached to the apex of the heart to demonstrate inotropy. Although they also used an intraventricular balloon for one part of their study, the effect of apelin infusion on developed pressure was not reported. Secondly, the published study reported an increase in dP/dt max when

apelin was infused at diastolic pressures of 10 mmHg and 15 mmHg, but not at a diastolic pressure of 5 mmHg which was the pressure used in the present study. Taken together, these studies suggest that inotropic effects of apelin may only be apparent at higher levels of preload. Experiments with increased preload *in vitro* by increasing diastolic pressure using an intraventricular balloon or *in vivo* by increasing venous blood volume would increase our understanding of the effect of apelin under conditions of increased preload.

The literature demonstrates that apelin has a greater inotropic effect in tissue from heart failure animals (Berry *et al.*, 2004; Dai *et al.*, 2006). Further experiments involving measurement of cardiac contractility following *in vivo* administration of apelin to control rats and rats with heart failure using a pressure-volume catheter and echocardiography would complement the data presented in this thesis.

In summary, although the presence of the APJ receptor protein on the tissues studied is demonstrated here, we were unable to confirm the inotropic response to apelin that has been shown in other published studies.

Chapter 4 The vasoactive effects of apelin

4.1 Introduction

Apelin is synthesised as a prepropeptide of 77 amino acids and is cleaved by unknown endopeptidases to the active apelin isoforms which have reported effects on the vasculature. Apelin molecules with biological activity have been postulated to be degraded by angiotensin converting enzyme-2 (ACE-2) (El Messari *et al.*, 2004), although recent data suggests that treatment of apelin peptides with ACE-2 does not in fact abolish biological activity (Davenport *et al.*, 2009; Davenport *et al.*, 2010).

The first report of a functional effect of apelin on the vasculature was published in 2001 when it was demonstrated that pyr-apelin-13 constricted human saphenous vein in the absence of a functional endothelium (Katugampola *et al.*, 2001). Salcedo *et al*. (2007) reported that human mesenteric arteries with intact endothelium dilated in response to apelin. However, human mesenteric arteries denuded of endothelium did not constrict to apelin in this study. *In vivo,* in healthy volunteers, pyr-apelin-13 and apelin-36 caused nitric oxide dependent vasodilatation in forearm resistance vessels. However, neither peptide had an effect on dorsal hand vein blood flow (Japp *et al.*, 2008).

In rats, the only published study that demonstrates a functional effect of apelin on vasculature *in vitro* is that of Hus-Citharel *et al*. (2008) who report that in juxtamedullary afferent arterioles of the kidney, apelin-17 induces vasodilation in ATII preconstricted vessels (see Table 4.1). Jia *et al*. (2007) reported that apelin caused nitric oxide production and increased L-arginine uptake in cultured rat aortas, but there has been no report of a functional effect of apelin in this tissue. In rat portal

vein, preincubation of vessels with apelin attenuated the vasoconstrictor response to ATII, but apelin had no effect on its own in vessels with intact or removed endothelium (Gurzu *et al.*, 2006).

Vessel	Apelin effect in *in vitro* tissue		Reference
	Rat	Human	
mesenteric artery	not reported	vasodilator, not vasoconstrictor	Salcedo *et al*., 2007
saphenous vein	not reported	vasoconstrictor	Katugampola *et al.*, 2001, Maguire *et al*., 2009
internal mammary artery	not reported	vasodilator and vasoconstrictor	Maguire *et al*., 2009
aorta	not reported	not reported	
kidney arteriole	vasodilator and vasoconstrictor	not reported	Hus-Citharel *et al*., 2008
portal vein	no effect	not reported	Gurzu *et al*., 2006

Table 4.1: Apelin *in vitro* functional studies in rat and human vessels reported in the literature.

Despite the limited number of studies on rat *in vitro* vascular preparations, a number of rodent studies have shown a decrease in mean arterial pressure (MAP) in response to apelin *in vivo*. In anaesthetised rats, intravenous apelin-12 decreased mean arterial pressure (MAP) and HR (Tatemoto *et al.*, 2001). In conscious rats, intravenous apelin-12 decreased MAP and increased HR (Cheng *et al.*, 2003). Conversely, intravenous pyr-apelin-13 increased both MAP and HR in conscious rats (Kagiyama *et al.*, 2005). In the same study, intracerebroventricular pyr-apelin-13 increased both MAP and HR and the effect was more potent at this site than in the periphery. Thus, although the majority of publications assessing MAP in an *in vivo* model report a

decrease in MAP, there is some evidence that suggest the opposite may occur in some settings.

As functional vascular responses to apelin *in vitro* in rats had not been thoroughly investigated, this study aimed to further investigate the vasoactive effects of apelin. As human mesenteric artery reportedly vasodilated in response to apelin (Salcedo *et al.*, 2007), rat mesenteric artery was utilised in the present study as a readily available and previously widely used *in vitro* model for the testing of vasoactive compounds (Gitterman *et al.*, 2000; Meens *et al.*, 2009; Retailleau *et al.*, 2010).

This chapter aimed to use both *in vivo* and *in vitro* techniques to study the vasoactive effects of apelin. The hypothesis investigated in this chapter was that apelin-13 and apelin-36 will vasodilate rat mesenteric resistance vessels with intact endothelium and vasoconstrict rat mesenteric resistance vessels denuded of endothelium *in vitro*. The *in vivo* vasoactive effects of apelin in the rat were also inconsistent throughout the published literature. Therefore, in order to assess if selected apelin isoforms used in this study had activity in an *in vivo* model, we performed a series of experiments in the instrumented, anaesthetised rat. These experiments addressed the hypothesis that apelin-13, pyr-apelin-13 and apelin-16 will decrease MAP, with no change in HR, when administered intravenously.

4.2 Methods

4.2.1 Myography

Following mounting and tensioning of mesenteric vessels as described in section 2.4, each vessel was given three 5 minute exposures to high potassium with a 5 minute washout period between each exposure. This was followed by a phenylephrine (PE) concentration response curve (1 nM – 100 µM) to determine the PE EC_{80} of each vessel. Following washout, this EC_{80} concentration of PE was used to preconstrict the vessels before performing an ACh concentration response curve (1 nM – 100 µM) to assess endothelium dependent relaxation. A single concentration of SNP (10 µM) was added at the end of the ACh curve to determine endothelium independent relaxation. Following a final 20 minute washout period, the relaxant and contractile effect of apelin-13 and apelin-36 (1 – 100 nM) was examined in vessels that were and were not preconstricted with PE, respectively. Apelin-13 was added to third order mesenteric arteries in the presence of captopril (100 µM) which was added to the bath 30 minutes before the addition of apelin. Captopril, an ACE inhibitor, was used to inhibit apelin degradation in the bathing medium as ACE-2 had been postulated to be responsible for apelin degradation at the time when the study was performed (see Japp and Newby *et al.*, 2008). This, however, does not appear to be the case according to the most recent literature (Davenport *et al.*, 2010) and the degradation pathway of apelin is unclear.

The endothelium was said to be intact when, in response to ACh, clear relaxations were observed on the trace and maximal relaxation was greater than 80%. Preconstriction of the vessels before the addition of ACh was 2.28 ± 0.36 mN/mm

(n = 11) and 2.51 ± 0.37 mN/mm (n = 6) in second and third order mesenteric arteries, respectively. Vessels that were stripped of endothelium accidentally were discarded; likewise vessels that were thought to be denuded, but relaxed to ACh were excluded.

Data is expressed as mean response above resting tension ± SEM. Responses of vasoconstricting agents are expressed as mN/mm length of vessel. Responses of vasodilating agents are expressed as percentage relaxation of the preconstriction prior to the addition of the vasodilator.

4.2.2 In vivo blood pressure measurements

Male Wistar rats (300 - 400 g) were anaesthetised and the carotid artery and jugular vein were cannulated by insertion of cannula tubing. Apelin-13, apelin-16 or pyr-apelin-13 (10 nM/kg) was delivered to the jugular vein via the inserted cannula and blood pressure was measured at the carotid artery via a fluid filled transducer attached to the inserted cannula.

4.3 Results

4.3.1 In vitro vascular responses

In order to validate the technique, concentration response curves to PE and ACh were analysed. Second order and third order rat mesenteric arteries with intact endothelium constrict comparably to PE and relax similarly to ACh (Table 4.2; Fig 4.1 and 4.2).

	pD_2	Slope	Max contraction (mN)	Max relaxation (%)	n
Second order					
PE	5.63 ± 0.06	2.35 ± 0.11	3.11 ± 0.37	-	11
ACh	7.51 ± 0.05	-1.42 ± 0.15	-	93.72 ± 2.10	11
Third order					
PE	5.78 ± 0.09	2.02 ± 0.09	3.70 ± 0.52	-	6
ACh	7.48 ± 0.04	-1.64 ± 0.29	-	89.18 ± 2.43	6

Table 4.2: Response of second and third order rat mesenteric arteries with intact endothelium to PE and ACh.

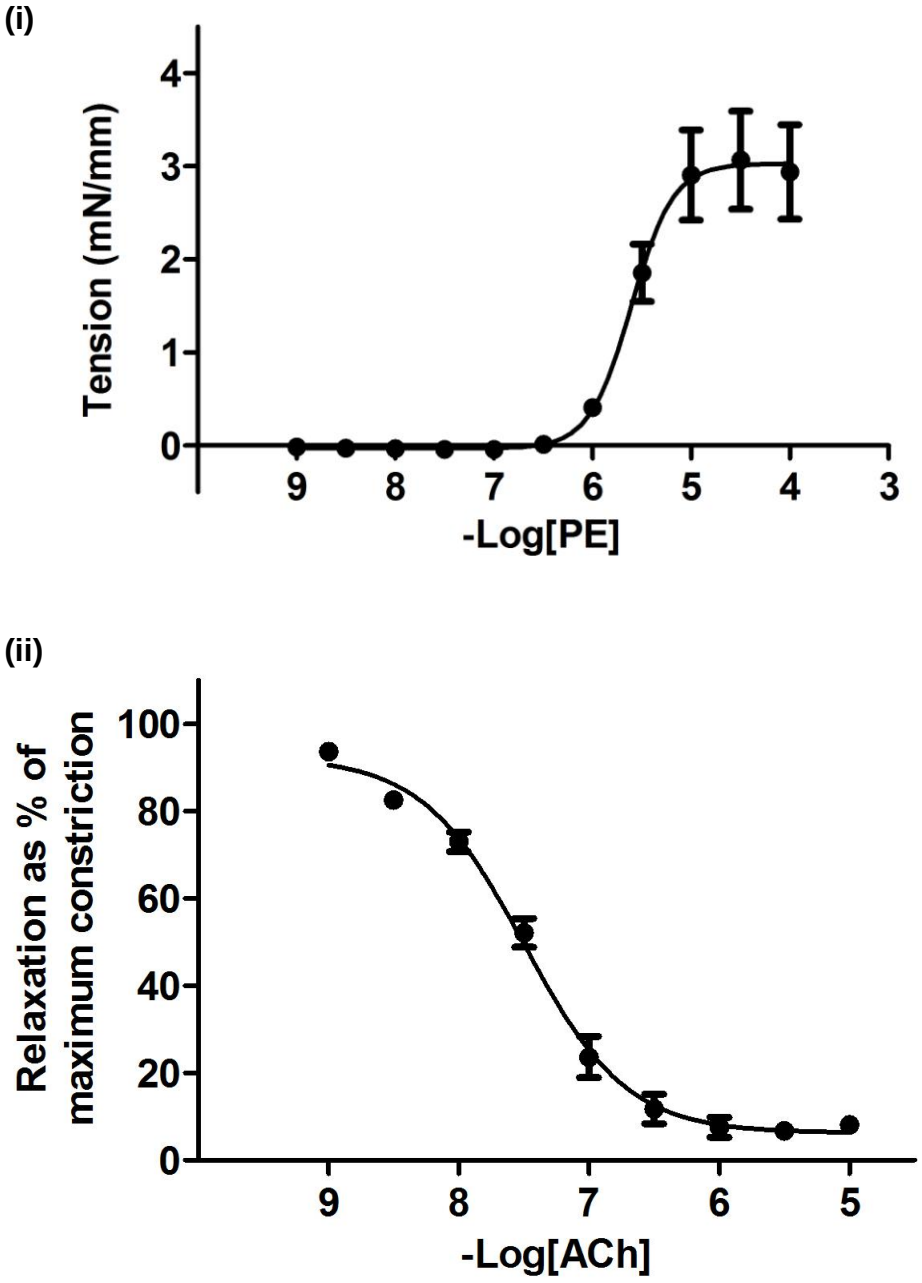

Figure 4.1: Constriction with PE (i) and relaxation of PE preconstricted vessels with ACh (ii) in rat second order mesenteric arteries.
Both n = 11.

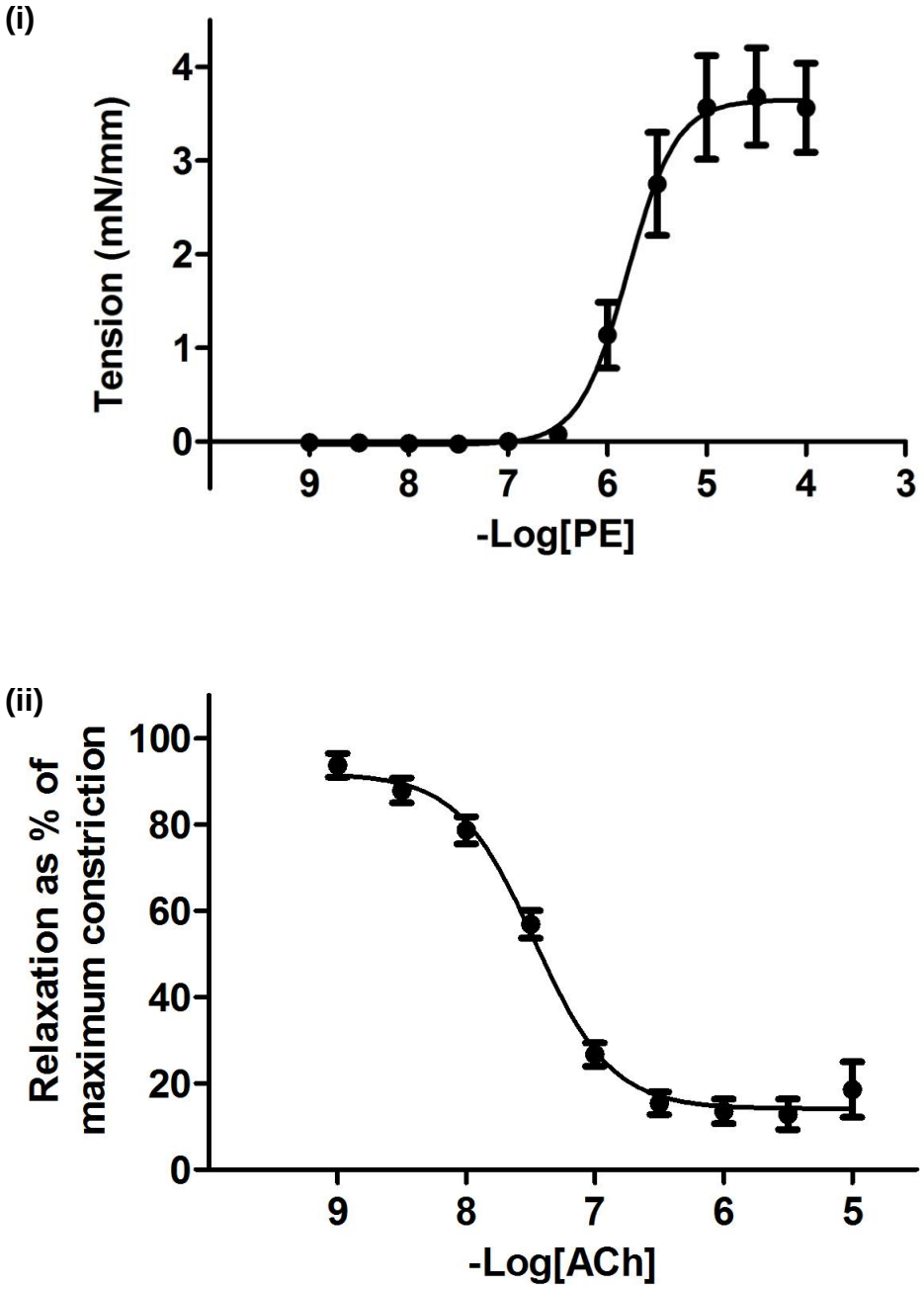

Figure 4.2: Constriction with PE (i) and relaxation of PE preconstricted vessels with ACh (ii) in rat third order mesenteric arteries
Both n = 6.

Apelin-13 and apelin-36 had no effect on rat second order mesenteric arteries; both with (apelin-13, n = 5; apelin-36, n = 3; Fig 4.3) and without endothelium (apelin-13, n = 4; apelin-36, n = 3; Fig 4.3). Both forms of apelin also had no effect on second order mesenteric vessels with intact endothelium that were firstly preconstricted with PE (apelin-13, n = 6; apelin-36, n = 4; Fig 4.3). Likewise, preconstricted vessels denuded of endothelium failed to respond to apelin-13 (n = 4) and apelin-36 (n = 3) (Fig 4.3).

In the presence of captopril (100 µM), apelin-13 had no effect on third order mesenteric arteries with intact endothelium (n = 6) or denuded of endothelium (n = 6). In third order vessels incubated in captopril and preconstricted with PE, apelin-13 had no effect (intact endothelium n = 5, denuded of endothelium n = 4) (Fig 4.3). Prism® was unable to perform successful nonlinear regression on these data sets as there was no concentration-dependent response to any of the apelin isoforms in these experiments.

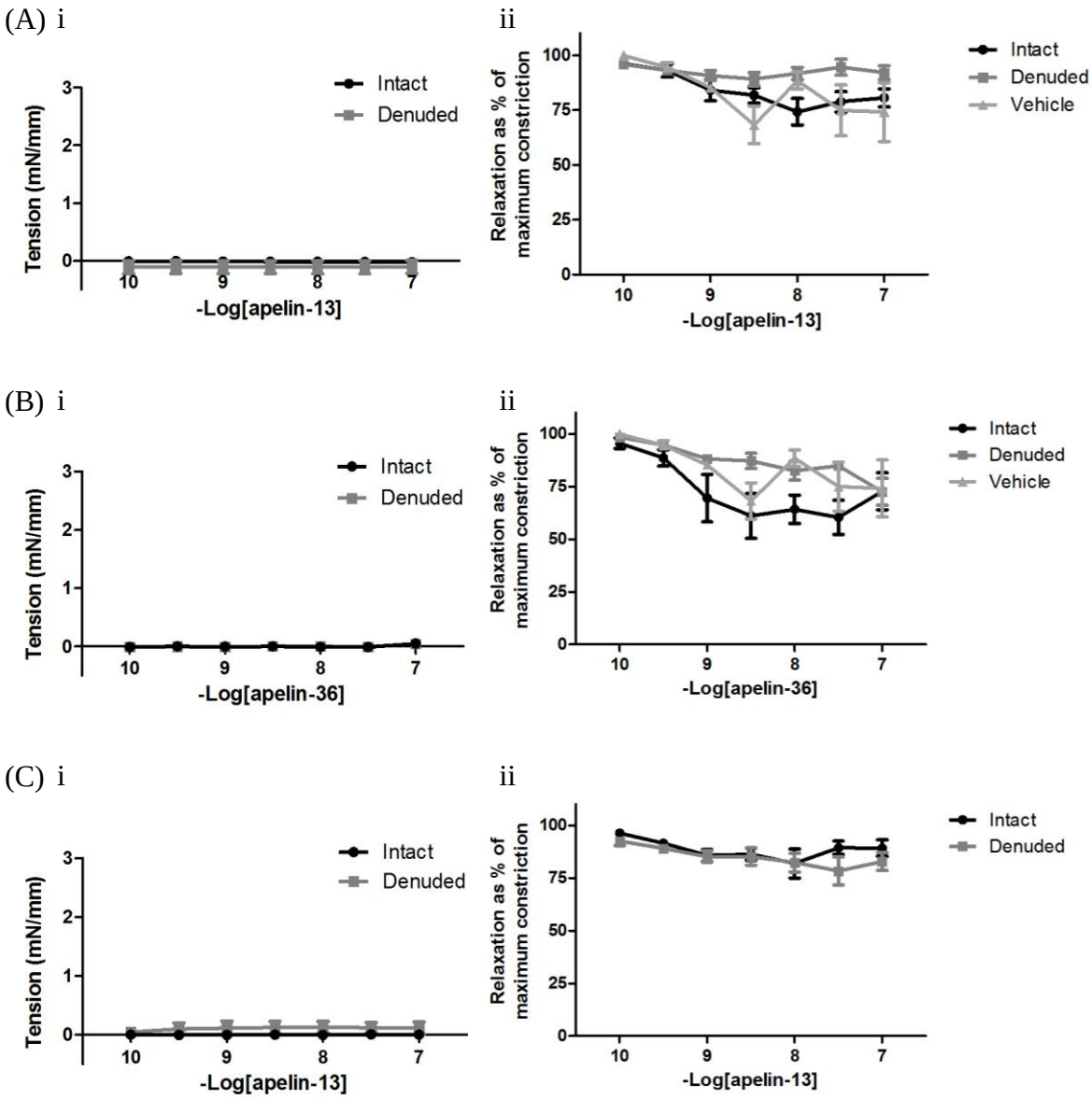

Figure 4.3: Effect of apelin on isolated rat mesenteric arteries.
Effect of apelin-13 (A) and apelin-36 (B) on vessel tone in rat second order mesenteric vessels at resting tension (i) and after constriction with PE (ii) and the effect of apelin-13 (C) in rat third order mesenteric vessels in the presence of captopril at resting tension (i) and after constriction with PE (ii).

4.3.2 In vivo effect on blood pressure and heart rate

In vivo effects of apelin on MAP and HR were examined. Pyr-apelin-13 (n = 5) and apelin-16 (n = 5) (bolus 10 nM/kg) had no effect on MAP (pyr-apelin-13 vs saline $P = 0.10$, apelin-16 vs saline $P = 0.50$ two-way ANOVA) when compared to the effect of administering the same volume of saline in the same animals over 10 minutes (n = 5 per group). Apelin-13 (bolus 10 nmol/kg) produced a maximum decrease in MAP of 22 ± 8 mmHg (apelin-13 vs saline $P = 0.002$ two-way ANOVA; n = 6). This effect was rapid and was observed within 30 s of administering apelin; the maximum decrease was observed after 2 min and recovered towards baseline after 10 minutes, although complete recovery was not observed after 20 minutes (Fig 4.4(i)).

HR was decreased by administration of apelin-13 by 22 ± 17.5 bpm 30 s after addition of apelin ($P = 0.003$ two-way ANOVA). Pyr-apelin-13 had no effect on HR ($P = 0.08$ two-way ANOVA), while apelin-16 decreased HR significantly within 30 s of administration and recovered by 2 min ($P < 0.0001$ two-way ANOVA) (Fig 4.4(ii)).

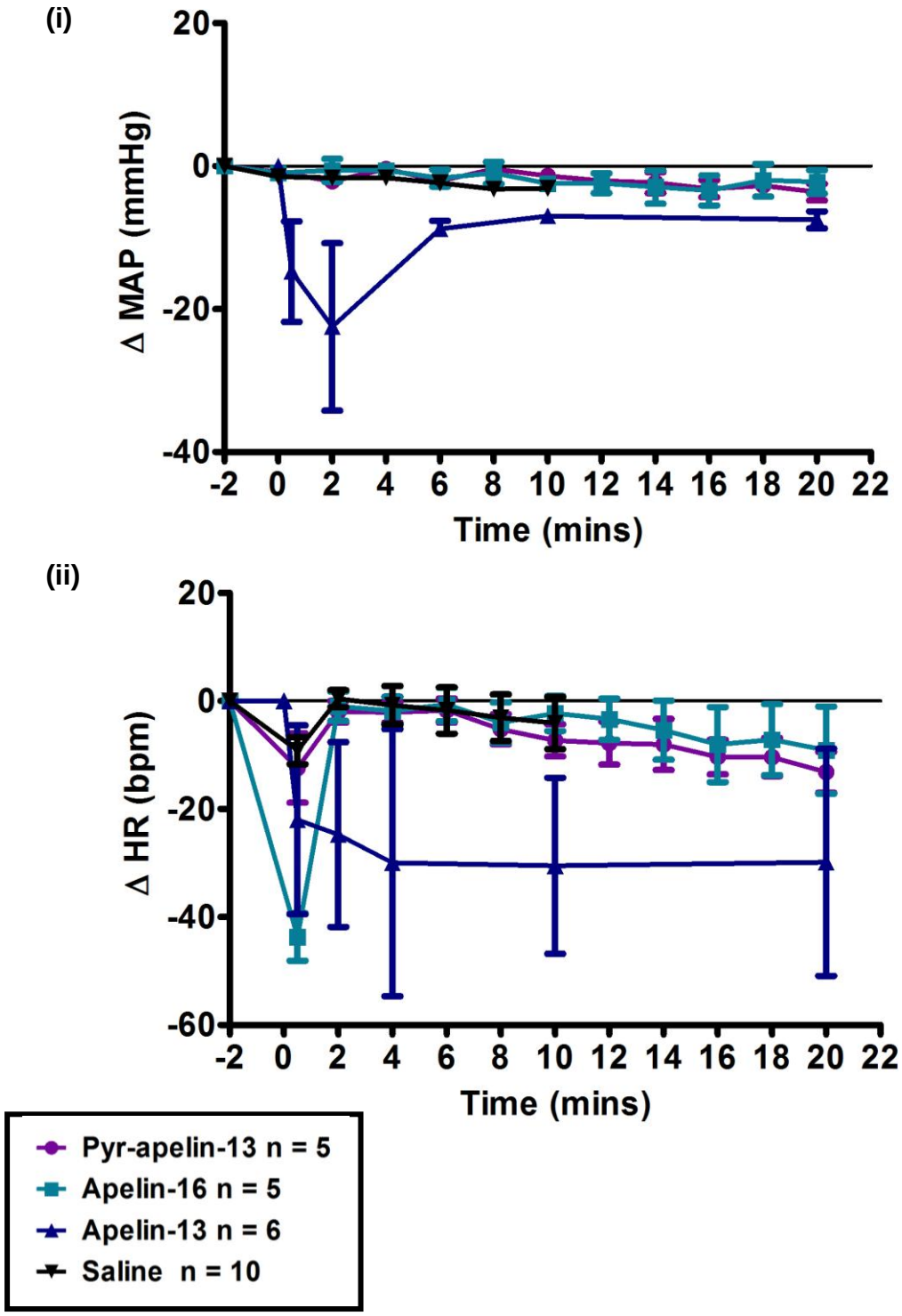

Figure 4.4: The effect of pyr-apelin-13, apelin-16 and apelin-13 on MAP (i) and HR (ii).

(i) P = 0.10 pyr-apelin-13, P = 0.50 apelin-16, P = 0.002 apelin-13 two-way ANOVA, (ii) P = 0.08 pyr-apelin-13, P < 0.0001 apelin-16, P = 0.003 apelin-13 two-way ANOVA

4.4 Discussion

4.4.1 In vitro vessel responses

In isolated rat mesenteric resistance arteries, apelin-13 and apelin-36 did not produce a vasodilatory response in the current study. *In vitro* in the rat, there are only two reports in the literature of the vasoactive effects of apelin and of these reports only in the arterioles of the kidney has apelin been shown to have a consistent vasodilatory effect (Hus-Citharel *et al*., 2008). This result suggests a species difference in the effect of apelin in the mesenteric vascular bed as human mesenteric arteries with intact endothelium vasodilate in response to apelin (Salcedo *et al.*, 2007). Our results, together with the existing limited published data in these preparations, suggest that there may be several vessel beds in the rat that do not respond to apelin. Although rat aortic smooth muscle cells have been shown to produce nitric oxide following stimulation with apelin, a functional effect has not been demonstrated. Indeed previous work in our own laboratory using fixed mount myography found no effect on treatment with apelin in rat aortas (Emery, Japp and Gray, unpublished data).

In the present study, apelin-13 and apelin-36 had no vasoconstrictor effect in rat mesenteric arteries denuded of endothelium. In contrast to the species difference observed when studying the potential vasodilatory effects of apelin, this was in agreement with the human mesenteric artery study by Salcedo *et al*. (2007).

4.4.2 In vivo blood pressure measurements

Apelin-13, apelin-16 and pyr-apelin-13 were administered to anaesthetised rats via the jugular vein and blood pressure measured via the carotid artery. Apelin-13 produced a decrease in MAP as demonstrated by Tatemoto *et al*. (2001). However, the decrease in MAP measured in the current study was larger and more variable (28 ± 11 mmHg) than that of Tatemoto *et al*. (2001) (11 ± 4 mmHg). Apelin-13 also lowered HR. Apelin-16 did not alter MAP compared to a bolus of saline in the same animals, but did produce a significant transient decrease in HR which recovered 2 minutes after the bolus was administered. No effect of apelin-16 on MAP or HR has been previously reported. Neither a decrease in MAP nor HR was observed following intravenous administration of pyr-apelin-13 in these experiments which is in contrast to the work of Ishida *et al*. (2004) who observed a decrease in MAP in response to pyr-apelin-13.

Surprisingly, administration of apelin-13 *in vivo* decreased heart rate and MAP, while apelin-16 depressed only heart rate. A decrease in MAP is usually associated with reflex tachycardia mediated via baroreceptors (Noll et al., 1997). Therefore, the observation that apelin-13 decreases both heart rate and MAP, suggests that these two effects are mediated via different mechanisms. A decrease in MAP in response to apelin-13 has been previously reported *in vivo* (Tatemoto *et al.*, 2001). Interestingly, I noted that the majority of publications describing a vasoactive effect of apelin used apelin-13. Furthermore, the majority of publications describing an inotropic effect of apelin used apelin-16. No publication has compared apelin-13 and apelin-16 in a model assessing vasoactivity, yet the *in vivo* experiments presented in

this thesis demonstrate that different apelin isoforms may have different physiological effects. Since the twelve C-terminal amino acids have been shown to be responsible for the activity of the apelin peptide (De Mota *et al.*, 2000; Reaux *et al.*, 2001), it is unlikely that the activity of two different apelin isoforms on the same receptor in the same tissue produces a different effect. However, different effects may be elicited in different tissues by the same ligand and receptor if the receptor is coupled to different signal transduction pathways eg. G_i in one tissue and G_q in another. The APJ receptor may also be expressed more highly in one tissue than in another which could be studied by qPCR or histology with an APJ antibody. It is also possible that the apelin receptor may have different receptor subtypes (as in zebrafish), although to date there is no data to suggest this (Pitkin *et al.*, 2010).

The decrease in MAP has been previously reported to be nitric oxide dependent (Tatemoto et al., 2000). Therefore, if the decrease in MAP and decrease in heart rate are two unrelated effects, I hypothesise that in the presence of L-NAME, the decrease in blood pressure would be abolished, but the decrease in heart rate would be observed. It is also possible that the heart rate effect may be centrally mediated, while the decrease in MAP may be a local effect. To test this hypothesis, vagal tone could be inhibited with atropine. In the presence of atropine, if mean arterial pressure decreases in response to apelin, but heart rate does not, we conclude that the change in heart rate is a central effect of the apelin peptide. Secondly, the femoral artery could be isolated *in vivo* to eliminate central effects and apelin applied to the artery, an experimental model previously reported by Zhang *et al.* (2010) in a mouse model.

This experiment would confirm that the decrease in mean arterial pressure is a local effect and is not mediated centrally.

The vasoactive effect of apelin *in vivo* in rats remains a subject of debate in the literature. In conscious rats, an increase in MAP was observed following both IV injection and intracerebroventricular (ICV) injection of apelin (Kagiyama *et al*., 2004), inferring a direct action on central cardiovascular autonomic centres. Indeed, apelin has been reported to cross the blood-brain barrier (Higuchi *et al.*, 2007). Although these publications are small in number, equal numbers report an increase in HR as report no change in HR. These studies are summarised in Table 4.3.

Model	**Administered**	**Measured**	**Effect**	**Reference**
anaesthetised rat (inactin)	femoral vein, bolus apelin-13	common carotid artery	decrease in MAP (≈ 10 mmHg), slight increase in HR	Lee *et al*., 2000
anaesthetised rat (pentobarbital)	femoral vein, bolus, 10 nM/kg apelin-12, apelin-13, apelin-36	femoral artery	decrease in MAP (11 mmHg), no change in HR	Tatemoto *et al*., 2001
conscious rat (halothane for insertion of cannulae)	iliac vein and jugular vein, bolus, 10, 20 and 40 nM/kg apelin-12	left iliac artery	decrease in MAP at 20 and 40 nM/kg, increase in HR	Cheng *et al*., 2003
conscious rat (pentobarbital for insertion of cannulae)	femoral vein or ICV, 5-50 nmol/rat pyr-apelin-13	femoral artery	ICV and IV apelin increase MAP (20 mmHg) and HR	Kagiyama *et al.*, 2004
anaesthetised rat (pentobarbital)	right femoral vein, bolus 10 nM/kg pyr-apelin-13	right femoral artery	decrease in MAP (≈ 8 mmHg), no change in HR	Ishida *et al*., 2004

Table 4.3: Summary of apelin vasoactive studies *in vivo* in the rat.

4.4.3 Conclusion

In the published literature, there is variation of *in vivo* rat vasoactive effects described in response to apelin and only one paper demonstrating a vasoactive effect *in vitro* in isolated vessels from the rat. The use of several different models and different apelin isoforms in these vasoactive studies makes comparison of the published work difficult. In addition, the surprisingly small body of published literature in comparison to that of other reportedly vasoactive peptides, such as endothelin-1, point to a well described publication bias (Callaham *et al.*, 1998; Timmer *et al.*, 2002; Young *et al.*, 2008) (discussed further in chapter 7). We conclude that the small number of publications in this area is indicative of the challenges of working with this peptide.

Chapter 5 The apelin system in the zebrafish embryo and zebrafish adult heart

5.1 Introduction

5.1.3 The Apelin/APJ system in the zebrafish

The apelin/APJ system is present in the zebrafish. However, unlike in mammals, there are two forms of the apelin receptor in zebrafish: angiotensin receptor-like 1a (agtrl1a) and angiotensin receptor-like 1b (agtrl1b). There is significant sequence homology both in the apelin peptide and the apelin receptor, respectively, when comparing the zebrafish amino acid sequence with that of mammalian organisms (Figs 5.3 and 5.4). It is important to note that pyr-apelin-13 was used in all zebrafish experiments which is the thirteen amino acids at the C-terminal end of the apelin sequence. As shown in Fig 5.3, the last twelve amino acids are identical to that of mammalian species and it is these twelve amino acids that are important for the biological activity of the peptide (De Mota *et al.*, 2000; Reaux *et al.*, 2001).

Although it is known to be present, little is known about the functional role of the apelin system in the zebrafish. In fact there are only 4 original research publications (see below) involving apelin and zebrafish embryos in the PubMed database (September 2010).

```
HUMAN              LVQPRGSRNGPGPWQGGRRKFRRQRPRLSHKGPMPF
RAT                LVKPRTSRTGPGAWQGGRRKFRRQRPRLSHKGPMPF
MOUSE              LVKPRTSRTGPGAWQGGRRKFRRQRPRLSHKGPMPF
BOVINE           1 LVQPRGPRSGPGPWQGGRRKFRRQRPRLSHKGPMPF 36
ZEBRAFISH          PLRQNPARAGRSQRPAGWRR-RRPRPRLSHKGPMPF
Xenopus laevis     LVNPKMVRNSAPQRQANRRKLIRQRPRLSHKGPMPF
                         *          *    * ***********
```

Figure 5.1: Apelin peptide sequence for human, rat, mouse, bovine, zebrafish and xenopus apelin-36.
* identical amino acids, residues that differ from the human sequence are highlighted in red. Figure from Pitkin *et al*. (2010).

The amino acids of the human APJ receptor thought to be responsible for ligand binding are aspartate residues at positions 184 and 282, phenylalanine residues at positions 125, 210 and 257, and tryptamine residues at positions 154 and 261 (Iturrioz *et al.*, 2009). All are conserved in the zebrafish agtrl1a receptor with the exception of the aspartate residue at position 282 and all are conserved in the zebrafish agtrl1b receptor with the exception of the phenylalanine residue at position 125 and the aspartate residue at position 282. Therefore, it is likely that the mammalian apelin used in this study will bind to the zebrafish apelin receptors.

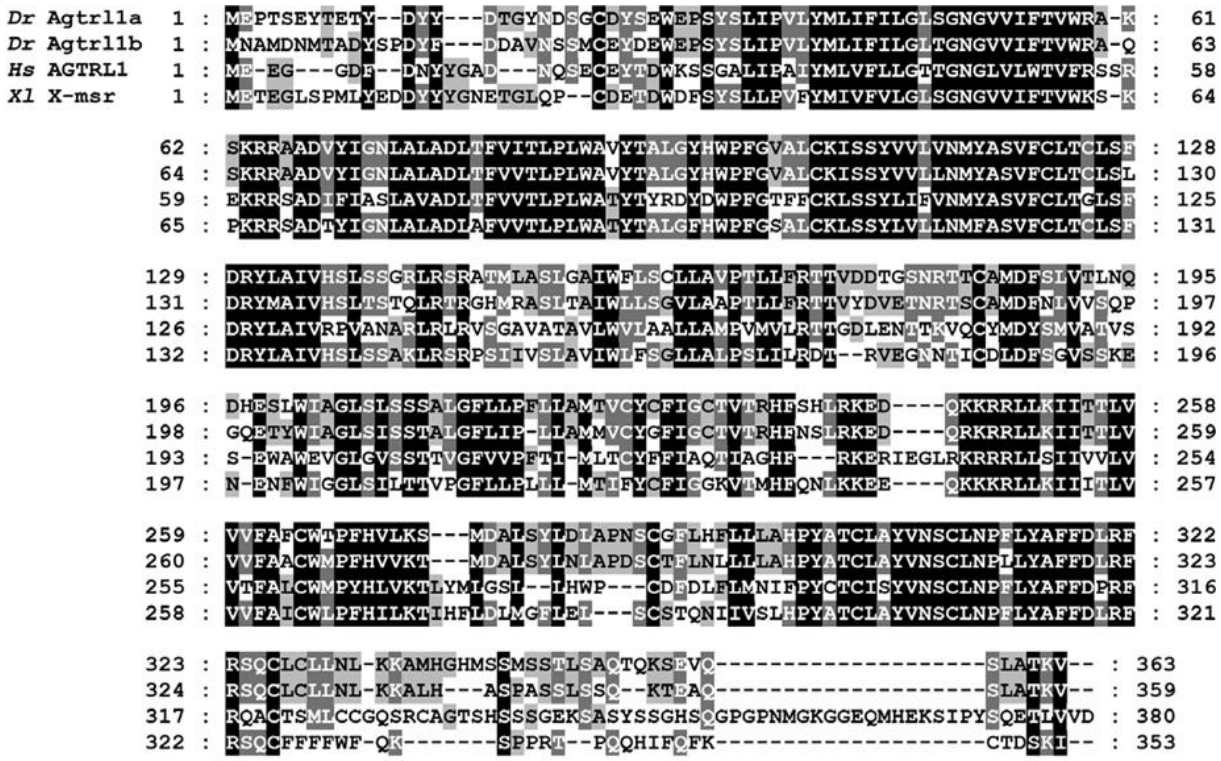

Figure 5.2: Amino acid sequence of the apelin receptor orthologues, agtrl1a (Dr Agtrl1a) and agtrl1b (Dr Agtrl1b), in the zebrafish, and the human (Hs AGTRL1) and xenopus (Xl X-msr) sequences.
Conserved residues in all four species are highlighted in black; those conserved in three of these four species are highlighted in dark grey (white lettering); those conserved in two of four species are highlighted in light grey (black lettering). Figure from Tucker *et al*. (2007).

5.1.4 Genetic manipulation of apelin and its receptors in zebrafish embryos

5.1.4.1 Apelin

Overexpression of apelin by injection of apelin RNA into embryos results in a delay in epiboly, lack of extension of the anteroposterior axis and no visible beating heart at 2 dpf (Zeng *et al.*, 2007). Overexpression of apelin also resulted in a reduction in cardiac myosin light chain 2 expression and no cardiac differentiation in work by another group (Scott *et al.*, 2007). Knockdown of apelin using both translation blocking and splice site blocking morpholinos resulted in a reduction in the size of the region expressing cardiac myosin light chain 2 and ventricular myosin heavy chain cardiac markers at 17 hpf (Zeng *et al.*, 2007), suggesting that a balance of apelin levels is necessary during development for normal expression of cardiac markers. Despite the reduction in cardiac markers, the structure of the heart was grossly normal at 24 hpf and, surprisingly, the paper does not report any observations beyond this time point.

5.1.4.2 Agtrl1a receptor

Knockdown of agtrl1a using three non-overlapping translation blocking morpholinos results in delayed development in zebrafish embryos (Nornes *et al.*, 2009). Nornes *et al*. (2009) demonstrate that agtrl1a knockdown delays epiboly, as reported in apelin knockdown experiments by Zeng *et al.* (2007). The agtrl1a knockdown phenotype can be rescued by injection of agtrl1a RNA at the 32-cell stage, although not when injected with the morpholino at the single cell stage (Nornes *et al.*, 2009).

5.1.4.3 Agtrl1b receptor

Overexpression of agtrl1b by injection of agtrl1b RNA into one-cell stage zebrafish embryos results in an uneven surface between the blastoderm and yolk cell in contrast to the smooth surface observed in control embryos. However, the agtrl1b RNA injected embryos do develop normally despite this, although in some cases exhibited a shorter body length than controls at 24 hpf (Zeng *et al.*, 2007). Knockdown of agtrl1b using a translation blocking morpholino results in absence of a beating heart at 2 dpf in 93% of injected embryos. Co-injection with agtrl1b RNA, lacking the morpholino binding site, partially rescued this phenotype as 54% of embryos in this group did have a beating heart at 2 dpf. However, in those with a beating heart, the heart appeared to be of reduced size (Zeng *et al.*, 2007). The authors reason that their experiments demonstrate only partial rescue of the agtrl1b knockdown phenotype as both overexpression and knockdown of agtrl1b influence normal development.

Scott *et al*. (2007) identified a single mutation in zebrafish *agtrl1b* which results in hearts of reduced size, and in the most severe cases of the mutation few or no cardiac myosin light chain-positive cardiomyocytes. This mutation, known as grinch, appears to be specific to the heart, as development of the grinch mutants is otherwise no different to that of wild-type embryos. However, severe grinch mutants survive only until 7 dpf.

Manipulation of apelin and its receptors have severe developmental consequences in zebrafish embryos which are summarised in Table 5.1. In particular, overexpression of apelin or knockdown of agtrl1b results in the loss of a beating heart (Zeng *et al.*, 2007). However, in knockout mouse models, apelin knockout and APJ knockout do not appear to have severe developmental consequences. There are some physiological consequences in adult mice, including the development of heart failure in aged apelin knockout mice (Kuba *et al.*, 2007) (discussed in section 1.2.3).

	Overexpression	**Knockdown**
Apelin	reduction in cardiac markers no beating heart delay in epiboly	reduction in cardiac markers grossly normal heart at 24 hpf
Agtrl1a	not reported	delay in epiboly
Agtrl1b	uneven blastoderm/yolk cell surface	no beating heart

Table 5.1: Summary of reported effects of overexpression and knockdown of apelin, agtrl1a and agtrl1b in zebrafish embryos.
Data from Nornes et al. (2009), Scott et al. (2007) and Zeng et al. (2007).

5.1.5 Aims of this chapter

This chapter investigates the apelin system in the zebrafish and the specific aims were:

i. to determine the abundance of apelin, agtrl1a and agtrl1b mRNA transcripts during the first 5 days of development

ii. to demonstrate whether or not apelin, agtrl1a and agtrl1b mRNA are present in the adult zebrafish heart

ii. to study the effect of exogenous apelin on heart function of zebrafish embryos *in vivo* and on isolated zebrafish embryonic hearts

iii. to investigate mRNA knockdown of the apelin system using a morpholino targeted to apelin preRNA

5.2 Methods

5.2.1 qPCR

qPCR was carried out as described in section 2.7.2.4. RNA was extracted from whole zebrafish embryos (12 – 15 embryos per stage) at each of the following developmental stages (8, 18, 24, 36, 48, 72, 96 and 120 hpf) and transcribed to cDNA. Apelin, agtrl1a and agtrl1b assays were performed in addition to assays for the reference genes, elongation factor 1 alpha (EF1a) and ribosomal subunit L13A (RPL13a) (see Table 5.2). EF1a and RPL13a mRNA expression did not change across the developmental stages (EF1a $P = 0.06$ one-way ANOVA; RPL13a $P = 0.43$ one-way ANOVA; n = 2 (12 – 15 embryos per stage per experiment)). Apelin, agtrl1a and agtrl1b mRNA were corrected for the mean of reference genes, EF1a and RPL13a, and expressed as a percentage of abundance at 8 hpf.

Target gene	Accession number	UPL Probe number	Primer sequences (5' – 3')	Product size (bp)
Apelin	NM_001166124	19	F:ACTCCTTTGCGGCAGAATC R:GGAGGGCACTCTAAGCTGTG	138
Agtrl1a	NM_001075105.1	49	F:CTCAGAAGTCAGAGGTGCAGTC R:CCCAGAGTTTTGTCCTCATGT	78
Agtrl1b	NM_001030197.1	24	F:AAAAAGCTCTTCACGCCAGT R:ACTGGGCCTCGGTCTTCT	60
EF1a	NM_131263.1	67	F: CCTTCGTCCCAATTTCAGG R: CCTTGAACCAGCCCATGTT	72
RPL13a	NM_212784.1	3	F: TCCCGTGGATCATATCACTTC R: GGTTTTGTGTGGAAGCATACC	78

Table 5.2: UPL probes and primer sequences for RT qPCR in the zebrafish.

5.2.2 PCR to detect the presence or absence of mRNA of interest

PCR to detect apelin, agtrl1a and agtrl1b was performed on zebrafish adult hearts (n = 3, 3 hearts per group) as described in section 2.7.2.3, using primer sequences from Table 5.3.

Target gene	NCBI accession number	Primer sequences (5' – 3')	Product size (bp)
Apelin	NM_001166124	F:CTAGCGACTGGCAGGGAAAC R:GGAGGGCACTCTAAGCTGTG	297
Agtrl1a	NM_001075105.1	F:CGGAATACACCGAGACATACG R:CGAGGTAGCGGTCAAAACTC	384
Agtrl1b	NM_001030197.1	F:GCCCAGATTACTTCGACGAT R:AGCAGGAGGTTCAGGAAGGT	850
GAPDH	NM_001115114	F:GTCTGGTGACCCGTGCTGCT R:GTTTGCCGCCTTCTGCCTTAAC	153

Table 5.3: Primer sequences for RT-PCR in the zebrafish.

5.2.3 Video edge detection

5.2.3.1 Embedded zebrafish embryos 3 dpf

Zebrafish embryos 3 dpf were embedded in agar as described (section 2.6.1). An Axioskop II MOT compound microscope with a x 40 water dipper objective lens was used to visualise the hearts of the embryos and video edge detection was carried out as described in section 2.6.1. Zebrafish were incubated in pyr-apelin-13 (150 nM) for 1h. In apelin incubated embryos, measurements of ventricle wall motion were made at baseline and at 15 minute intervals thereafter. In vehicle incubated embryos, measurements were made at baseline and after 1h incubation. Contraction velocity,

relaxation velocity, wall motion amplitude and heart rate were expressed as a percentage of the measurement at baseline in each group.

5.2.3.2 Zebrafish isolated embryonic hearts 3 dpf and 4 dpf

Zebrafish hearts were isolated as described in section 2.6.1.2. Briefly, zebrafish were anaesthetised before being placed into HEPES buffer containing BSA. Their hearts were isolated mechanically using one pair of forceps to hold the tail of the embryo and the other to detach the heart by quickly and carefully freeing it from the surrounding tissue. Hearts were then placed in a well in a prepared agar mould and HEPES buffer (without BSA). Video edge detection, as described above, was used to measure the following parameters of isolated embryonic heart function: contraction velocity, relaxation velocity, wall motion amplitude and heart rate.

Protocol

The baseline bathing calcium concentration in these experiments was 2.5 mM. In isolated embryonic hearts from zebrafish 3 dpf, calcium 3.5 mM, 4.5 mM, 5.5 mM and 6.5 mM was added cumulatively at 2 minute intervals. In isolated embryonic hearts from zebrafish 3 dpf and 4 dpf, apelin 50 nM, 100 nM and 150 nM was added cumulatively at 3 minute intervals. At the end of each apelin experiment, calcium 5.5 mM was added to each preparation.

5.2.4 Morpholino (MO)

5.2.4.1 Design of a morpholino targeting apelin

A morpholino targeted to apelin preRNA was designed and synthesised by GeneTools (5' – ATTGTGCTGGAATGTCAAACTGACC-carboxyfluorescein - 3'). In order to determine that the sequence of the morpholino was specifically targeting apelin, the sequence was checked against the zebrafish genome using BLAST (http://blast.ncbi.nlm.nih.gov/Blast.cgi) and UCSC genome browser (http://genome.ucsc.edu/). Figure 5.5 shows schematically that the morpholino binds at the exon 2/intron 2 junction. A five mispair control was also designed and synthesised by GeneTools for our experiment (5' – ATTGTCCTGCAATCTGAAACTCACC-carboxyfluorescein - 3'; mispairs underlined). The carboxyfluorescein added to the 3' end of both morpholinos allowed us to determine whether or not successful uptake of the morpholino had occurred.

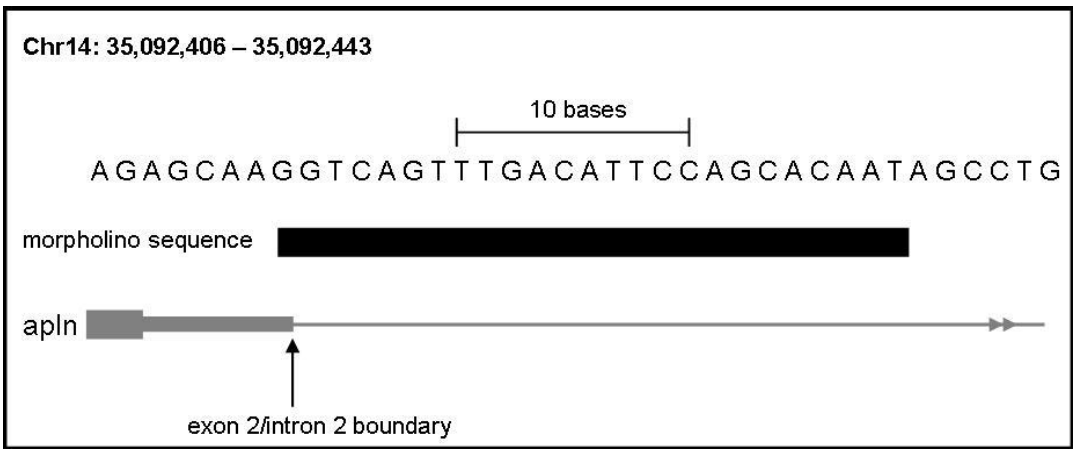

Figure 5.3: Morpholino targeting apelin.
Morpholino targeting apelin is shown schematically binding to the exon/intron boundary of exon 2/intron 2 in the apelin gene sequence. Reverse complementary sequence of the morpholino is shown in diagram (5' – GGTCAGTTTGACATTCCAGCACAAT – 3'); Morpholino sequence is 5' – ATTGTGCTGGAATGTCAAACTGACC – 3'.

5.2.4.2 Determining the optimal injection quantity of the apelin morpholino

The first step in our experimental design was to determine a suitable dose at which to inject our morpholinos. In preliminary experiments, the morpholino targeting apelin (MO-apelin) and its mispair control (MO-mispair) were injected using a 0.1 mm diameter bolus of 1 mM, 0.5 mM, 0.25 mM and 0.125 mM.

To determine the size of the bolus administered, each morpholino was injected into a pool of mineral oil on a graticule (Fig 5.6). The radius of the bolus was determined and, making the assumption that the bolus in the oil is spherical, the volume (V) injected could be calculated. For these experiments, where the radius is 0.05 mm:

$$V = \frac{4}{3} \pi r^3$$

$$V = \frac{4}{3} \pi r^3$$

$$V = 0.0005 \text{ mm}^3$$

$$V = 0.5 \text{ nl}$$

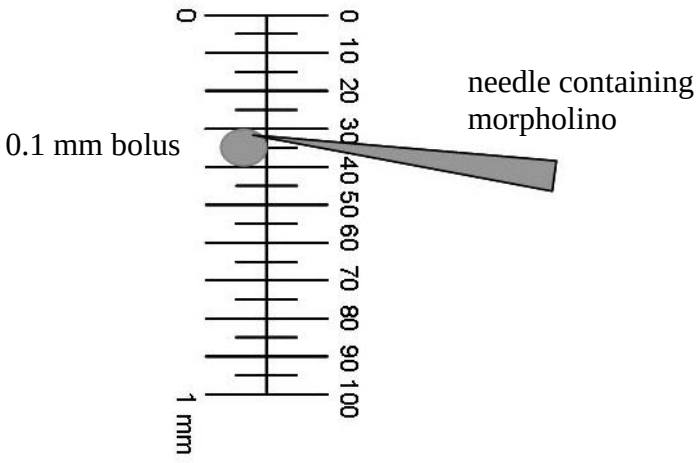

Figure 5.4: Calculation of bolus size in morpholino experiments.
Diagram shows that morpholino bolus is injected into mineral oil on a graticule before each experiment to determine bolus size.

The molecular weights of MO-apelin and MO-mispair are 8972 and 8852 respectively. This means that injecting 1 nl of 1 mM stock morpholino would result in 8.9 ng of morpholino being injected into the cytoplasmic streaming area of each embryo.

5.2.4.3 Morpholino microinjection in 1 - 4 cell zebrafish embryos

Morpholino injections were performed as described in section 2.6.4.2. MO-apelin was injected undiluted (1 mM) and diluted 0.5 mM, 0.25 mM and 0.125 mM in preliminary experiments. As calculated above, 0.5 nl was injected in these experiments, resulting in each embryo receiving 4.5 ng, 2.3 ng, 1.1 ng and 0.6 ng depending on the dilution injected.

As a result of these preliminary experiments, we went on to perform the experiment injecting 1.1 ng/embryo in three independent experiments. In all experiments the injected embryos were treated in the same way. Non-injected controls, embryos injected with the morpholino targeted to apelin (MO-apelin) and the mispair morpholino control (MO-mispair) were kept in three separate petri dishes. Three hours post injection, embryos damaged by injection were removed from each experimental group as well as any abnormally developing embryos in the non-injected control group. Non-fluorescing embryos (indicating unsuccessful uptake of the morpholino) were removed from both MO-apelin and MO-mispair groups. This accounted for a small proportion of all injected embryos and these embryos are not included in any subsequent analysis.

Embryos were then observed under light microscopy (x 40) for gross anatomical and specific cardiac phenotypes. A gross structural phenotype score was used (see Table 5.3). The six features were included in this score were head size, body axis, heart rate (HR), presence/absence of blood in heart, presence/absence of blood pooling and tail circulation. Normal embryos were described as having a head size similar to that described by Kimmel et al. (1995), a straight body axis, a HR of around 150 bpm, blood clearly present in the heart, no blood pooling and normal tail circulation (determined subjectively using non-injected zebrafish embryos as a control). The number of assessed normal characteristics for each embryo was counted and the embryos were classified as detailed in Table 5.4. This classification was performed each day until the embryos reached 5 dpf.

Number of normal characteristics	**6**	**4-5**	**2-3**	**1**	**0**
Phenotypic score	**6**	**4.5**	**2.5**	**1**	**-**
Phenotype	**Normal**	**Mild**	**Moderate**	**Severe**	**Dead**

Table 5.4: Characterisation of morpholino phenotype.
Zebrafish were classified according to the number of normal characteristics following morpholino injection. Normal characteristics used for the classification were normal head size, straight body axis, normal HR, blood present in the heart, no blood pooling and normal tail circulation (further details in text).

5.2.4.4 Calculation of ejection fraction of MO-apelin embryos

In a single experiment, 10 embryos were selected 3h post injection from the MO-apelin, MO-mispair and non-injected control embryos. The selection criteria was simply that the embryos were of grossly normal appearance for this developmental timepoint according to Kimmel *et al*. (1995) and that fluorescence indicating successful uptake of the morpholino was observed. The groups of embryos were placed (1 fish per well) in a twelve well plate. Ejection fraction was measured in 6 fish per group (unless death occurred) at 2 dpf, 3 dpf and 4 dpf as described in section 2.6.2.

5.3 Results

5.3.1 The abundance of apelin, agtrl1a and agtrl1b mRNA transcripts during development

Quantitative PCR revealed differences in the abundance of mRNA transcripts of apelin and its receptors, agtrl1a and agtrl1b, during development in the zebrafish embryo. Apelin mRNA abundance was lowest at 8 hpf and increased steadily from 18 hpf, reaching a peak at 48 hpf. Apelin mRNA expression then decreased until 96 hpf, but reached its largest expression level at 120 hpf (5 dpf) (Fig 5.7).

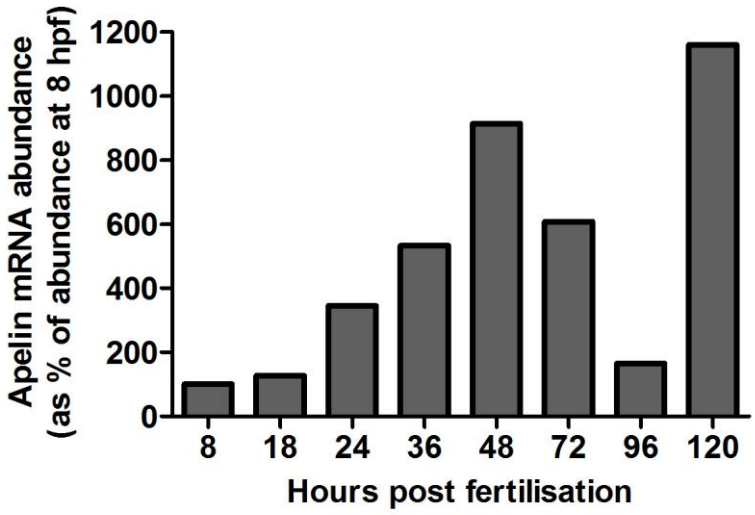

Figure 5.5: The abundance of apelin mRNA in zebrafish embryos during development from 8 hpf to 120 hpf.
Abundance of mRNA measured by qPCR (corrected for EF1a and RPL13a as reference genes and expressed as a percentage of abundance at 8 hpf; n = 2 (12-15 embryos per timepoint per experiment).

The expression of both apelin receptors was highest at 8 hpf and reduced by 16 hpf. Agtrl1a and agtrl1b expression was maintained at a comparably low level until 120 hpf (Figs 5.8 and 5.9).

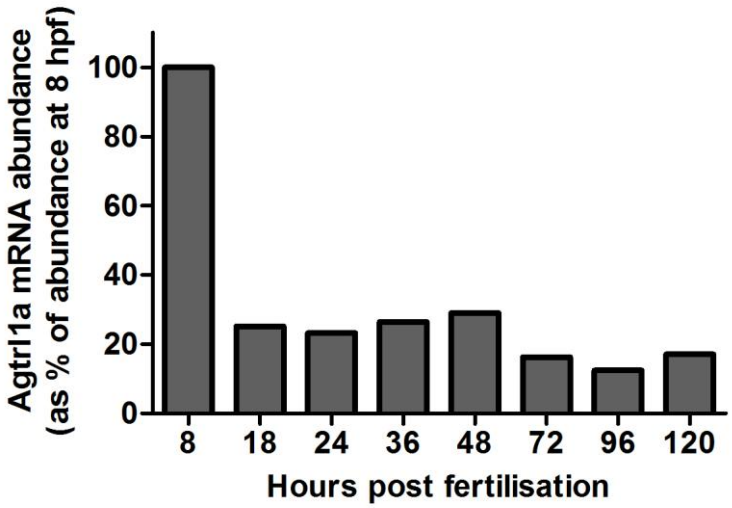

Figure 5.6: The abundance of agtrl1a mRNA in zebrafish embryos during development from 8 hpf to 120 hpf.
Abundance of mRNA measured by qPCR (corrected for EF1a and RPL13a as reference genes and expressed as a percentage of abundance at 8 hpf; n = 2 (12-15 embryos per timepoint per experiment).

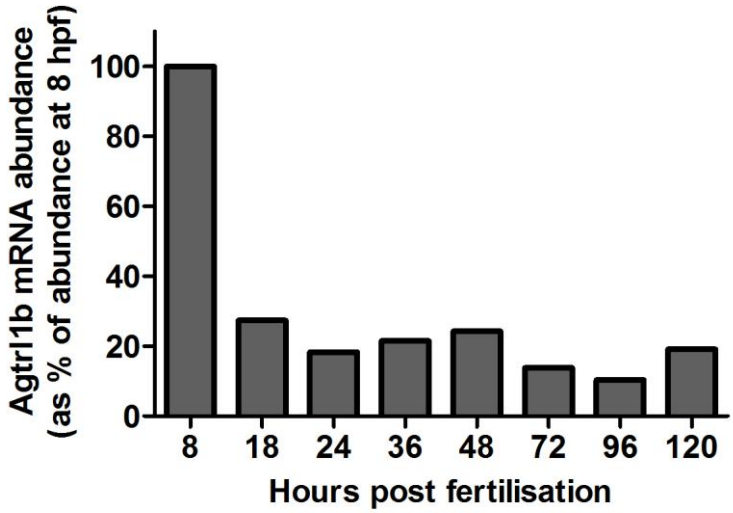

Figure 5.7: The abundance of agtrl1b mRNA in zebrafish embryos during development from 8 hpf to 120 hpf.
Abundance of mRNA measured by qPCR (corrected for EF1a and RPL13a as reference genes and expressed as a percentage of abundance at 8 hpf; n = 2 (12-15 embryos per timepoint per experiment).

5.3.2 Apelin, agtrl1a and agtrl1b are present in the zebrafish adult heart

Apelin, agtrl1a and agtrl1b mRNA transcripts are present in the zebrafish adult heart (n = 3, 3 hearts per experiment; Fig 5.10).

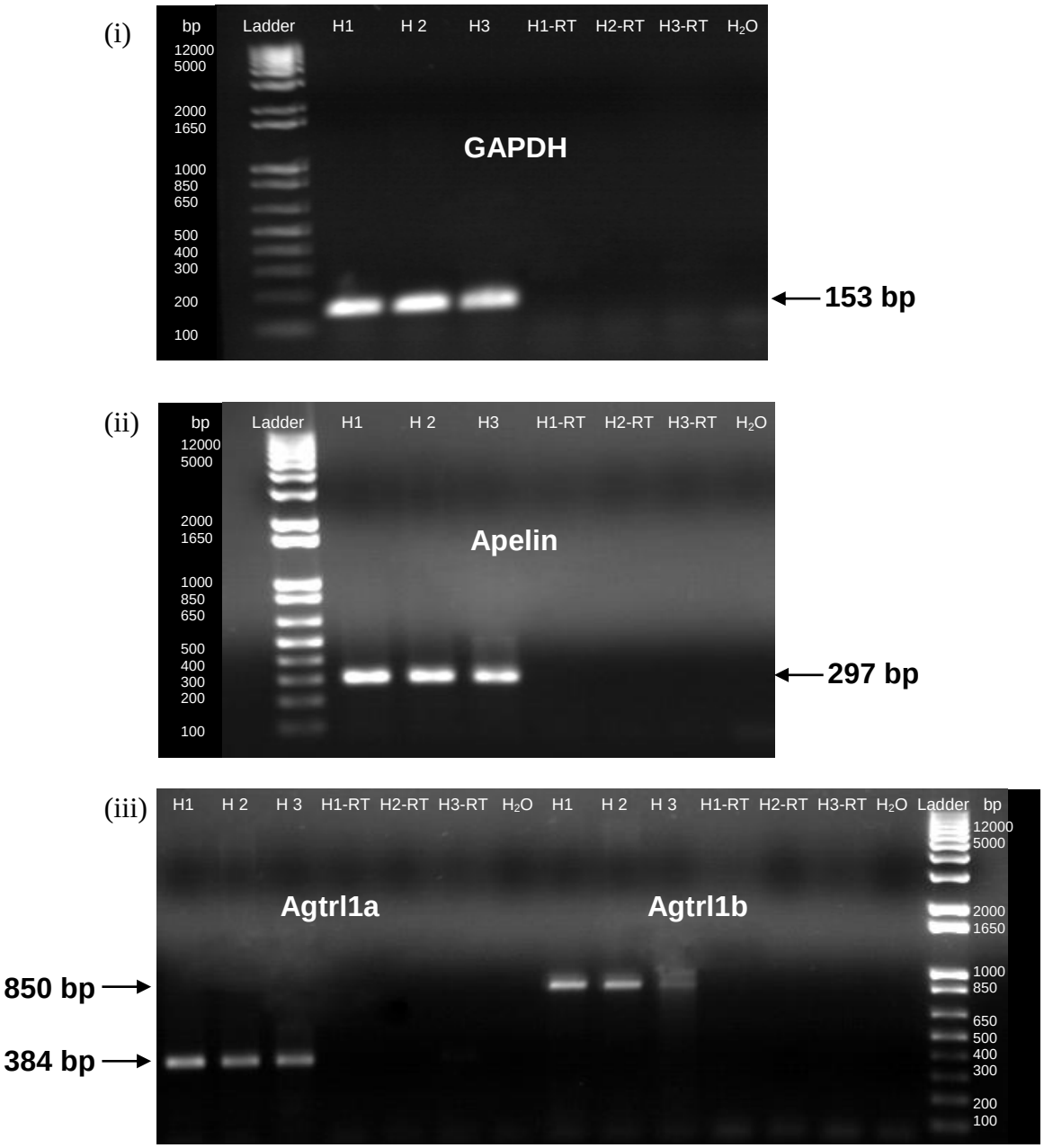

Figure 5.8: Apelin, agtrl1a and agtrl1b mRNA was detected in the zebrafish adult heart.
GAPDH is used as a positive control (i). Apelin (ii), agtrl1a and agtrl1b (iii) mRNA is present in zebrafish adult heart (n = 3; 3 hearts pooled per experiment).

5.3.4 The effect of apelin on cardiac function in zebrafish embryos

Incubation of zebrafish embryos for 1h in pyr-apelin-13 (150 nM) had no effect on contraction velocity (P = 0.38 one-way ANOVA; P = 0.09 apelin vs vehicle two-way ANOVA; Fig 5.11(i)), relaxation velocity (P = 0.37 one-way ANOVA; P = 0.37 apelin vs vehicle two-way ANOVA; Fig 5.11(ii)) or wall motion amplitude (P = 0.48 one-way ANOVA; P = 0.04 apelin vs vehicle two-way ANOVA; Fig 5.11(iii)) of the ventricle. Apelin incubation also had no effect on HR in zebrafish embryos (P = 0.97 apelin vs vehicle two-way ANOVA; Fig 5.11(iv), although HR increased throughout the experiment in both apelin and vehicle treated groups (apelin $P < 0.0001$ one-way ANOVA) (Apelin n = 6, 3 – 5 embryos per experiment; vehicle n = 3, 3 embryos per experiment).

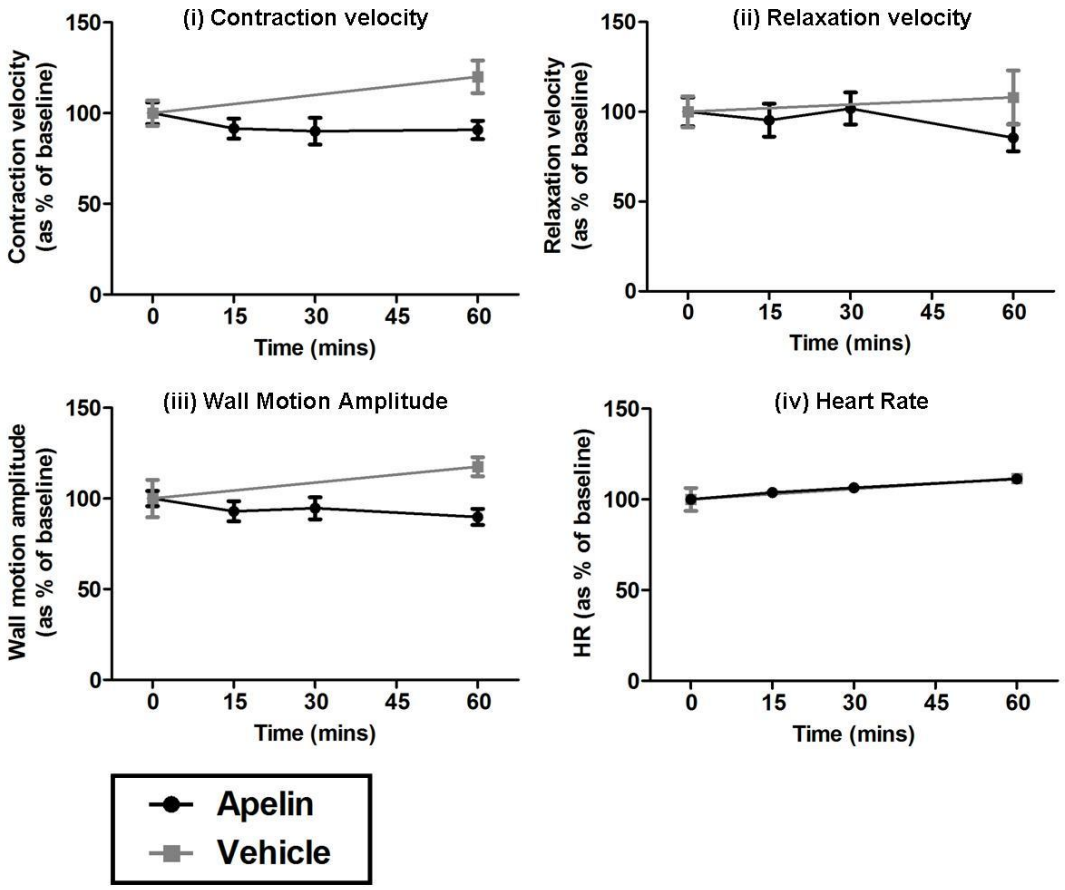

Figure 5.9: The effect of pyr-apelin-13 (150 nM) on wall motion parameters in zebrafish 3 dpf.

(i) contraction velocity $P = 0.09$ apelin vs vehicle two-way ANOVA, (ii) relaxation velocity $P = 0.37$ apelin vs vehicle two-way ANOVA, (iii) wall motion amplitude $P = 0.48$ apelin vs vehicle two-way ANOVA, (iv) heart rate $P = 0.97$ apelin vs vehicle two-way ANOVA (apelin n = 6, 3 – 5 embryos per experiment; vehicle n = 3, 3 embryos per experiment).

5.3.5 The effect of calcium on isolated zebrafish embryonic hearts

The peak response to calcium was observed at a calcium concentration of 5.5 mM in isolated hearts from zebrafish 3 dpf. Calcium (5.5 mM) significantly increased wall motion amplitude (P = 0.03 one-tailed paired t-test 2.5 mM vs 5.5 mM calcium) in isolated embryonic hearts from zebrafish 3 dpf (n = 3). There was also an increase in contraction velocity (P = 0.08 one-tailed paired t-test 2.5 mM vs 5.5 mM calcium) and relaxation velocity (P = 0.053 one-tailed paired t-test 2.5 mM vs 5.5 mM calcium) which approached significance. However, increasing calcium concentrations had no effect on intrinsic HR (P = 0.15 paired t-test) (Fig 5.12).

5.3.6 The effect of pyr-apelin-13 on isolated zebrafish embryonic hearts

Pyr-apelin-13 (50 - 150 nM) had no effect on contraction velocity (P = 0.21 one-way ANOVA) or HR (P = 0.77 one-way ANOVA) in isolated hearts 3 dpf. There was a small increase in wall motion amplitude which approached significance (P = 0.07 one-way ANOVA) and a significant increase in relaxation velocity (P = 0.049 one-way ANOVA, P = 0.01 post test for linear trend) (Fig 5.13).

In isolated hearts from zebrafish 4 dpf, pyr-apelin-13 (50 – 150 nM) had no effect on contraction velocity (P = 0.81 one-way ANOVA), relaxation velocity (P = 0.57 one-way ANOVA), wall motion amplitude (P = 0.91 one-way ANOVA) or HR (P = 0.92 one-way ANOVA) (Fig 5.13).

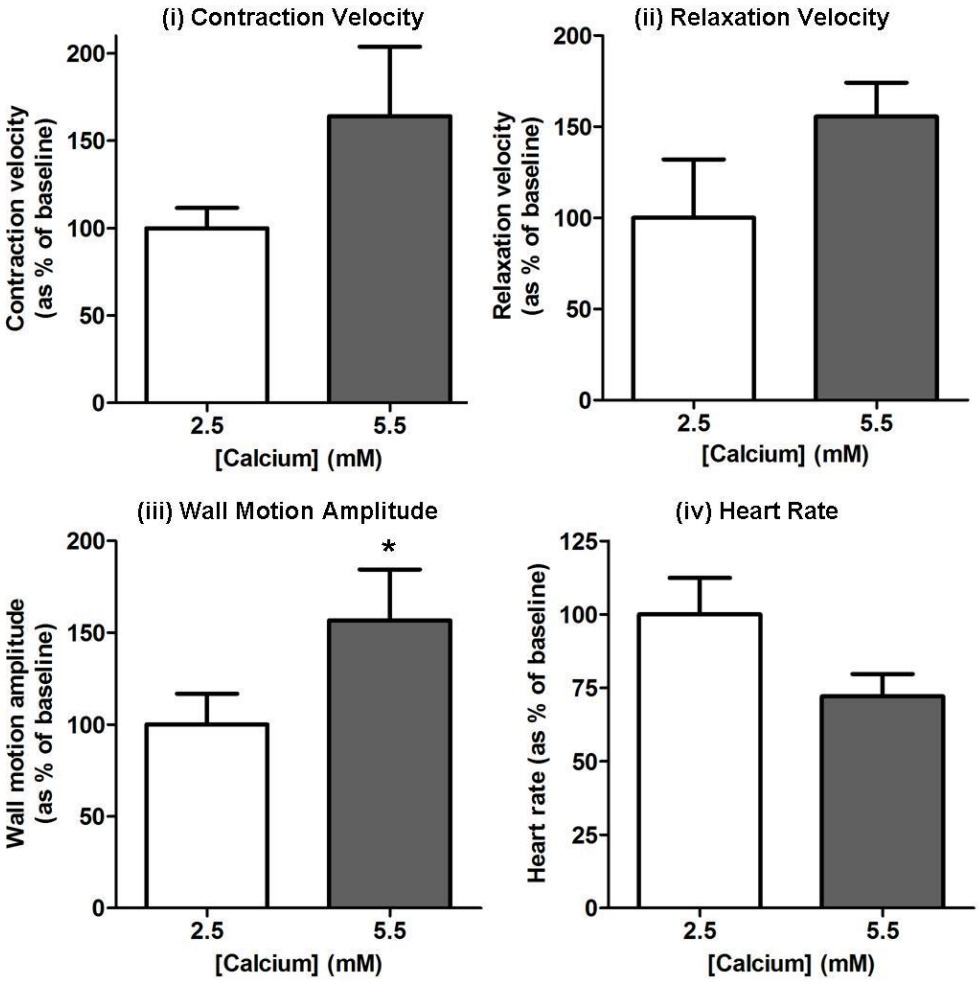

Figure 5.10: The effect of calcium (5.5 mM) on wall motion parameters in isolated hearts of zebrafish 3 dpf.

* $P < 0.05$, (i) contraction velocity $P = 0.08$ one-tailed t-test, (ii) relaxation velocity $P = 0.053$ one-tailed t-test, (iii) wall motion amplitude $P = 0.03$ one-tailed t-test, (iv) heart rate $P = 0.15$ paired t-test (n = 3).

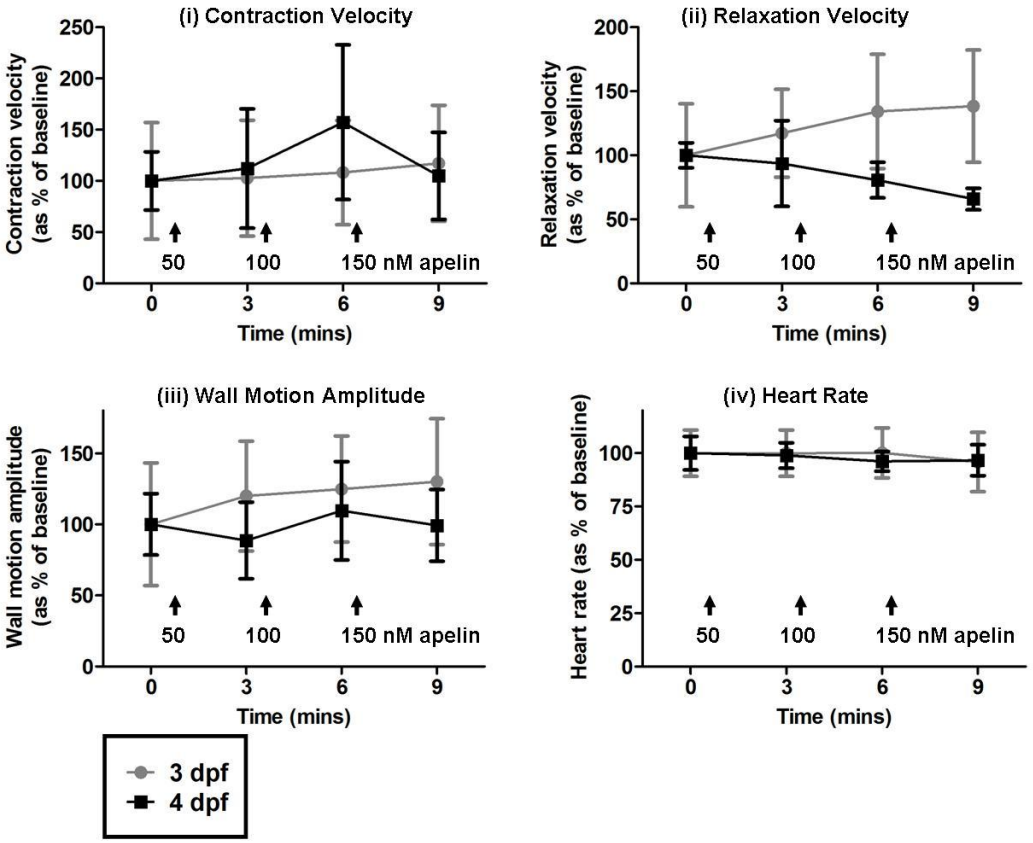

Figure 5.11: The effect of pyr-apelin-13 (50 - 150 nM) on wall motion parameters in isolated hearts of zebrafish 3 dpf and 4 dpf.
(i) contraction velocity $P = 0.21$ (3 dpf) $P = 0.81$ (4 dpf) one-way ANOVA, (ii) relaxation velocity $P = 0.049$ (3 dpf) $P = 0.57$ (4 dpf) one-way ANOVA, (iii) wall motion amplitude $P = 0.07$ (3 dpf) $P = 0.91$ (4 dpf) one-way ANOVA, (iv) heart rate $P = 0.77$ (3 dpf) $P = 0.92$ (4 dpf) one-way ANOVA; n = 3 (3 dpf) and 5 (4 dpf).

5.5.6 The effect of knockdown of apelin gene expression using a targeted morpholino

Preliminary experiments using different morpholino concentrations were carried out, from which we decided to inject 1.1 ng per embryo for further experiments (Fig 5.14).

Apelin mRNA knockdown of approximately 90% compared to embryos injected with the mispair control was shown by qPCR in embryos 3 dpf (n = 2; 7 embryos per experiment). Data was corrected for the reference gene EF1a which did not change between groups (n = 2; 7 embryos per experiment) (Fig 5.15).

The probe used in qPCR binds at the exon 2/intron 2 boundary. The forward primer binds in exon 2 and the reverse primer binds in exon 3. As the morpholino binds at the same exon/intron boundary, this qPCR assay is ideal to detect apelin knockdown as a result of morpholino injection.

5.5.6.1 Survival in embryos with apelin knockdown

MO-apelin injected embryos had greater mortality than non-injected controls and MO-mispair injected embryos ($P < 0.0001$ log rank (Mantel-Cox) test; n = 3, 100 embryos per group per experiment (Fig 5.16).

5.5.6.2 Phenotypic analysis of embryos with apelin knockdown

Cardiovascular phenotypes and gross anatomy of the zebrafish embryos were assessed. We observed that a large proportion of MO-apelin injected embryos had reduced HR, a lack of blood in hearts and reduced or absent circulation, in addition to gross anatomical changes such as twisted tails or the absence of a tail, compared to MO-mispair controls. The phenotypic score (Table 5.4) was significantly reduced in MO-apelin embryos compared to MO-mispair embryos ($P < 0.0001$ two-way ANOVA MO-apelin vs MO-mispair) (Figs 5.17, 5.18, 5.19).

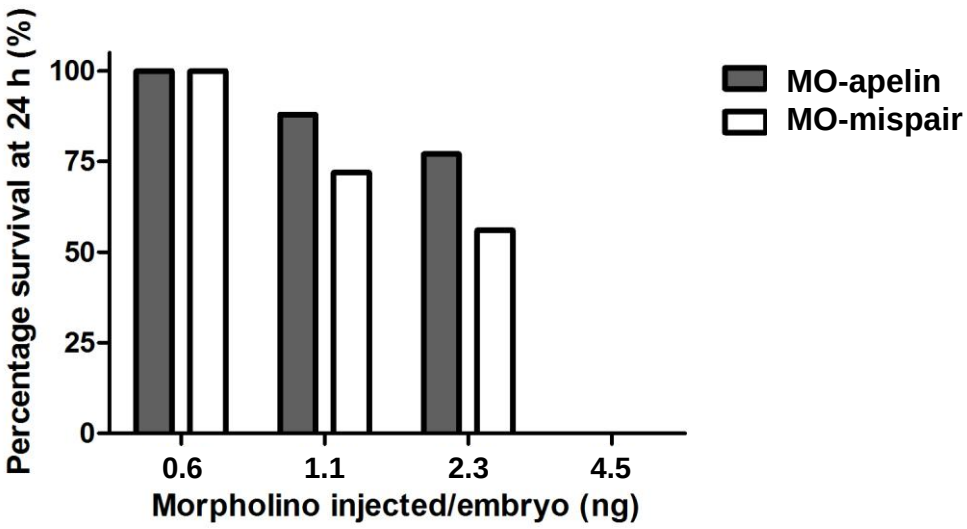

Figure 5.12: Percentage survival at 24h in morpholino injected embryos (n = 1 experiment per dose; n = 30 embryos per morpholino per dose)

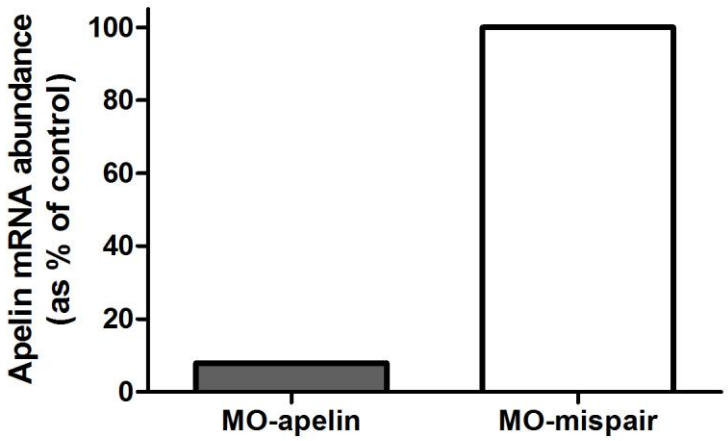

Figure 5.13: Apelin mRNA in MO-apelin injected embryos versus MO-mispair injected embryos
Knockdown of apelin mRNA is shown by qPCR in zebrafish embryos 3 dpf (n = 2; 7 embryos per experiment). Data corrected for EF1a as a reference gene. Both the morpholino and qPCR probe bind at the exon2/intron 2 boundary. The forward primer binds in exon 2 and the reverse primer binds in exon 3.

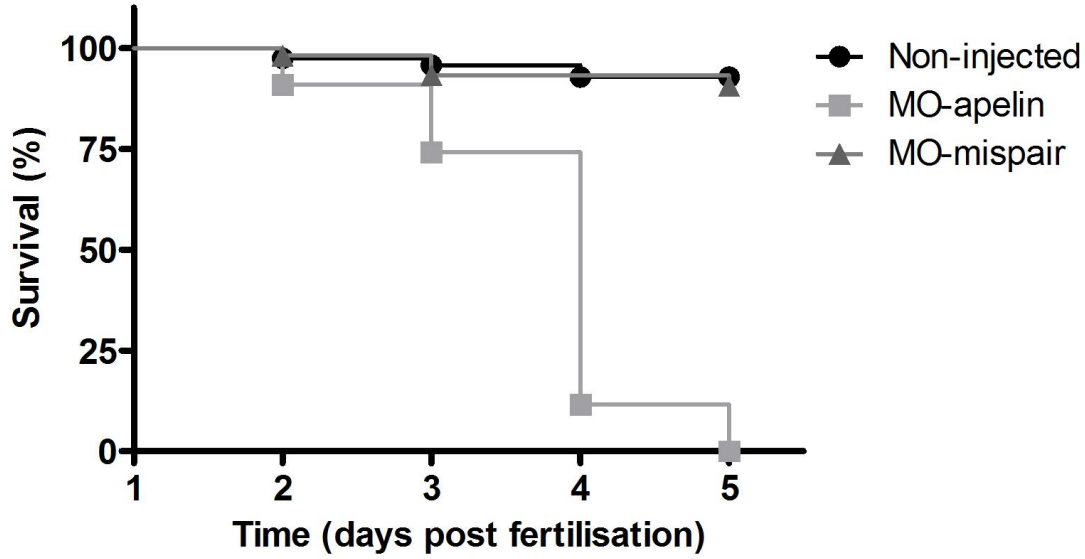

Figure 5.14: Kaplan-Meier survival curve of MO-apelin embryos compared to non-injected and MO-mispair controls.
P < 0.0001 Log-rank (Mantel-Cox) test, n = 3, 100 embryos per group per experiment.

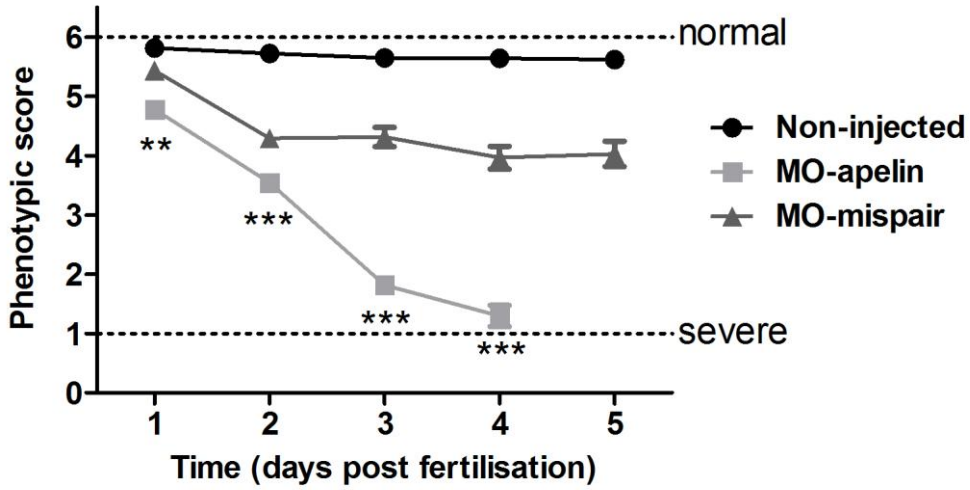

Figure 5.15: Mean phenotypic score in non-injected control, MO-apelin and MO-mispair embryos.
A phenotypic score of 6 denotes a normal phenotype and a score of 1 denotes an embryo with a severe phenotype according to the characteristics listed in Table 5.4. ** $P < 0.01$ *** $P < 0.001$ two-way ANOVA MO-apelin vs MO-mispair embryos; n = 3, 100 embryos per group per experiment.

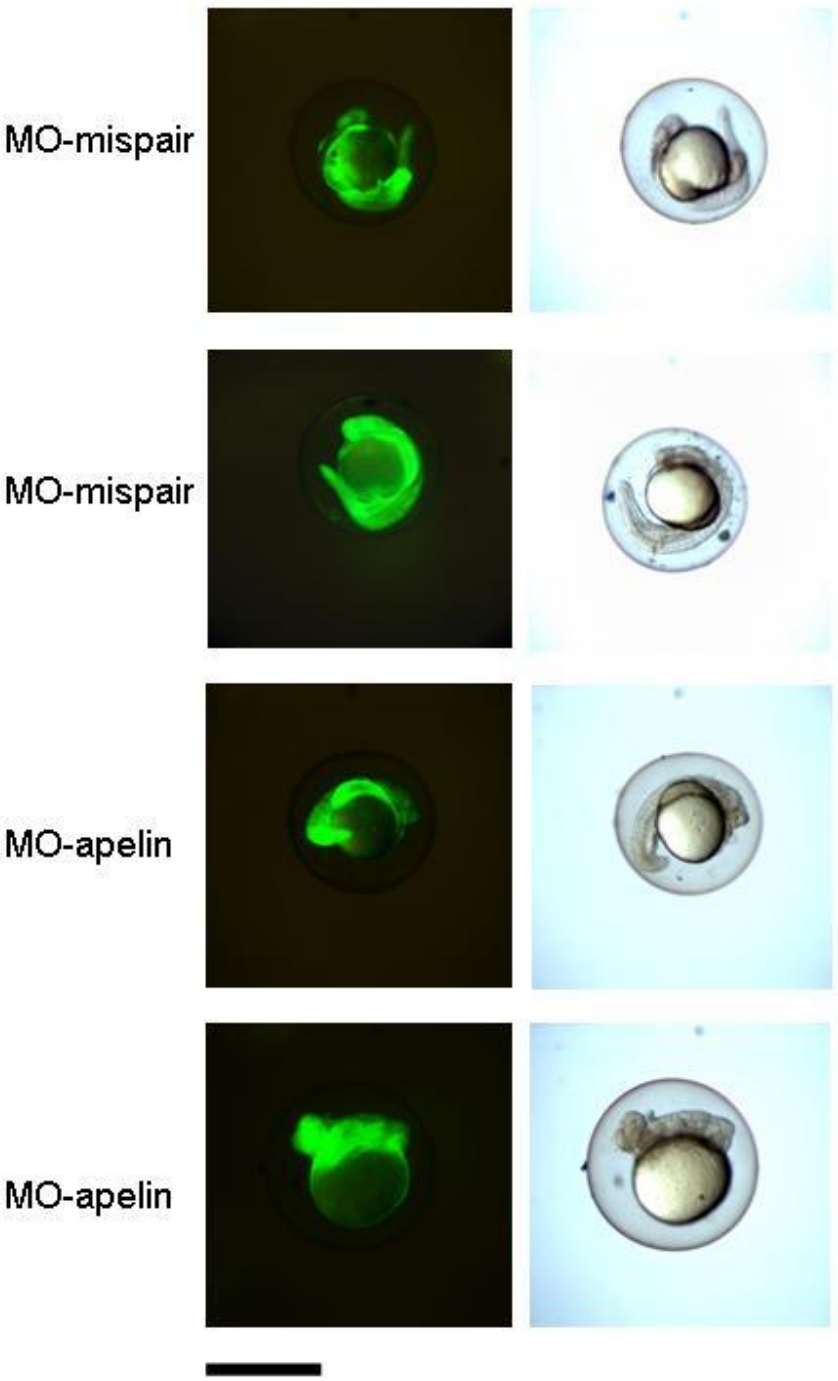

Figure 5.16: MO-apelin and MO-mispair injected zebrafish embryos at 1 dpf. Fluorescent images show successful uptake of the morpholino and a severe anatomical phenotype can be seen in a typical MO-apelin injected embryo. Scale bar 0.1 mm.

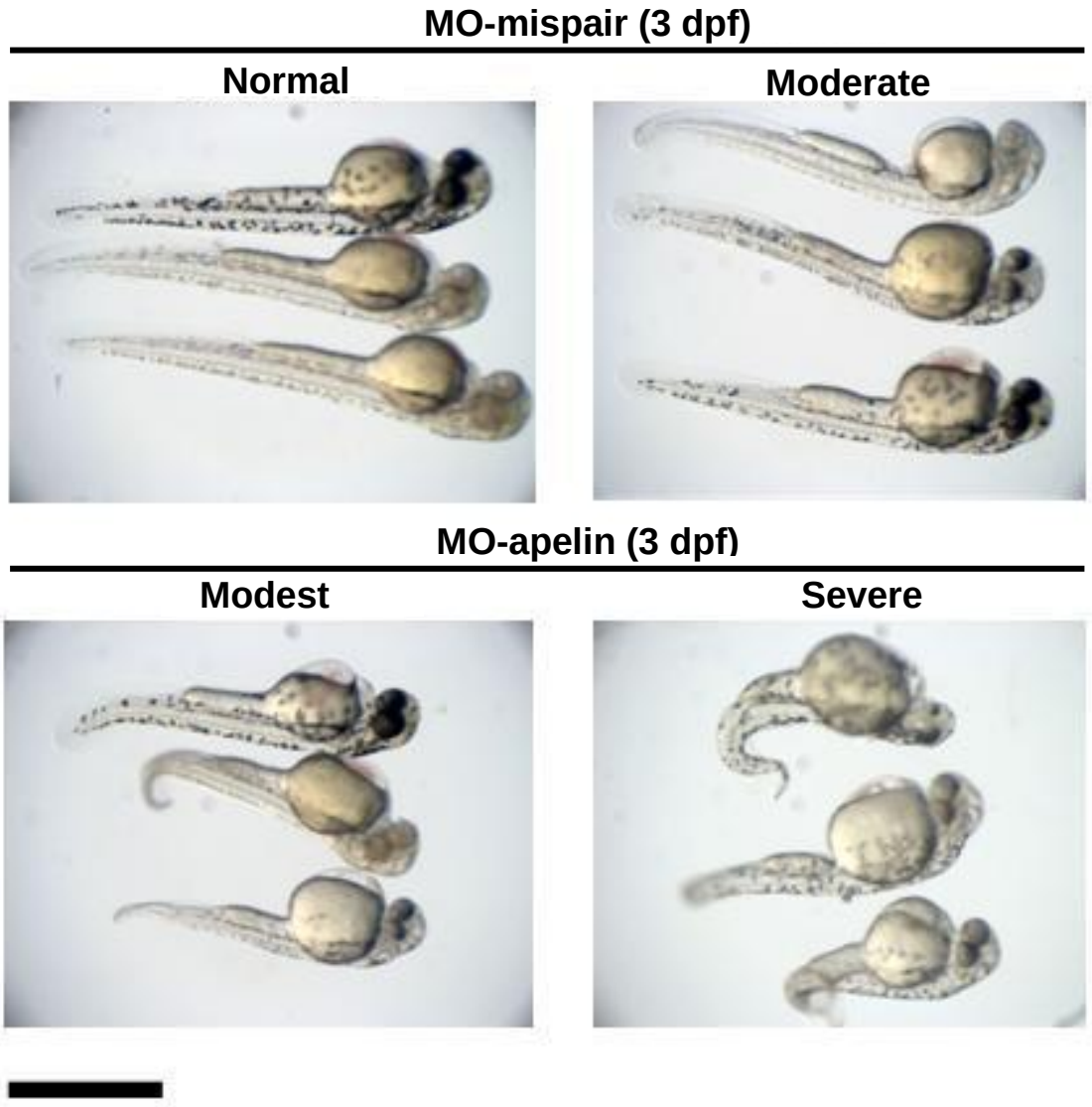

Figure 5.17: MO-apelin and MO-mispair injected embryos at 3 dpf.
The majority (71 ± 6%, n = 3) of MO-mispair injected embryos display a normal or mild phenotype at 3 dpf, while the majority (87 ± 9%, n = 3) of MO-apelin injected embryos display moderate or severe phenotypes at 3 dpf. Scale bar 0.5 mm.

5.5.6.3 Ejection fraction in MO-apelin embryos

Despite observing greater mortality and a more severe total body and cardiovascular phenotype in MO-apelin injected embryos, we were unable to detect an effect of MO-apelin on ejection fraction in surviving zebrafish embryos at 2 dpf, 3 dpf and 4 dpf (P = 0.94 two-way ANOVA; Fig 5.20).

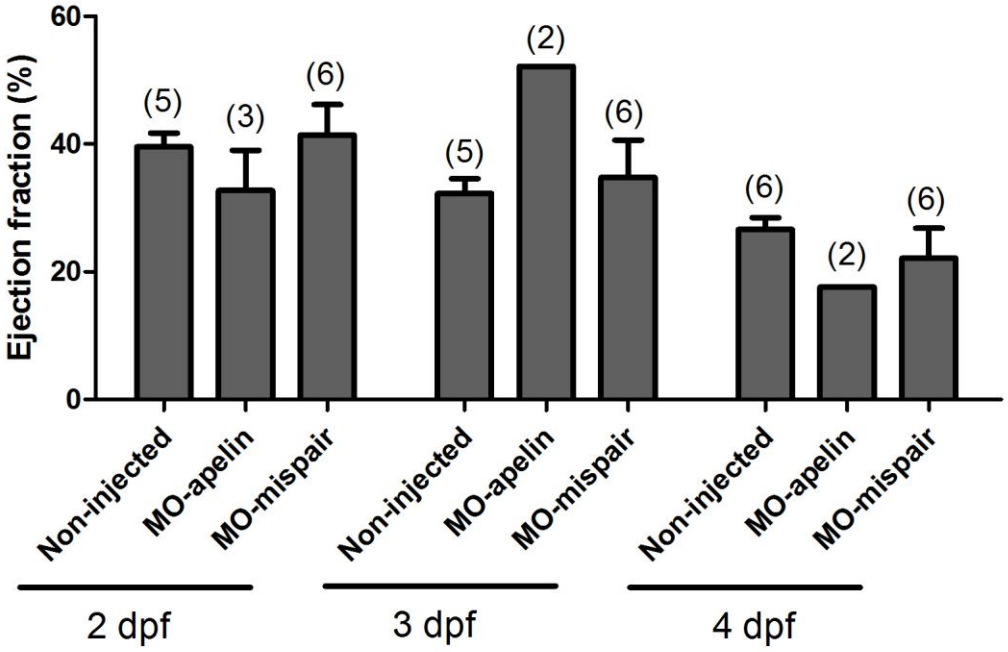

Figure 5.18: Ejection fractions in non-injected controls, MO-apelin and MO-mispair morpholino injected embryos.
Ejection fractions do not differ between groups at 2 – 4 dpf (P = 0.94 two-way ANOVA; n = 2 – 6, shown in brackets).

5.4 Discussion

5.4.1 mRNA studies of apelin and its receptors in zebrafish embryos and the adult zebrafish heart

The pattern of mRNA of apelin and its receptors in whole embryos during the first five days of development is striking. Apelin mRNA increases steadily from 8 hpf and reaches a peak at 48 hpf. This confirms the work of Zeng *et al*. (2007) who showed using RT-PCR that apelin mRNA is not detected at 7 hpf, but is present from 8.5 hpf and increases until 48 hpf. These authors stop their time course at this point. We were able to show that apelin mRNA declines at 72 hpf and again at 96 hpf where it reaches a level comparable with that of 18 hpf. However, there is a sharp increase at 120 hpf (5 dpf) when apelin mRNA reaches its highest level in all of the developmental time points studied, a five fold increase in apelin mRNA abundance from 96 hpf.

In contrast to the pattern of the abundance of the ligand, apelin, both receptors, agtrl1a and agtrl1b, have similar mRNA patterns. The assays used have been checked with BLAST for specificity for other genes and we can be confident that although the homology between the receptor isoforms is significant (approximately 80% (Tucker *et al.*, 2007)), each of our assays is detecting only one form of the receptor. The receptor mRNA patterns show the highest levels of both forms of the receptor in our time course are expressed at 8 hpf. Midblastula transition (MBT), a time when zygotic transcription begins and maternal regulated transcription decreases, occurs at 5.5 hpf (Kimmel *et al.*, 1995). The high levels of agtrl1a and agtrl1b mRNA detected at 8 hpf may be in part due to maternally controlled

transcription. From 18 hpf until 120 hpf, the levels of both receptors are around 20 – 30% of that observed at 8 hpf. Protein extracted from zebrafish embryos (5 dpf) was probed in a western blot with rat anti-APJ receptor antibody, but the antibody was unable to detect the zebrafish protein. *In situ* hybridisation studies would allow us to further investigate the expression of the apelin receptor in zebrafish in the absence of a suitable antibody.

Apelin, agrtrl1a and agtrl1b mRNA were also detected in zebrafish adult heart. Our embryo mRNA studies represent the mRNA of the whole embryo so we are unable to determine the degree to which specific tissues contribute to the pattern of mRNA in the embryo. As I now have the technical skill to isolate embryonic hearts from zebrafish 3 – 5 dpf, it would be possible, in a future study, to investigate cardiac specific changes in apelin, agtrl1a and agtrl1b mRNA during this window of development. Using qPCR, it would then be possible to relate cardiac apelin mRNA abundance in the embryonic heart to that in the adult zebrafish heart.

5.4.2 The effect of exogenous apelin on cardiac function in zebrafish embryos

Although we detected the presence of endogenous apelin, agtrl1a and agtrl1b mRNA in whole zebrafish embryos, exogenous apelin had no effect on cardiac function *in vivo* of zebrafish embryos 3 dpf. Pyr-apelin-13 was administered to zebrafish via the bathing water. This particular apelin isoform was chosen for these studies as the terminal pyroglutamate is thought to afford it protection from degradation by endopeptidases (Russo *et al.*, 2002). The zebrafish embryos were incubated in pyr-apelin-13 for 1h. Previous work demonstrated that 10 minutes was sufficient time for

small molecule drugs, such as noradrenaline, to have an effect on cardiac function in zebrafish embryos embedded in agar (Denvir *et al.*, 2008). Although the incubation time should have been long enough, we could not be sure that the peptide was entering the zebrafish embryos. Drugs have been successfully administered to embryonic zebrafish via the bathing water in a number of studies (Berghmans *et al.*, 2008; Denvir *et al.*, 2008; Loynes *et al.*, 2010; Milan *et al.*, 2003; Parng *et al.*, 2006); however, it is unclear whether or not small peptides enter the zebrafish embryo when administered via the bathing medium.

One way to investigate whether or not the human apelin was entering the zebrafish embryo would have been to use a fluorescently tagged apelin and subsequently perform immunohistochemistry. However, the available fluorescent tags were much larger than apelin itself meaning that if apelin did not get in we could not determine if this was due to the fluorescent tag. Another possibility was to use a radiolabelled apelin and perform autoradiography after bathing the embryos in system water containing the radiolabelled peptide. We also attempted to inject apelin into the circulation of zebrafish embryos at 3 dpf.

The injection of apelin into the circulation of zebrafish embryos at 3 dpf was attempted. Microinjection of drugs (sotalol, pentamidine and procainamide) that induce bradycardia have been shown to be effective when injecting directly into the yolk sac at 2 dpf (Milan et al., 2003); injecting directly overcomes the hydrophilicity and possible poor absorption of the compound. However, in embryos 3 dpf, the yolk sac is further separated from the circulation than at 2 dpf (Isogai *et al.*, 2001),

therefore, microinjection into the caudal vein and dorsal aorta whilst attempted did prove to be technically too difficult. Injection into the caudal vein and dorsal aorta is not only compounded by the dimensions of the vessels available but also the need to inject, under pressure, the apelin compound into the vasculature.

The only way to be certain of whether apelin had a direct action on the heart in zebrafish embryos was to isolate embryonic hearts and expose hearts directly to pyr-apelin-13 in the bathing medium. Two developmental stages of embryo were chosen for these experiments: 3 dpf when endogenous apelin mRNA was relatively high and 4 dpf when endogenous apelin mRNA was relatively low. Exogenous pyr-apelin-13 administered to hearts isolated from embryos at 3 dpf and 4 dpf had no inotropic effect i.e. there was no increase in wall motion amplitude or contraction velocity. There was also no change in heart rate. However there was a small, but significant, increase in relaxation velocity in isolated hearts (3 dpf) in response to apelin.

Nevertheless, embryonic isolated heart preparations were not without their own limitations. The hearts were unpaced and HR was around 60 bpm compared to 150 bpm *in vivo* in zebrafish embryos. This did, however, allow us to determine that apelin had no effect on HR in these preparations. The experiments were also performed on unloaded hearts. The Frank-Starling law where increasing stretch results in increased cardiac contractility, has been shown to apply to all vertebrates (see Shiels and White, 2008). Therefore, applying stretch to the isolated embryonic hearts may improve this experimental approach. Other considerations are temperature, oxygenation and physical trauma to the tissue. The experiments were

carried out at room temperature (22 °C), whereas a physiological temperature for these preparations would be 28.5 °C. As zebrafish are poikilothermic organisms (they do not regulate body temperature so body temperature varies with the environment), this may have influenced heart rate and function. The bathing medium was buffered by HEPES, but was not oxygenated. Therefore, it is likely that the tissue was experiencing a small level of hypoxia. The physical trauma that may have been caused to the cardiac tissue during isolation of the heart is another limitation of the preparation. For these reasons, the experimental protocol was kept short in length. Despite these limitations, the hearts were removed from the embryos quickly and all were beating well for the duration of the experimental protocol. A similar technique has been utilised and reported using isolated embryonic zebrafish hearts to assess voltage mapping of the zebrafish ventricle (Panakova *et al.*, 2010).

5.4.3 Knockdown of apelin mRNA using a targeted morpholino

Knockdown of apelin expression generated severe, abnormal total body and cardiovascular phenotypes. The pattern of abundance of mRNA of the ligand, apelin, appears to mirror the survival curve of the MO-apelin embryos i.e. the greater the level of endogenous apelin mRNA in our developmental time course; the greater the mortality rate in embryos with knockdown of apelin expression. Since no MO-apelin embryo has survived to 5 dpf in our morpholino experiments, we can conclude that at 5 dpf apelin is essential for survival or that the severe abnormalities generated by apelin knockdown prior to this cause death by 5 dpf. A combination of both of these reasons may be responsible.

We established that (a) apelin was successfully knocked down using our morpholino and (b) a five mispair control morpholino demonstrated significantly greater survival and a less severe phenotype as determined by our phenotypic score. However, the specificity of the action of the morpholino requires further experiments. One way would be to perform a second morpholino experiment using a non-overlapping morpholino which also targets apelin mRNA. If the resulting phenotype was the same, we would conclude that the total body and cardiovascular phenotype observed is specific to knockdown of apelin in these experiments. Another experiment that would illustrate the specificity of the apelin morpholino would be to perform a "rescue experiment", in which apelin mRNA lacking the morpholino binding site would be co-injected with the morpholino. If this attenuated the observed phenotype, then we would conclude that the phenotype is specifically due to apelin knockdown. These future experiments are further discussed in section 7.2.3.

The effect of apelin knockdown in zebrafish embryos was in contrast to the effect of apelin knockout in mice reported in the literature. Apelin knockout mice develop normally with no notable phenotype (Kuba *et al.*, 2007). This questions whether (i) apelin does have a developmental role in zebrafish, but not in mice or (ii) the effect observed in these experiments is not specific to knockdown of the apelin gene. The experiments described above would help in answering this question. In addition p53-mediated cell death has been shown to be responsible for several morpholino-induced phenotypes (Robu *et al.*, 2007). Co-injection of a p53 morpholino and apelin morpholino would determine whether or not the developmental abnormalities observed on knockdown of the apelin gene are due to p53-mediated cell death.

Other approaches which were considered to generate embryos in which apelin gene expression is knocked down were Targeted Induced Local Lesions in Genomes (TILLING) and zinc finger nucleases. These methods have advantages over the use of morpholinos as they both produce a mutation in the gene of interest.

TILLING involves exposure of adult male zebrafish to a mutagen, for example, *N*-ethyl-*N*-nitrosourea (ENU) which are crossed with untreated females in order to generate mutations which are passed to the offspring via the germline (see Moens *et al.*, 2008). It is used in huge screens as a way of generating multiple mutant lines which may have phenotypes of interest to a particular field. Interesting phenotypes in the resulting embryos can then be followed up by sequencing the genome to find the mutation responsible for the phenotype (see Sood *et al.*, 2006). However, TILLING cannot be used to target a particular gene of interest and therefore, although it would ultimately provide a more specific apelin mutant than could be generated by morpholino, it was not a viable option for this study.

Zinc finger nucleases bind to the targeted DNA and produce double stranded breaks in the DNA. These breaks are repaired by non-homologous end joining which join the ends of the break back together. However, errors are often made in this process and it can result in insertions or deletions in the gene sequence leading to a frame-shift which results can result in a non-functional protein. Zinc finger nucleases produce a specific mutant which may be more reliable than knockdown of gene expression by morpholino (see Urnov *et al.*, 2010). The mutation generated by a zinc finger nuclease can also be passed to offspring and therefore a mutant line can be

created. This is in contrast to the use of a morpholino where the gene knockdown will last only for the first 5-7 days of development. In some cases, zinc finger nucleases produce non-specific effects (Gupta *et al.*, 2011). Furthermore, the generation of a zinc finger nuclease can take months in the lab, whereas GeneTools are able to design a morpholino to target a specific gene in days. For these reasons, morpholinos were used in this study.

5.4.4 Summary

In summary, the endogenous apelin system appears to be established early in development and is essential at these early timepoints. Although we observed a total body and cardiovascular phenotype following apelin knockdown with a targeted morpholino, exogenous apelin had no inotropic effect on the heart function of embedded embryos 3 dpf or isolated embryonic hearts (3 dpf and 4 dpf). The functional role of the apelin system in the zebrafish remains unclear, although these data support a developmental role for the peptide

Chapter 6 The development of an acute hypoxia-recovery model in zebrafish embryos

6.1 Introduction

6.1.1 Cardioprotection: a definition

Cardioprotection can be defined as a mechanism which reduces injury to the cardiovascular system following an ischaemic or hypoxic insult, for example by a pharmacological agent. Cardioprotection is measured by a decrease in myocardial infarct size (Simpkin *et al.*, 2007) or, as in this study, by a lesser degree of depression in cardiac function in response to an ischaemic insult.

6.1.2 Cardioprotective effects of apelin

The cardioprotective effects of apelin have been previously reported in a limited number of publications. A thorough search of the literature for studies involving apelin and hypoxia or ischaemia revealed a limited number of publications. The published data demonstrates reduced cardiac injury in the presence of apelin compared to saline alone in rat and mouse models of ischaemia-reperfusion (Simpkin *et al.*, 2007). The cellular mechanisms responsible for cardioprotection by apelin remain unclear. Apelin-mediated cardioprotection was shown to be independent of P13K/Akt and P70S6 kinases in a study carried out by Kleinz and Baxter (2008). However, Smith *et al.* (2007) demonstrate in isolated, perfused mouse hearts that phosphorylation and activity of the kinases, Akt and P44/42, are increased following reperfusion with apelin.

6.1.1.2 The relationship between the apelin and HIF-1 pathways

Cardioprotection associated with activation of the hypoxia-inducible factor 1α (HIF-1α) pathway has been well documented and this has been reviewed recently by Tekin *et al*. (2010). The relationship between HIF-1α and apelin pathways has been explored in a small number of studies (Eyries *et al.*, 2008; Glassford *et al.*, 2007; Han *et al.*, 2008; Ronkainen *et al.*, 2007). However, the role of apelin in HIF-1α mediated cardioprotection has not yet been studied.

The link between HIF-1α and apelin was first established by the discovery of a hypoxia-response element on the human apelin gene (Eyries *et al.*, 2008). Under hypoxic conditions, HIF-1α translocates to the nucleus, pairs with HIF-1β, and binds to hypoxia-response elements on a variety of genes to induce transcription (Qutub *et al.*, 2006). In adipocytes, an increase in apelin mRNA expression in response to hypoxia was shown to be mediated via HIF-1α (Glassford *et al.*, 2007). Another study suggested that HIF-1α-mediated apelin expression promotes enteric cell proliferation in response to hypoxia (Han *et al.*, 2008). In rat myocardium and cultured rat cardiomyocytes exposed to hypoxia, an increase in apelin mRNA was mediated via HIF-1α, as inhibition of HIF-1α abolished the increase in apelin mRNA expression (Ronkainen *et al.*, 2007). Although the link between the HIF pathway and apelin pathway has been documented in these systems, these models do not directly demonstrate a cardioprotective effect of apelin when activated via HIF-1α. Using the zebrafish as a model organism allowed us to expose the whole organism to hypoxia, monitor heart function non-invasively and influence the apelin system, in order to

further understand the potential cardioprotective role of apelin and its relationship with the HIF-1α pathway.

6.1.2 Hypoxia studies in the zebrafish

Zebrafish are adaptive organisms which respond to a changing environment and may experience hypoxia in their natural environment of shallow, slow moving waters (Spence *et al.*, 2008). However, zebrafish embryos (3 dpf and older) are unable to survive exposure to severe hypoxia (5% oxygen) for more than 12h (Ton *et al.*, 2003), while embryos can survive less severe hypoxia for days (Schwerte *et al.*, 2003). In our experience, zebrafish embryos (3 dpf and older) are unable to survive very severe hypoxia (1% oxygen) for longer than 4 - 8h. Therefore, hypoxia studies in the zebrafish fall into two groups: (i) longer term less severe hypoxia assessing the developmental and adaptive capabilities of zebrafish embryos (Schwerte *et al.*, 2003) and (ii) shorter more severe hypoxia studies assessing hypoxia-induced injury.

Longer term hypoxia studies, in which zebrafish are exposed to hypoxia throughout development, demonstrate the adaptive responses of zebrafish embryos. In response to long-term hypoxia there is an apparent change in red blood cell distribution with more red blood cells in the tail and less in the gut after hypoxia (Schwerte *et al.*, 2003). Bagatto (2005) describes slower growth, slower HR and more variation in development in chronic hypoxia studies. One study showed that complete anoxia (24h) caused development to halt, but when oxygen was returned to normal levels, development restarted normally (Padilla *et al.*, 2001).

Short term very severe hypoxia (< 5% oxygen) studies are fewer in number. Most have focussed on changes in HR or the developmental impact of acute hypoxic exposure. Indeed, the majority of short term hypoxic insults are exposure to 5% oxygen for between 4h and 24h. HIF-1α expression is up-regulated in response to 5% oxygen for 24h from 24 hpf to 48 hpf, in zebrafish embryos and these changes can be reversed by normoxic exposure (Gray *et al.*, 2007; Ton *et al.*, 2003). HIF-1α mRNA was also increased in zebrafish 4 dpf exposed to 5% oxygen for 4h (Gray *et al.*, 2007). The mechanisms which underpin the cardiovascular response to acute hypoxia have not been studied in depth to date.

The aims of this chapter were to develop a hypoxia-recovery model in zebrafish embryos. Establishing the model involved defining a reproducible effect of hypoxia on the heart and circulation by incubation in a hypoxic environment for a defined time period. This also involved defining the time scale of normoxic recovery using global cardiovascular function (heart rate, heart contraction and tail circulation) as surrogate measure. Once these parameters were explored and defined, we used the model to:

i. assess the response to hypoxia at different developmental stages
ii. study the possible effects of apelin on the hypoxia-recovery response
iii. study the effect of other drugs (including HIF modulators) on the hypoxia-recovery response
iv. assess changes in the abundance of mRNA transcripts of apelin and HIF-1α on exposure to hypoxia and subsequent recovery

6.2 Methods

6.2.1 Hypoxia-recovery model measured using a semi-quantitative scoring system

To determine semi-quantitative differences in the cardiac response of zebrafish 3 dpf and 5 dpf to hypoxia, zebrafish (15 – 20 embryos per dish) in dechlorinated system water were placed in the hypoxic chamber (1% oxygen, 94% nitrogen, 5% carbon dioxide; 26 °C) for 2h or 4h. After the assigned time in the hypoxic chamber, heart and circulatory function were assessed under a light microscope (at 22 °C) and each fish was described as having normal, reduced or absent heart rate (HR) and circulation compared to normoxic controls (Table 6.1, Fig 6.1).

Category	Normal	Reduced	Absent
Criteria	HR > 100 bpm, normal global circulation compared to normoxic controls	HR < 100 bpm, reduced global circulation compared to normoxic controls	no HR or circulation

Table 6.1: Criteria for categorising HR and global circulation in the hypoxia-recovery model.

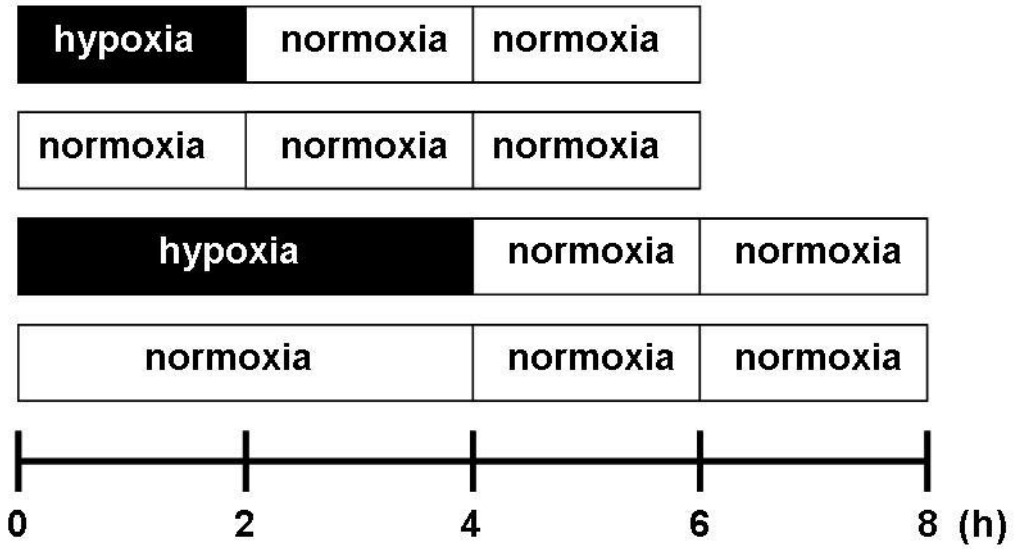

Figure 6.1: Hypoxia-recovery model.
Zebrafish were exposed to hypoxia or normoxia for 2h or 4h as shown followed by 4h recovery in normoxia. Measurements were made at the end of each block.

6.2.1.1 The effect of pharmacological agents on the hypoxia-recovery model

Zebrafish 5 dpf exposed to 2h hypoxia with recovery in normoxia was chosen as a suitable model for the assessment of a possible influence of pharmacological agents on the hypoxia-recovery response. A series of experiments tested the effect of the following drugs in this model: pyr-apelin-13 (150 nM), desferrioxamine (0.1 mM), α-ketoglutarate (2.5 mM), glibenclamide (0.1 mM) and nicorandil (0.1 mM).

Desferrioxamine is an iron chelator which can potentiate the HIF pathway by inhibiting the formation of the degradation complex formed by PHD enzymes. The drug also has antioxidant activity (Parng *et al.*, 2006). Desferrioxamine has previously been administered to zebrafish embryos via the bathing water in an assay used to identify neuroprotectant compounds (Parng *et al.*, 2006). The maximal effect was seen at 0.1 mM and therefore the same concentration was used in the experiments described in this thesis. Alpha-ketoglutarate can inhibit the HIF pathway as α-ketoglutarate is required for the PHD complex that is responsible for the degradation of HIF. Preliminary experiments at 0.1 mM, 2.5 mM and 25 mM demonstrated that the maximal effect in our model was observed at 2.5 mM and therefore this concentration was used in subsequent experiments.

Glibenclamide acts by inhibiting ATP-dependent potassium channels. Glibenclamide was used in a previous study in zebrafish 2 dpf in which it produced a small decrease in heart rate at 100 µg/ml which equates to 0.02 mM (Milan *et al.*, 2003). The concentration used in this study was five times greater which I used bearing in mind that the zebrafish used in the experiments presented here were older at 5 dpf. The

action of glibenclamide has been shown to abolish the cardioprotective effects of other drugs in rat models of cardioprotection (Taliyan *et al.*). Nicorandil is an ATP-dependent potassium channel activator and has been shown to be beneficial in patients undergoing reperfusion after myocardial infarction (Iwakura *et al.*, 2009). Although no published study exists in which nicorandil was administered to zebrafish embryos, the concentration used was the same as that of glibenclamide as nicorandil targets the same potassium channel and is of a similar size.

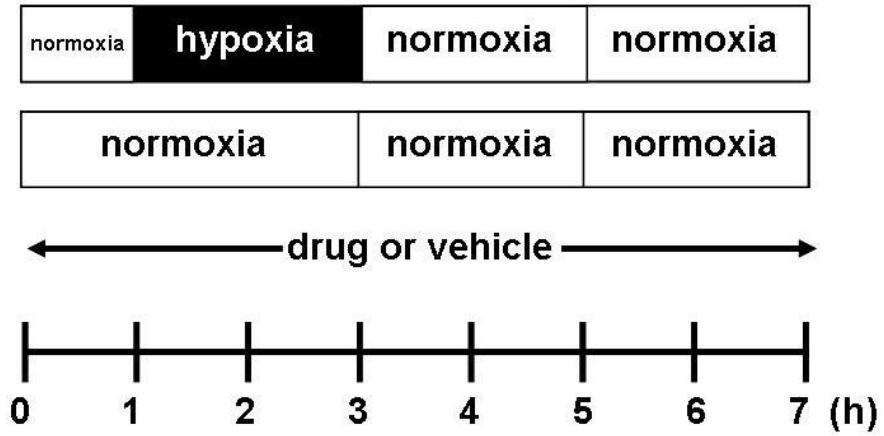

Figure 6.2: The effect of drugs on the hypoxia-recovery model.
Zebrafish (5 dpf) are incubated in drug, followed by a 2h exposure to normoxia (a) or hypoxia (b). Alternatively, zebrafish are incubated in vehicle followed by a 2h exposure to normoxia (c) or hypoxia (d). All fish are allowed to recover in normoxia for 4h and are observed at arrowed timepoints.

These experiments were performed blinded which meant that the investigator was unaware of which dish of embryos had drug or vehicle added in all experiments. In all cases, zebrafish were incubated (10 embryos per dish) in drug or its vehicle throughout the experimental protocol. In the cases where DMSO was used as a vehicle, the final concentration of DMSO in the bathing solution was 0.1%.

Incubation began 1h prior to hypoxic exposure. Assessments of HR and global circulation (Table 6.1) were made in the same way as for the experiments comparing the response in 3 dpf and 5 dpf embryos and at the same timepoints, i.e. immediately after hypoxia, after 2h recovery in normoxia and after 4h recovery in normoxia (Fig 6.2).

6.2.1.2 The effect of hypoxia on MO-apelin embryos

In a single experiment (n = 7 per group), MO-apelin embryos (described in chapter 5) were exposed to hypoxia with MO-mispair embryos and non-injected controls at 3 dpf. Normoxic embryos of all three groups were also observed as a control. To ensure that the MO-apelin embryos were not highly susceptible to severe hypoxic conditions, the hypoxia-recovery protocol was adapted. Assessment of HR and global circulation (see Table 6.1) of embryos was performed at 30 minute intervals for the first 1h 30 and at 1h intervals thereafter for a total exposure time of 5h 30.

6.2.2 Hypoxia-recovery model measured using video edge detection

6.2.2.1 Apelin

Agar-embedded zebrafish (3 dpf) were incubated in pyr-apelin-13 (150 nM) for 1h prior to hypoxia and throughout the experimental protocol. Zebrafish were exposed to hypoxia (1% oxygen) for 2h and then placed in a normoxic environment for 2h. Vehicle controls were exposed to hypoxia and normoxia in the same way and embryos exposed to normoxia throughout the experiment were used as an additional control. Video edge detection (as described in section 2.6.1) was performed on apelin and vehicle treated embryos immediately after hypoxia and after 1h and 2h recovery

in normoxia. Similarly, video edge detection measurements of normoxic controls were performed at each of the above timepoints and at baseline. Contraction velocity, relaxation velocity, wall motion amplitude and heart rate were expressed as a percentage of baseline normoxic control measurements.

6.2.2.2 Desferrioxamine

At 5 dpf the ventricle wall was difficult to track in wild-type embryos due to overlying skin pigmentation reducing optical clarity of the heart region. Therefore, the effect of desferrioxamine on the hypoxia-recovery model was assessed using transgenic *cardiac myosin light chain 2: green fluorescent protein (cmlc2:GFP)* zebrafish (5 dpf). Agar-embedded *cmlc2:GFP* zebrafish were incubated in desferrioxamine (0.1 mM) for 1h prior to hypoxia and throughout the experimental protocol. Embryos were exposed to hypoxia for 2h followed by recovery in normoxia for 4h. Video edge detection (as performed in section 6.2.2.1) was performed on desferrioxamine and vehicle treated embryos immediately after 2h hypoxia and after 2h and 4h of recovery. Similarly, video edge detection measurements of normoxic controls were performed at each of the above timepoints and at baseline. Contraction velocity, relaxation velocity, wall motion amplitude and heart rate were expressed as a percentage of baseline normoxic control measurements.

6.2.3 Quantitative PCR

6.6.1.2 Measuring mRNA of genes of interest in the hypoxia-recovery model

At each timepoint in the model described above (Fig 6.1) qPCR was carried out in groups of whole zebrafish embryos 3 dpf and 5 dpf (see section 2.7.2.4). Apelin,

agtrl1a, agtrl1b, HIF-1α, EF1a and ribosomal subunit 18S assays (Table 6.3) were run on each of the samples (10 embryos pooled per sample) against standard curves for each primer-probe set made by serial dilutions of pooled cDNA from all samples. EF1a and 18S reference (housekeeping) gene mRNA did not change across the groups in zebrafish 3 dpf (EF1a P = 0.75 one-way ANOVA; 18S P = 0.24 one-way ANOVA) or 5 dpf (EF1a P = 0.89 one-way ANOVA; 18S P = 0.76 one-way ANOVA). There was also no change in EF1a or 18S mRNA between zebrafish 3 dpf and 5 dpf at any of the timepoints measured (EF1a P = 0.32 two-way ANOVA; 18S P = 0.46 two-way ANOVA) (n = 6 - 8, 10 embryos per timepoint per experiment). Abundance of mRNA of our genes of interest was corrected for the mean of reference genes EF1a and 18S and expressed as a percentage of the normoxic control.

6.2.1.1 Measuring the abundance of HIF-1α mRNA during development

qPCR of HIF-1α mRNA transcript was carried out as described in section 2.7.2.4. RNA was extracted from zebrafish embryos at each of the following developmental time points (8, 18, 24, 36, 48, 72, 96 and 120 hpf) as was previously carried out for apelin, agtrl1a and agtrl1b (see chapter 5). EF1a, RPL13a and HIF-1α assays were run on each of the samples against standard curves for each primer-probe set made by serial dilutions of pooled cDNA from all samples. EF1a and RPL13a mRNA did not change across the groups (EF1a P = 0.06 one-way ANOVA; RPL13a P = 0.43 one-way ANOVA; n = 2 (12 – 15 embryos per time point per experiment)). HIF-1α mRNA abundance was corrected for the reference genes EF1a and RPL13a and expressed as a percentage of abundance at 8 hpf.

Target gene	Accession number	UPL Probe number	Primer sequences (5' – 3')	Product size (bp)
Apelin	NM_001166124	19	F:ACTCCTTTGCGGCAGAATC R:GGAGGGCACTCTAAGCTGTG	138
Agtrl1a	NM_001075105.1	49	F:CTCAGAAGTCAGAGGTGCAGTC R:CCCAGAGTTTTGTCCTCATGT	78
Agtrl1b	NM_001030197.1	24	F:AAAAAGCTCTTCACGCCAGT R:ACTGGGCCTCGGTCTTCT	60
HIF-1α	NM_200233	111	F:AATGATGTCATGCTGCCTTCT R:GTCGTAGCGTGTGAGCTGAG	92
EF1a	NM_131263.1	67	F: CCTTCGTCCCAATTTCAGG R: CCTTGAACCAGCCCATGTT	72
RPL13a	NM_212784.1	3	F: TCCCGTGGATCATATCACTTC R: GGTTTTGTGTGGAAGCATACC	78
18S	BX296557	77	F: CTCAACACGGGAAACCTCAC R: CGCTCCACCAACTAAGAACG	110

Table 6.2: UPL probes and primer sequences for RT qPCR in the zebrafish.

6.3 Results

6.3.1 The effect of hypoxia-recovery on the cardiovascular response in zebrafish embryos

6.3.1.1 Hypoxia-recovery response of embryos 3 dpf compared to embryos 5 dpf

Clear differences were observed in the cardiovascular response of zebrafish 3 dpf and 5 dpf to severe hypoxia (Figs 6.3, 6.4). Zebrafish 3 dpf are less susceptible to a depression in HR and circulation in response to 2h or 4h hypoxia than zebrafish 5 dpf. After exposure to 2h hypoxia, 90% (95% CI 80, 96) more zebrafish 3 dpf had normal HR and circulation than zebrafish 5 dpf ($P < 0.0001$ comparison of proportions); while a larger proportion of zebrafish 5 dpf had reduced HR and circulation than zebrafish 3 dpf. After 4h hypoxic exposure, there were very few embryos with normal heart rate and circulation among zebrafish 3 dpf and zebrafish 5 dpf. There was no difference in the proportions of zebrafish 3 dpf and zebrafish 5 dpf with normal HR and circulation (difference 4% (95% CI 3, 12), $P = 0.32$ comparison of proportions). However, it was noted that a smaller proportion of zebrafish 3 dpf had absent HR and circulation than zebrafish 5 dpf after 4h hypoxia.

After hypoxic exposure, zebrafish were transferred to a normoxic environment. Following 2h hypoxic exposure, the cardiovascular effect of acute hypoxia was observed to recover in the majority of embryos 3 dpf and 5 dpf. As well as being less susceptible to the depression in HR and circulation after the initial hypoxic insult, zebrafish 3 dpf also recovered more rapidly than zebrafish 5 dpf. At 2h recovery, 59% (95% CI 46, 70) more zebrafish 3 dpf had normal HR and circulation than zebrafish 5 dpf ($P < 0.0001$ comparison of proportions). At 4h recovery, 28% (95%

CI 18, 40) more zebrafish 3 dpf had normal HR and circulation than zebrafish 5 dpf ($P < 0.0001$ comparison of proportions) (Fig 6.3).

Following 4h hypoxic exposure, the cardiovascular effect of hypoxia on zebrafish 3 dpf recovered, but zebrafish 5 dpf did not recover. Only 10% of zebrafish 5 dpf had normal HR and circulation after 4h recovery in normoxia. At 2h recovery, 88% (95% CI 77, 95) more zebrafish 3 dpf had normal HR and circulation than zebrafish 5 dpf ($P < 0.0001$ comparison of proportions). At 4h recovery, 83% (95% CI 69, 91) more zebrafish 3 dpf had normal HR and circulation than zebrafish 5 dpf ($P < 0.0001$ comparison of proportions) (Fig 6.4).

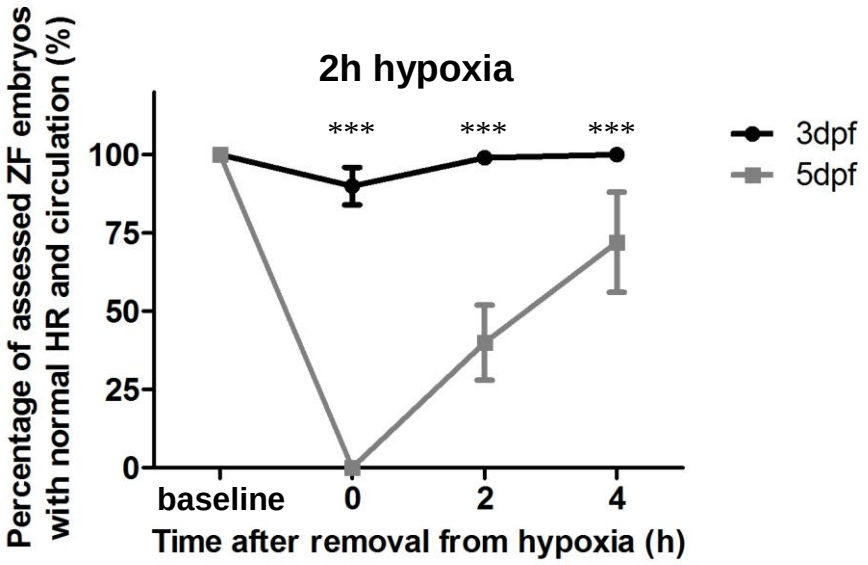

Figure 6.3: The percentage of assessed zebrafish embryos with normal HR and circulation after exposure to 2h hypoxia and 4h normoxia.
*** $P < 0.0001$ comparison of proportions, 3 dpf n = 4, 15 – 20 per experiment; 5 dpf n = 5, 15 – 20 embryos per group per experiment; data plotted as mean ± SEM.

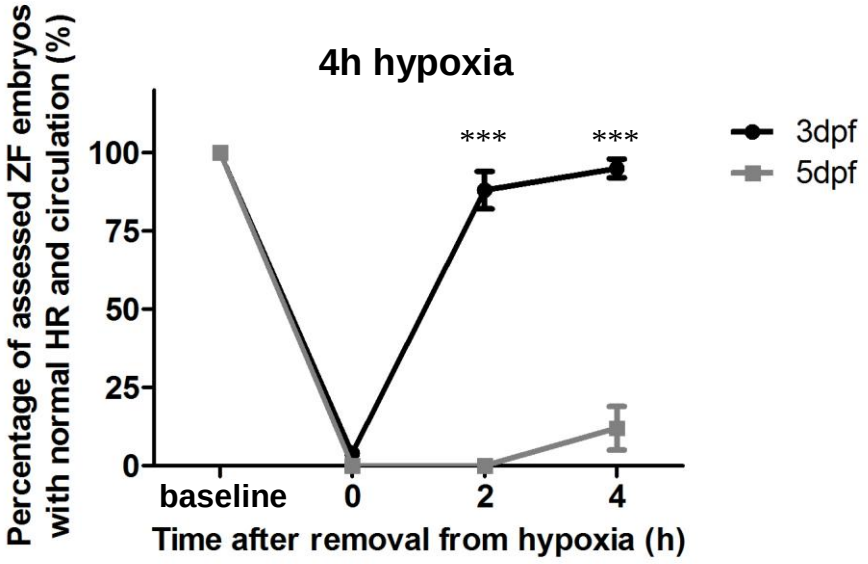

Figure 6.4: The percentage of assessed zebrafish embryos with normal HR and circulation after exposure to 4h hypoxia and 4h normoxia.
*** $P < 0.0001$ comparison of proportions, 3 dpf n = 3, 15 – 20 per experiment; 5 dpf n = 3, 15 – 20 embryos per group per experiment; data plotted as mean ± SEM.

6.3.1.2 Susceptibility to severe hypoxia by developmental stage: ventricle wall motion studies by video edge detection

The observed differences in cardiovascular response to hypoxia were further quantified in terms of cardiovascular function. As developmental stage increased, the depressive effect of hypoxia on wall motion parameters increased. The effect of 2h hypoxia was so profound that no wall motion could be detected. Contraction velocity (P = 0.84 one-way ANOVA, 2 – 4 dpf) and wall motion amplitude (P = 0.28 one-way ANOVA, 2 - 4 dpf) were unchanged across developmental stages. The decrease in relaxation velocity across developmental stages approached significance (P = 0.08 one-way ANOVA, 2 - 4 dpf), while the severity of the depression in HR increased with developmental stage (P = 0.02 one-way ANOVA, 2 - 4 dpf) (Fig 6.5).

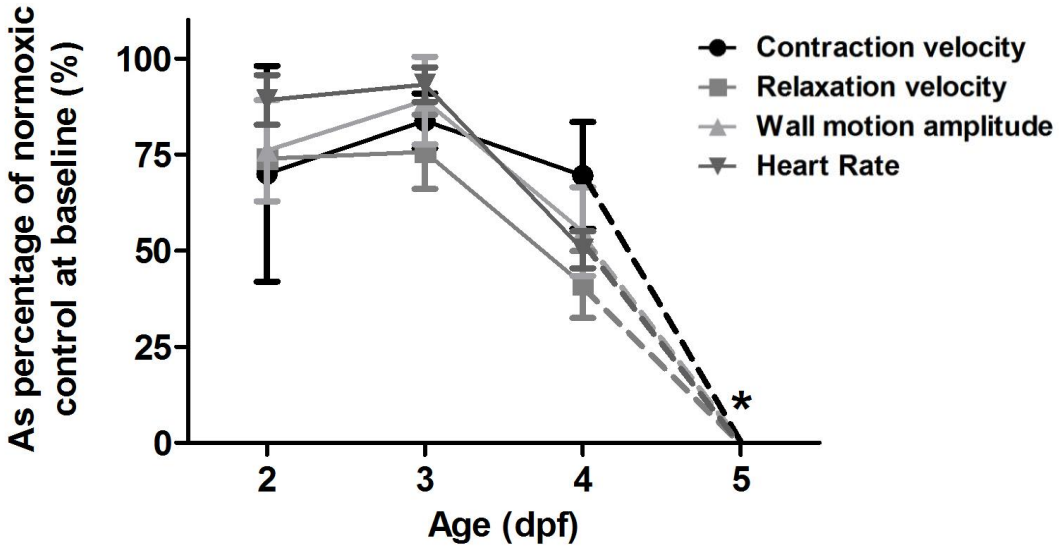

Figure 6.5: Wall motion parameters in zebrafish 2 – 5 dpf exposed to 2h hypoxia.
(i) contraction velocity P = 0.84 one-way ANOVA (2 – 4 dpf), (ii) relaxation velocity P = 0.08 one-way ANOVA (2 – 4 dpf), (iii) wall motion amplitude P = 0.28 one-way ANOVA (2 – 4 dpf), (iv) heart rate P = 0.02 one-way ANOVA (2 – 4 dpf), n = 2 (4 - 6 embryos per experiment), * embryos at 5 dpf had no wall motion following hypoxia in these experiments.

6.3.1.3 mRNA abundance in the apelin and HIF systems in the hypoxia-recovery model

Apelin mRNA was assessed in zebrafish embryos 3 dpf and 5 dpf following 2h and 4h hypoxia. In zebrafish 3 dpf exposure to hypoxia for 2h, resulted in no change in apelin mRNA abundance immediately following hypoxic exposure or during the recovery period (P = 0.10 one-way ANOVA; n = 5 – 8, 10 embryos per group per experiment). In zebrafish 3 dpf exposed to hypoxia for 4h, there was no change in apelin mRNA abundance after hypoxia or recovery in normoxia (P = 0.16 one-way ANOVA) (Fig 6.6 (i)).

In zebrafish 5 dpf exposed to hypoxia for 2h, there were no changes in apelin mRNA immediately after hypoxia or during the recovery phase (P = 0.10 one-way ANOVA). However, in zebrafish 5 dpf exposed to hypoxia for 4h, there was a marked decrease in apelin mRNA immediately after hypoxia. This decrease in apelin mRNA was maintained throughout the 4h normoxic recovery period (P = 0.02 one-way ANOVA) (Fig 6.6 (ii)).

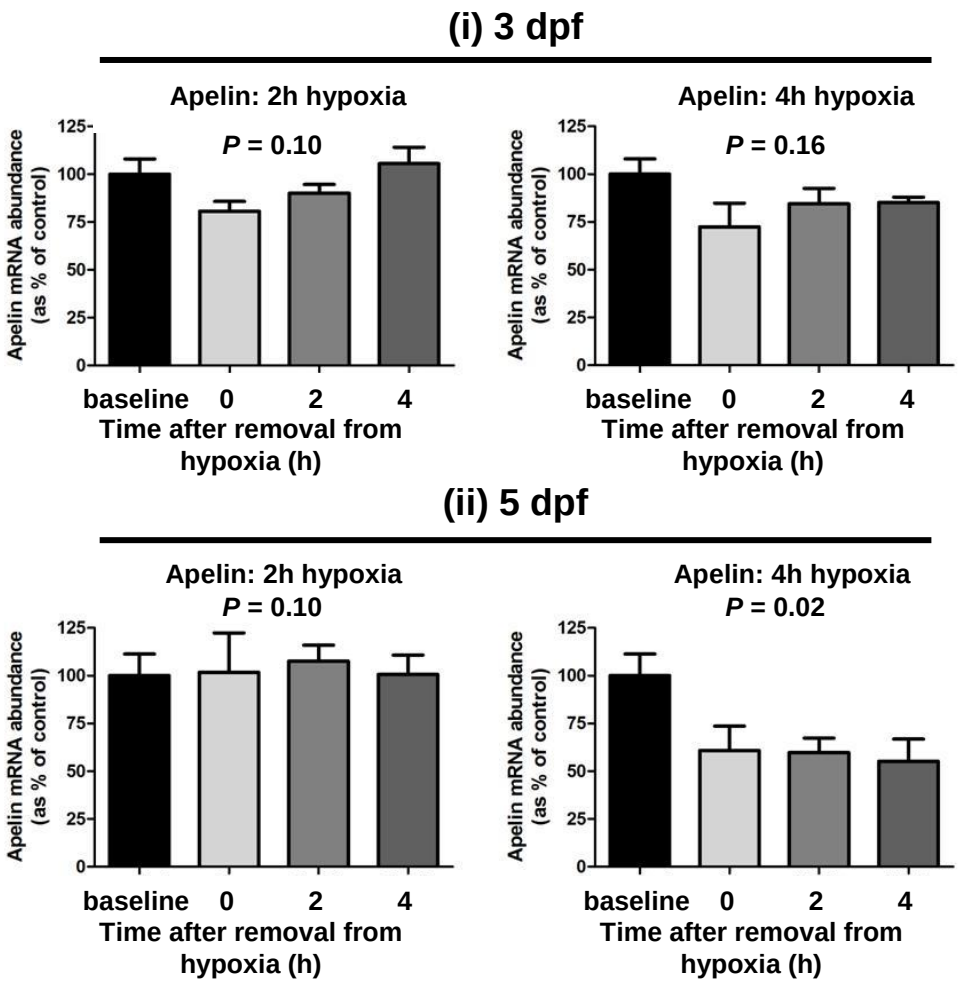

Figure 6.6: The abundance of apelin mRNA transcript as determined by qPCR in zebrafish 3 dpf (i) and 5 dpf (ii) following 2h and 4h hypoxia and subsequent recovery in normoxia.
P is the result of a one-way ANOVA; n = 5 – 8, 10 embryos per group.

The abundance of mRNA transcript of apelin receptors, agtrl1a and agtrl1b, were also determined following hypoxia. In a similar pattern to that of apelin mRNA, agtrl1a mRNA abundance was decreased following 2h hypoxia in zebrafish 3 dpf, but recovered following 4h in normoxia (P = 0.048 one-way ANOVA, n = 5 – 8, 10 embryos per group per experiment). In zebrafish 3 dpf, exposed to 4h hypoxia, no change in agtrl1a mRNA abundance was observed immediately after hypoxia. No difference in agtrl1a mRNA abundance was observed following 2h in normoxia or recovery in normoxia (*P* = 0.50 one-way ANOVA) (Fig 6.7 (i)).

In zebrafish 5 dpf exposed to 2h hypoxia, no change in agtrl1a mRNA was detected immediately following hypoxia. At 2h and 4h post-hypoxia, the abundance of agtrl1a mRNA was decreased by around 50%, although this did not reach significance (*P* = 0.28 one-way ANOVA). This was in contrast to apelin mRNA in this group which did not change following hypoxia or recovery. However, in a similar pattern to that of apelin mRNA abundance, in zebrafish 5 dpf exposed to 4h hypoxia, a decrease of around 40% in agtrl1a mRNA abundance was observed. This decrease in agtrl1a mRNA expression did not recover 4h post-hypoxia although this pattern did not reach statistical significance (*P* = 0.21 one-way ANOVA) (Fig 6.7 (ii)).

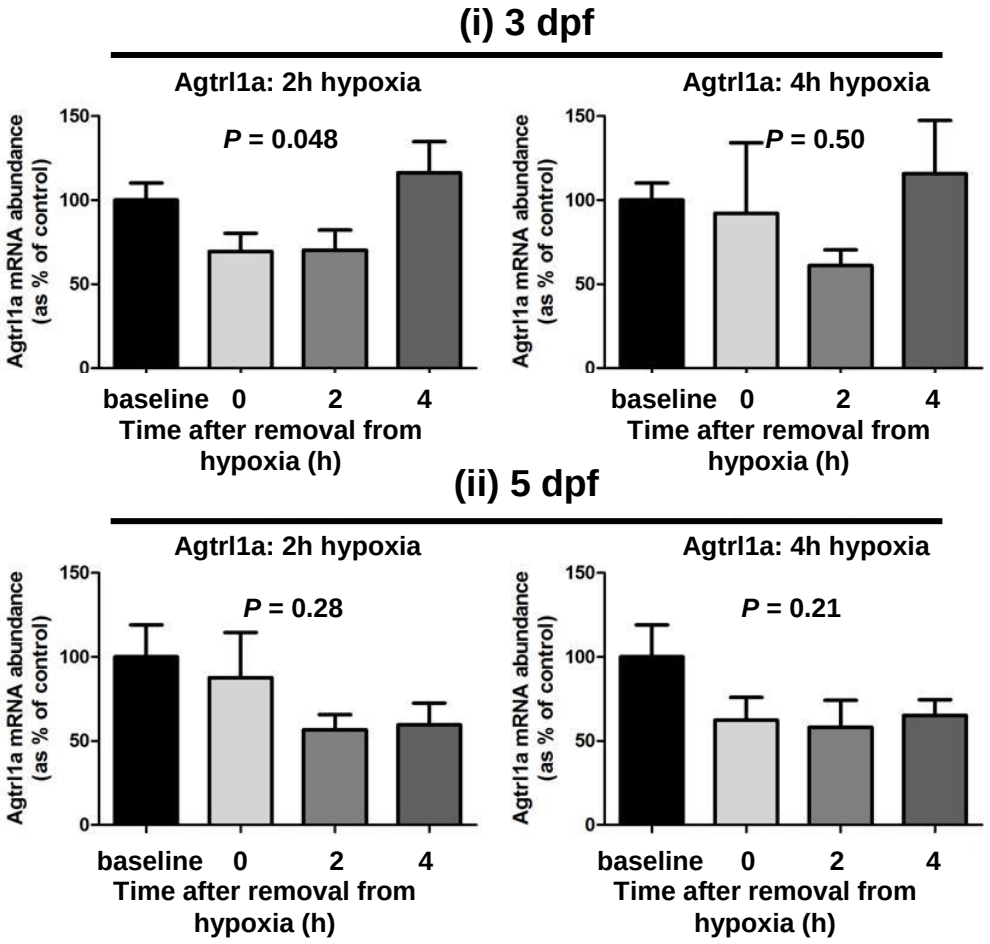

Figure 6.7: The abundance of agtrl1a mRNA transcript in zebrafish 3 dpf (i) and 5 dpf (ii) exposed to 2h and 4h hypoxia and subsequent recovery in normoxia.
P is the result of a one-way ANOVA; n = 5 – 8, 10 embryos per group.

Agtrl1b mRNA abundance was unchanged in zebrafish 3 dpf exposed to 2h hypoxia. No change in agtrl1b mRNA abundance was observed in this group 2h post-hypoxia which recovered 4h post-hypoxia (P = 0.46 one-way ANOVA, n = 5 – 8, 10 embryos per group per experiment). In zebrafish 3 dpf exposed to 4h hypoxia, agtrl1b mRNA abundance was more variable than in the other groups and no changes in abundance of the transcript were observed after hypoxic exposure or during the recovery phase (P = 0.71 one-way ANOVA) (Fig 6.8 (i)).

There was also no change in agtrl1b mRNA abundance in zebrafish 5 dpf exposed to 2h hypoxia and subsequent recovery (P = 0.14 one-way ANOVA). Agtrl1b mRNA abundance was unchanged in zebrafish 5 dpf exposed to 4h hypoxia, immediately after hypoxic exposure and during recovery in normoxia (P = 0.94 one-way ANOVA) (Fig 6.8 (ii)).

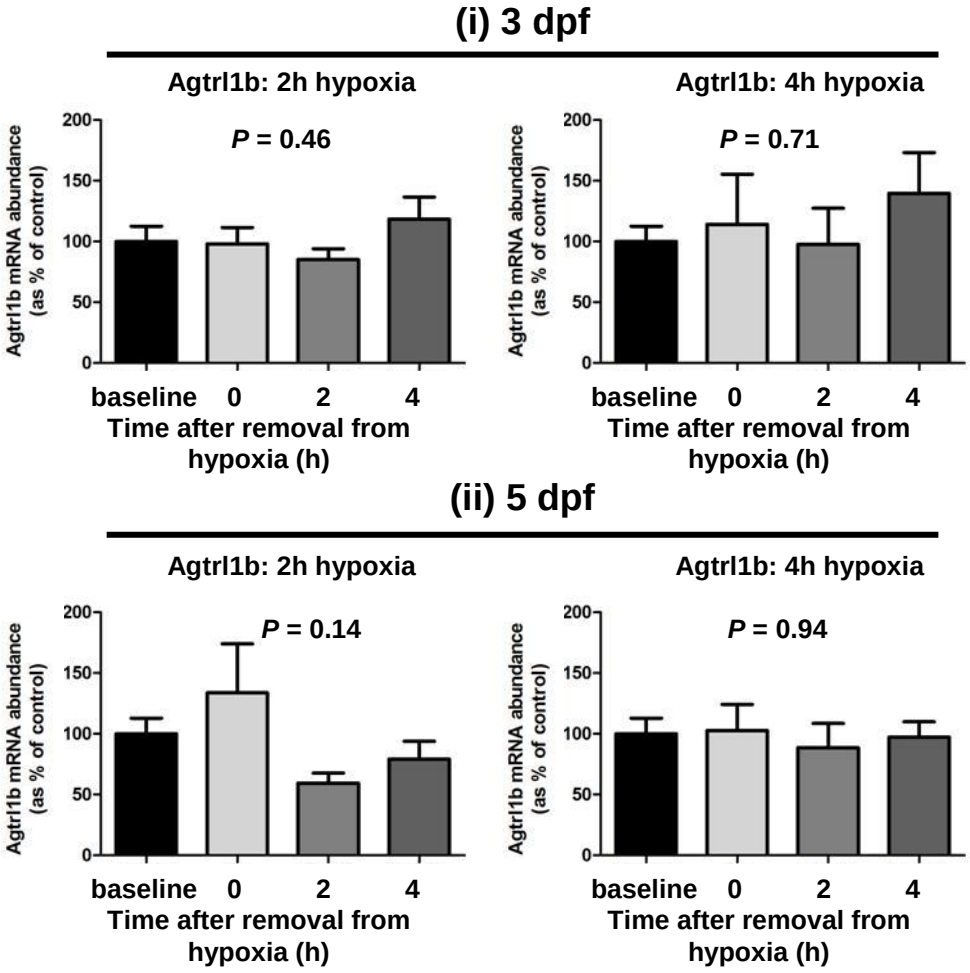

Figure 6.8: The abundance of agtrl1b mRNA transcript in zebrafish 3 dpf (i) and 5 dpf (ii) exposed to 2h and 4h hypoxia and subsequent recovery in normoxia.
P is the result of a one-way ANOVA; n = 5 – 8, 10 embryos per group.

The abundance of HIF-1α mRNA transcript was assessed during development (8 – 120 hpf) and subsequently in response to hypoxia at 72 hpf (3 dpf) and 120 hpf (5 dpf). HIF-1α mRNA abundance was highest at 8 - 18 hpf and lowest at 96 hpf of the measured developmental stages (Fig 6.9).

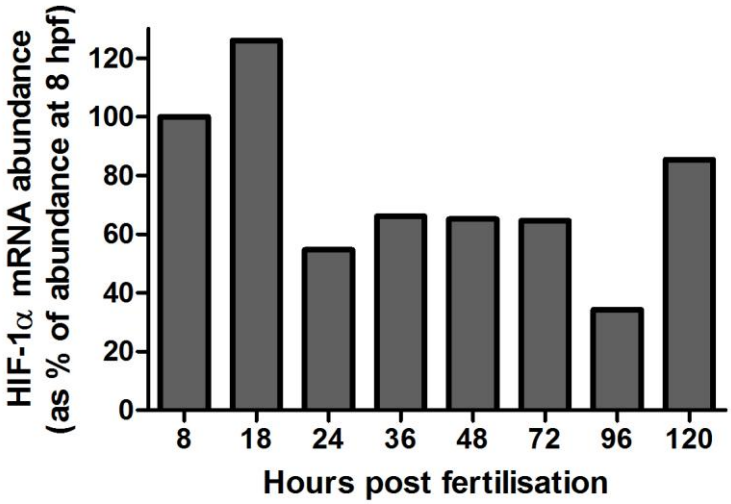

Figure 6.9: HIF-1α mRNA abundance in zebrafish embryos during development from 8 hpf to 120 hpf.
Abundance of mRNA measured by qPCR (corrected for EF1a and RPL13a as reference genes and expressed as a percentage of the abundance at 8 hpf). n = 2 (12-15 embryos per timepoint per experiment).

In zebrafish 3 dpf exposed to 2h hypoxia and 4h hypoxia, HIF-1α mRNA abundance was increased (2h hypoxia: $P = 0.39$ one-way ANOVA, 4h hypoxia: $P = 0.68$ one-way ANOVA; n = 5 – 8, 10 embryos per group per experiment) although this did not reach statistical significance. At 2h and 4h recovery in normoxia following both lengths of hypoxic exposure there appeared to be a reduction of HIF-1α mRNA back to control levels (Fig 6.10 (i)).

In zebrafish 5 dpf, exposed to 2h hypoxia, there were no changes in HIF-1α mRNA as a result of hypoxic treatment or recovery in normoxia ($P = 0.95$ one-way ANOVA). In zebrafish 5 dpf, exposed to 4h hypoxia, HIF-1α mRNA was unchanged following hypoxia, but there was a small increase in HIF-1α mRNA 4h post-hypoxia. However, this did not reach statistical significance ($P = 0.94$ one-way ANOVA) (Fig 6.10 (ii)).

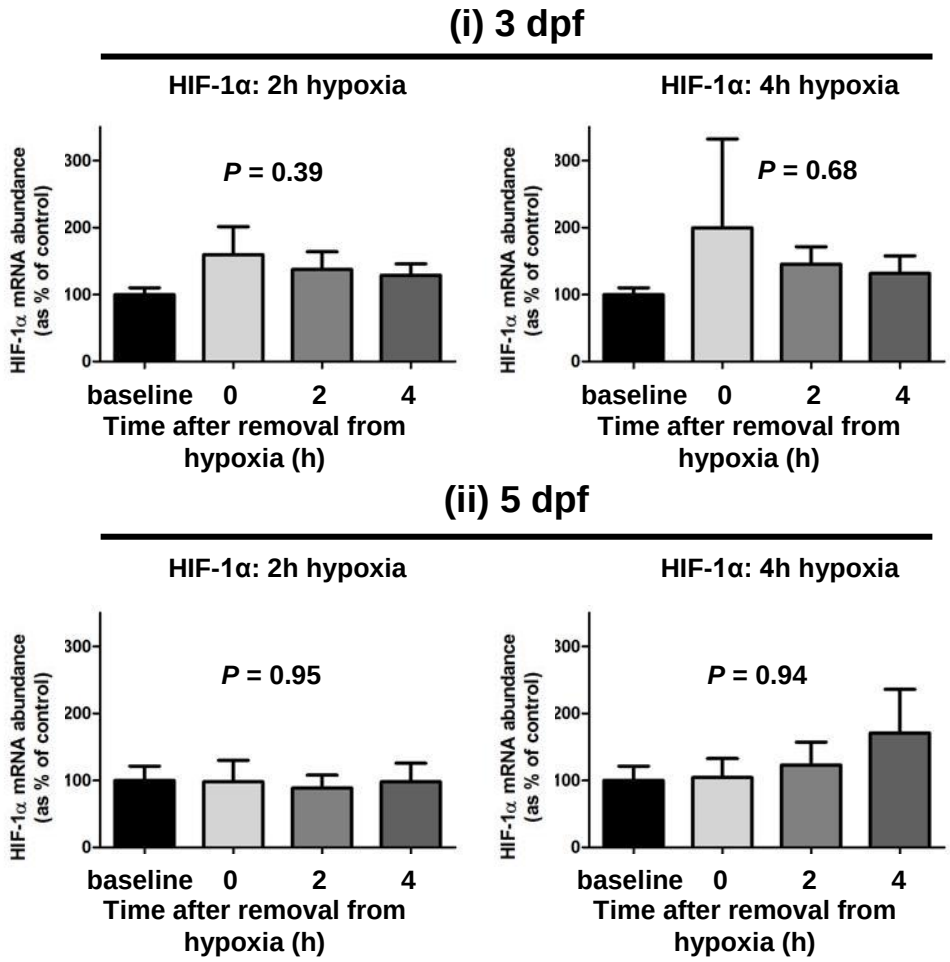

Figure 6.10: The abundance of HIF-1α mRNA transcript in zebrafish 3 dpf (i) and 5 dpf (ii) exposed to 2h and 4h hypoxia and subsequent recovery in normoxia.
P is the result of a one-way ANOVA; n = 5 – 8, 10 embryos per group.

6.3.2 The effect of pharmacological agents on the hypoxia-recovery response in zebrafish embryos

6.3.2.1 Global circulatory hypoxia-recovery model

Using the global circulatory hypoxia-recovery model, we assessed a number of pharmacological agents (apelin, nicorandil, glibenclamide, desferrioxamine and α-ketoglutarate) for their potential cardioprotective effect when added to the bathing water. In zebrafish embryos 5 dpf (n = 3, 10 embryos per group per experiment), pyr-apelin-13 (150 nM) did not affect the proportion of embryos with normal HR and circulation following hypoxia (difference 27% (95% CI 0, 50), P = 0.06 comparison of proportions). There was also no effect of apelin on the recovery phase at 2h (difference 10% (95% CI 15, 34), P = 0.57 comparison of proportions) or 4h (difference 0% (95% CI -26, 26), P = 0.79 comparison of proportions) in this model (Fig 6.11(i)).

The potassium channel activator, nicorandil (0.1 mM), did not affect the proportion of observed embryos with normal HR and circulation immediately after hypoxia (difference 6.3% (95% CI 5.9, 20.8), P = 0.47 comparison of proportions, n = 3, 10 embryos per group per experiment). There was also no difference in the proportion of embryos with normal HR and circulation following 2h recovery in normoxia (difference 9.4% (95% CI 15.4, 33.1) P = 0.59 comparison of proportions). Similarly, after 4h recovery in normoxia there was no difference in the proportion of embryos with normal HR and circulation (difference 0% (95% CI -25.0, 25.0), P = 0.80 comparison of proportions) (Fig 6.11(ii)).

Glibenclamide (0.1 mM), a potassium channel inhibitor, did not affect the global circulatory response to acute hypoxia in this model when compared to vehicle treated controls immediately after hypoxic exposure (difference 10% (95% CI -4.4, 26.5) *P* = 0.24 comparison of proportions, n = 3, 10 embryos per group per experiment). There was also no difference in the proportion of embryos with normal HR and circulation in glibenclamide and vehicle treated groups following 2h recovery in normoxia (difference 13.5% (95% CI -4.4, 31.7) *P* = 0.19 comparison of proportions) or 4h recovery in normoxia (difference 0% (95% CI -26.0, 26.0), *P* = 0.79 comparison of proportions) (Fig 6.11(iii)).

The HIF-1α activator, desferrioxamine (DFO) (0.1 mM), did not affect the proportion of embryos with normal HR and circulation following 2h hypoxia (difference 11.7% (95% CI 0.4, 23.8), *P* = 0.07 comparison of proportions, n = 4, 15 – 20 embryos per group per experiment). However, following 2h recovery in normoxia 31.1% (95% CI 14.6, 45.9) more desferrioxamine treated embryos had normal HR and circulation than vehicle treated embryos (*P* = 0.0002 comparison of proportions). Following 4h recovery in normoxia, 27.1% (95% CI 9.9, 42.7) more desferrioxamine treated embryos had normal HR and circulation than vehicle treated embryos (*P* = 0.002 comparison of proportions) (Fig 6.11(iv)).

The HIF-1α inhibitor, α-ketoglutarate (2.5 mM), did not affect the proportion of embryos with normal HR and circulation following 2h hypoxia (difference 10% (95% CI -4.0, 26.5), *P* = 0.24 comparison of proportions, n = 3, 10 embryos per group per experiment), but reduced the effect of severe hypoxia on the gross

circulatory response during the recovery phase. Following 2h recovery in normoxia 40% (95% CI 12.8, 61.4) more α-ketoglutarate incubated embryos had normal HR and circulation than those incubated in vehicle (*P* = 0.004 comparison of proportions). The protective effect of α-ketoglutarate was maintained after 4h recovery in normoxia when 36.7% (95% CI 9.6, 58.6) more α-ketoglutarate incubated embryos had normal HR and circulation than those incubated in vehicle (*P* = 0.009 comparison of proportions) (Fig 6.11(v)).

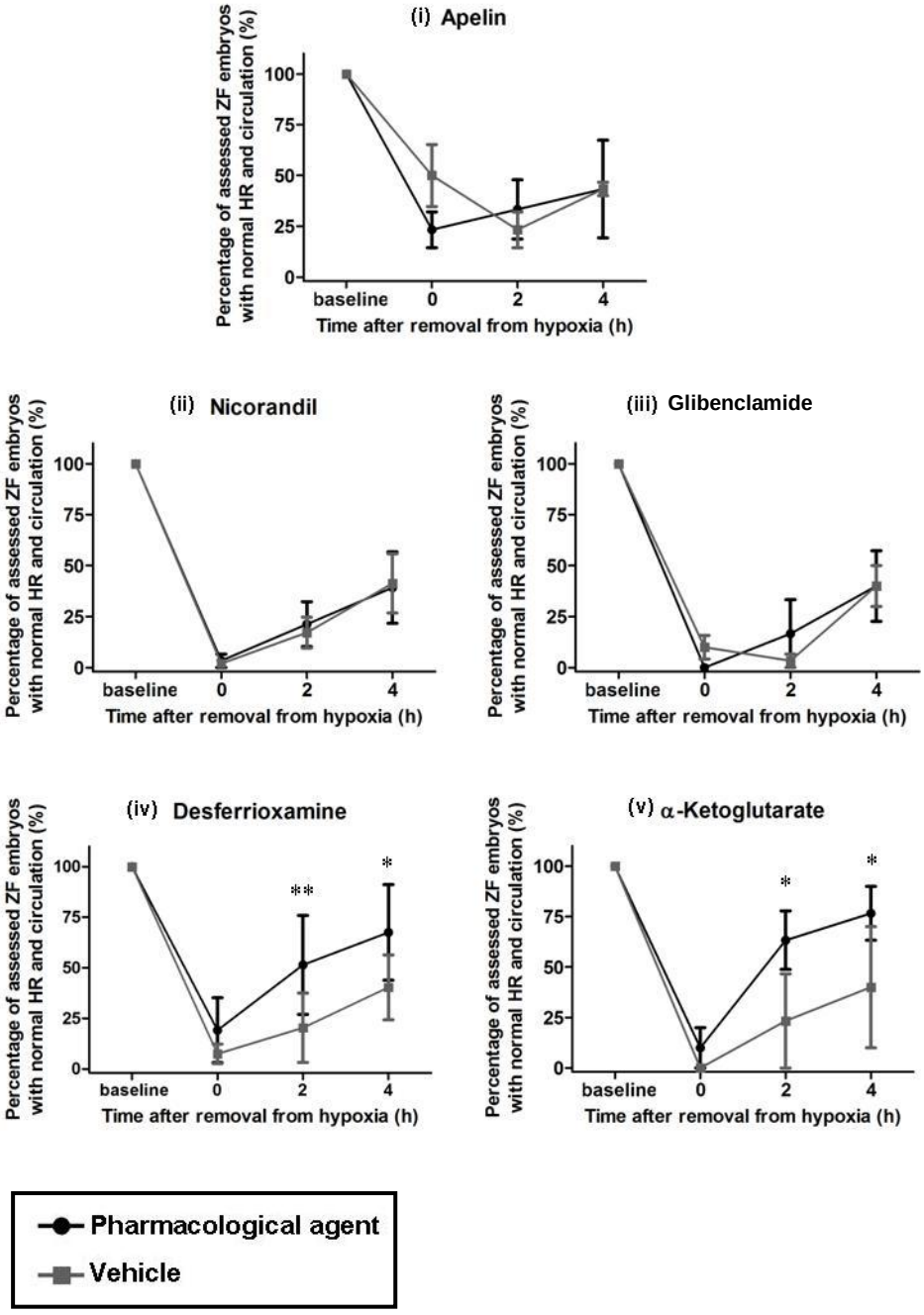

Figure 6.11: The effect of pharmacological agents on the global hypoxia-recovery response.
(i) Pyr-apelin-13 $P > 0.01$ comparison of proportions, (ii) nicorandil $P > 0.01$ comparison of proportions, (iii) glibenclamide $P > 0.01$ comparison of proportions, (iv) desferrioxamine $P = 0.07$ (0h) ** $P = 0.0002$ (2h) * $P = 0.002$ (4h) comparison of proportions, (v) α-ketoglutarate $P = 0.24$ (0h) * $P = 0.004$ (2h) * $P = 0.009$ (4h) comparison of proportions. n = 3 – 4, 10 – 20 embryos per group per experiment.

6.3.2.2 Video edge detection of cardiac function during hypoxia-recovery

Further experiments assessing the effect of apelin and desferrioxamine on ventricle wall motion during the hypoxia-recovery response were performed. Video edge detection experiments assessing the cardioprotective effect of apelin were performed in zebrafish 3 dpf. We observed that the depression in HR following acute hypoxic exposure and subsequent recovery in normoxia in zebrafish 3 dpf was similar in both apelin and vehicle treated embryos (P = 0.34 two-way ANOVA apelin vs vehicle; n = 8, 3 - 5 embryos per group per experiment; Fig 6.12(iv)). Contraction velocity was decreased in vehicle treated embryos, but not in apelin treated embryos after removal from hypoxia (P = 0.03 two-way ANOVA apelin vs vehicle). The depression in contraction velocity in vehicle treated embryos was reversed by 2h in normoxia (Fig 6.12(i)).

Relaxation velocity and wall motion amplitude displayed a trend towards apelin incubated zebrafish being less susceptible to the effects of acute hypoxia, but this did not reach statistical significance. Relaxation velocity was decreased by 27 ± 6% in vehicle treated embryos and by 5 ± 9% in apelin treated embryos (P = 0.09 two-way ANOVA apelin vs vehicle). Apelin treated embryos recovered to normoxic control levels following 1h in normoxia, while vehicle treated embryos recovered by 2h in normoxia (Fig 6.12(ii)). Wall motion amplitude was decreased by 13 ± 7% in vehicle treated embryos, but not in apelin treated embryos. At 1h recovery in normoxia, both groups had a wall motion amplitude comparable with normoxic control embryos (P = 0.09 two-way ANOVA apelin vs vehicle; Fig 6.12(iii)).

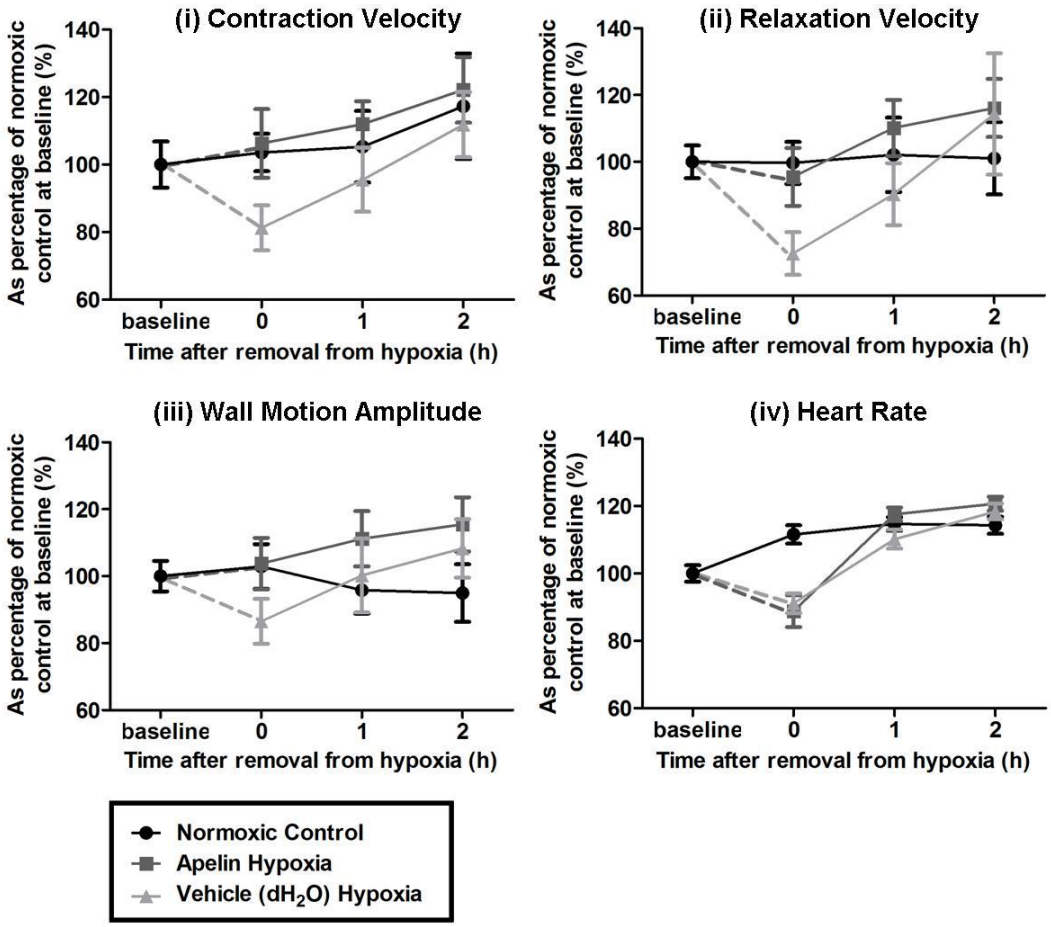

Figure 6.12: The effect of pyr-apelin-13 (150 nM) incubation on wall motion parameters of the zebrafish (3 dpf) ventricle in the hypoxia-recovery model.
(i) Contraction velocity $P = 0.03$ two-way ANOVA apelin vs vehicle, (ii) relaxation velocity $P = 0.09$ two-way ANOVA apelin vs vehicle, (iii) wall motion amplitude $P = 0.09$ two-way ANOVA apelin vs vehicle, (iv) heart rate $P = 0.34$ two-way ANOVA apelin vs vehicle; n = 8, 3 - 5 embryos per group.

Desferrioxamine protected against the depression in contraction velocity following hypoxia in zebrafish 5 dpf (P = 0.015 two-way ANOVA DFO vs vehicle; Fig 6.13 (i)). Relaxation velocity was decreased in vehicle treated embryos, but not in desferrioxamine treated embryos (P < 0.0001 two-way ANOVA DFO vs vehicle; Fig 6.13 (ii)). Contraction velocity and relaxation velocity recovered in both desferrioxamine and vehicle treated groups.

The depression in wall motion amplitude following hypoxia was also protected by incubation in desferrioxamine (P = 0.0008 two-way ANOVA DFO vs vehicle; Fig 6.13 (iii)). Wall motion amplitude remained reduced in vehicle treated embryos following 2h recovery in normoxia. The depression in HR was similar in both desferrioxamine and vehicle treated embryos, although there was a trend towards HR recovering more quickly in normoxia in desferrioxamine treated embryos than in those treated in vehicle (P = 0.06 two-way ANOVA DFO vs vehicle; Fig 6.13 (iv)).

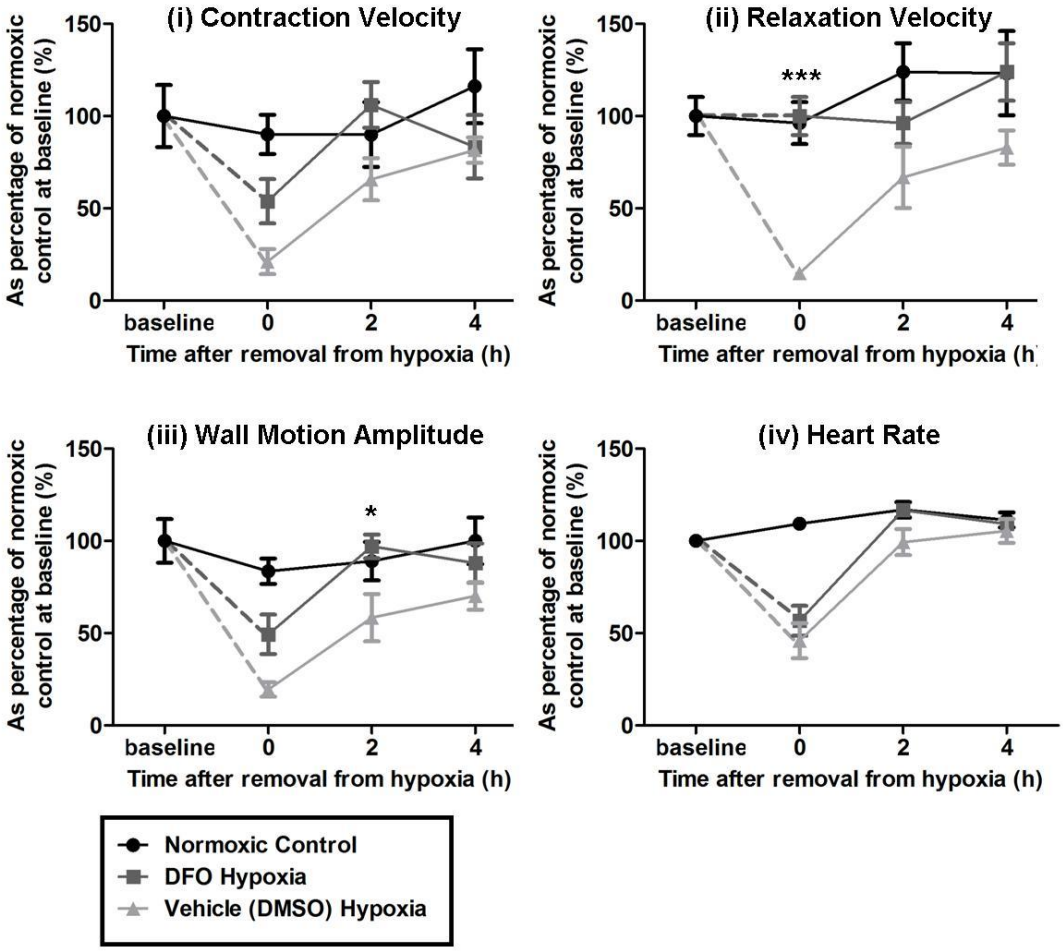

Figure 6.13: The effect of desferrioxamine (0.1 mM) incubation on wall motion parameters of the zebrafish (5 dpf) ventricle wall in the hypoxia-recovery model.

(i) Contraction velocity $P = 0.015$ two-way ANOVA DFO vs vehicle, (ii) relaxation velocity $P < 0.0001$ two-way ANOVA DFO vs vehicle, (iii) wall motion amplitude $P = 0.0008$ two-way ANOVA DFO vs vehicle, (iv) heart rate $P = 0.064$ two-way ANOVA DFO vs vehicle; n = 1, 5 embryos per group.

6.3.2.3 The effect of hypoxia-recovery in MO-apelin embryos

MO-apelin embryos 3dpf did not have an altered response to hypoxic exposure compared to that of MO-mispair (P = 0.99 comparison of proportions) or non-injected control zebrafish embryos (P = 0.99 comparison of proportions) (n = 1, 7 - 10 embryos per group) (Fig 6.14).

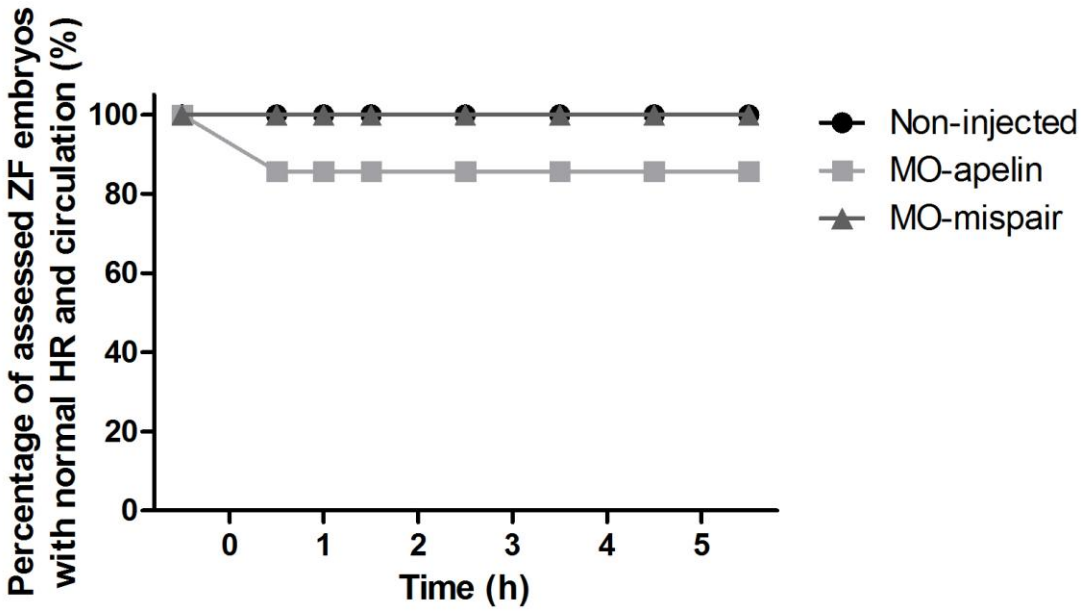

Figure 6.14: The response to hypoxia of MO-apelin, MO-mispair and non-injected controls (3 dpf).
Embryos were exposed to hypoxia and viewed briefly in normoxia at 30 minute intervals for the first 1.5 h and one hour intervals thereafter for a total time of 5.5 h. MO-apelin vs MO-mispair P = 0.99, MO-apelin vs non-injected control P = 0.99 comparison of proportions; n = 1, 7 – 10 embryos per group.

6.4 Discussion

As apelin had been reported to be cardioprotective in rodent studies (Jia *et al.*, 2006; Kleinz *et al.*, 2008; Simpkin *et al.*, 2007), I developed a hypoxia-recovery model in zebrafish embryos to test the hypothesis that exogenous apelin would protect against hypoxic injury in wild-type embryos. We hypothesised that hypoxia would increase apelin mRNA and that an increase in apelin mRNA would arise following induction of HIF-1α.

In order to test our hypothesis that apelin had a cardioprotective role, we developed a hypoxia-recovery model, firstly using a semi-quantitative scoring method and subsequently using video edge detection. In the development of our hypoxia-recovery model, we identified that with increasing age in the developmental period of the embryo (2 - 5 dpf) comes an increasing susceptibility to the cardiovascular effects of a severe hypoxic insult. We demonstrated that a semi-quantitative scoring method of HR and circulation was sensitive enough to detect differences between embryos 3 dpf and 5 dpf and allowed us to perform experiments with greater numbers of embryos. Increasing susceptibility to hypoxia with increasing developmental stage has been previously reported in the literature (Ton *et al.*, 2003), but this is the first study which has quantified the differences in term of contraction velocity, relaxation velocity and wall motion amplitude of the zebrafish embryo ventricle wall.

Despite the reproducibility of the model and its potential to screen compounds, it did have some limitations. In particular, to ensure that hypoxia was in fact induced in the

model, future experiments should involve degassing the solution overnight in the hypoxia chamber before adding the embryos and compounds. Induction of HIF-1α in zebrafish embryos exposed to hypoxia following overnight equilibration of the hypoxic water in a hypoxia chamber has been previously reported (Gray *et al.*, 2007). It would also have added to the model presented here if the oxygen concentration of the water throughout these experiments. Despite this, we have strong evidence that hypoxia was indeed induced in the model as we consistently observed a depression of cardiovascular which was reversible following removal from hypoxia.

Exogenous pyr-apelin-13 added to the bathing water did not protect against the depression in HR and circulation in response to severe hypoxia in zebrafish 5 dpf. Zebrafish embryos incubated in apelin did not recover more quickly than vehicle treated controls. However, using video edge detection in zebrafish 3 dpf we demonstrated that contraction velocity was less severely affected by hypoxia in apelin incubated embryos compared to vehicle incubated embryos. We also observed a trend towards relaxation velocity and wall motion amplitude being less severely affected by hypoxia in apelin treated embryos. Interestingly, HR was affected to the same degree following hypoxic exposure in both apelin and vehicle treated embryos. In preliminary experiments, in MO-apelin embryos in which apelin mRNA had been knocked down, we were unable to detect a difference in their cardiovascular response to severe hypoxia compared to MO-mispair embryos and non-injected controls.

The developed model could also be used to screen other pharmacological agents that may affect the hypoxia-recovery response. Activating and inhibiting potassium channels with nicorandil and glibenclamide respectively did not affect the number of embryos with normal HR and circulation in response to acute hypoxia or affect the rate at which the embryos recovered normal circulation during recovery in normoxia.

In particular we attempted to modulate endogenous apelin mRNA by influencing the HIF pathway. Apelin gene expression has been previously shown to be upregulated via HIF (Glassford *et al.*, 2007). Exposure of cultured adipocytes to hypoxia (1% oxygen) for 6h increased apelin mRNA expression as shown by qPCR. Apelin protein levels were also increased as shown by enzyme-linked immunosorbent assay. Mouse embryonic fibroblasts from HIF-1α knockout mice did not exhibit an increase in apelin mRNA in response to hypoxia, thus demonstrating that the increase in apelin expression in response to hypoxia is mediated via HIF-1α in these cells (Glassford *et al.*, 2007).

In a rat *in vivo* model of coronary artery ligation, apelin mRNA expression and APJ mRNA expression was increased in quadriceps muscle at 4 weeks post ligation and in the heart 8 weeks post ligation. Coronary artery ligation did not affect apelin mRNA or APJ mRNA in lung tissue at 4 weeks or 8 weeks post ligation. HIF-1α mRNA was increased in quadriceps muscle at 4 weeks post ligation, but HIF-1α mRNA expression was not reported for the heart or lungs. Continual systemic hypoxia (10% oxygen) for 1 week resulted in a 7-fold increase in apelin mRNA expression (Sheikh *et al.*, 2008). Eyries *et al.* (2008) also demonstrate in mice that

systemic hypoxia (10% oxygen) for 5h increases apelin mRNA expression almost 2-fold in the lung.

However, analysis of the abundance of mRNA transcripts in zebrafish embryos exposed to hypoxia did not support the hypothesis that an increase in HIF-1α following severe hypoxia results in increased apelin mRNA. In zebrafish 5 dpf, 2h hypoxia had no effect on HIF-1α or apelin mRNA levels. Yet a marked reduction in apelin mRNA was observed in embryos exposed to 4h hypoxia and after subsequent exposure to normoxia. This decrease in abundance of apelin mRNA was not associated with changes in HIF-1α mRNA. As this marked reduction was demonstrated in embryos 5 dpf exposed to 4h hypoxia which do not recover well from hypoxia, it is important to note that mRNA may be less stable in these hypoxic tissues and that although the reference genes used did not change across these groups, it is possible that apelin mRNA is less stable under hypoxic conditions. This has been previously demonstrated in the case of tumour necrosis factor α in human macrophages (Werno *et al.*, 2010).

Our mRNA expression studies represent the mRNA of 10 - 15 whole embryos pooled for each sample. This may account for the observation that there is no marked increase in the abundance of HIF-1α mRNA transcript following hypoxia. Increases in HIF-1α mRNA expression may be tissue specific, occurring in the embryonic heart or muscle, but not in other tissues. Tissue specific increases in HIF-1α, apelin and APJ mRNA have been demonstrated previously in the mouse (Sheikh *et al.*, 2008). Cardiac specific transcription of monocarboxylate transporters, involved in

the cellular transportation of important metabolites such as pyruvate, has been observed in adult zebrafish in response to chronic hypoxia for 48h and 96h (Ngan *et al.*, 2009). It is also a possibility that our acute hypoxic exposure was not sufficient for transcription to take place. In chronic hypoxia studies (5% oxygen, 24h) in zebrafish embryos 2 dpf, HIF-1α mRNA expression has been reported to increase 3-fold as detected by microarray (Ton *et al.*, 2003). In a cell culture system a 6h exposure to hypoxia (1% oxygen) was sufficient to observe induction of HIF-1α and apelin mRNA expression (Glassford *et al.*, 2007). In a mouse model of coronary artery ligation, increases in HIF-1α and apelin mRNA expression in the quadriceps muscle were observed only after a period of 4 weeks (Sheikh *et al.*, 2008).

Interestingly, both inhibition and activation of the HIF pathway had the same effect in the hypoxia-recovery model. Inhibition of the HIF pathway with α-ketoglutarate did not change the number of observed embryos with normal HR and circulation following hypoxic exposure, but did increase the ability of the embryos to recover. Activation of the HIF pathway with desferrioxamine produced similar findings. Embryos incubated in desferrioxamine were not protected from the cardiovascular effects of hypoxia immediately after hypoxic exposure. Yet, at 2h and 4h recovery in normoxia the proportion of embryos with normal HR and circulation was significantly greater in desferrioxamine treated embryos when compared to vehicle treated embryos. Using video edge detection, we further quantified the cardioprotective effect of desferrioxamine. The recovery in contraction velocity, relaxation velocity and wall motion amplitude following hypoxia was significantly enhanced in desferrioxamine treated embryos compared to vehicle treated controls.

We conclude that the protective effect of desferrioxamine is not likely to be due to the protective effect of endogenous apelin since we observed a reduction of apelin mRNA with increasing HIF-1α mRNA in our model. The observation that both inhibition and activation of the HIF-1α pathway had similar effects suggests that one or both of these compounds are having a protective effect via a mechanism unrelated to HIF.

The protective action of desferrioxamine may be due to its action as an iron chelator. Iron chelation has been shown to be important in free radical termination in a variety of studies (Morel *et al.*, 1992; Prus *et al.*, 2009; see Bendova *et al.*, 2010). Desferrioxamine has been used previously in an assay to identify neuroprotectant compounds in embryonic zebrafish (Parng *et al.*, 2006). Incubation in L-hydroxyglutaric acid caused apoptosis in the embryonic brain. Subsequent incubation in desferrioxamine reversed the apoptosis in a concentration-dependent manner. The concentration with maximal effect (0.1 mM) was the same as the concentration used in our study. Parng *et al*. (2006) reason that the neuroprotective effect of desferrioxamine observed in their model is due to its antioxidant activity. The same may be true in our hypoxia-recovery model. This would explain why no difference was observed immediately after hypoxia, but the protective effect of desferrioxamine was more apparent in the recovery phase where free radical generation would be expected to occur. In ischaemia-reperfusion models in rodents, free radicals are generated during the reperfusion phase (Khan *et al.*, 2010; Thu *et al.*, 2010) which we would liken to the recovery phase in our zebrafish model.

Alternatively, the accumulation of HIF-1α as a result of desferrioxamine incubation may result in cardioprotection via induction of another HIF inducible gene such as erythropoetin, tranferrin or vascular endothelial growth factor among others (see Semenza, 2009). In human endothelial cell culture, it has been demonstrated that more than 2% of human genes are regulated by HIF-1 (Manalo *et al.*, 2005). Therefore, in zebrafish embryos, it is also possible that the protective action of desferrioxamine is acting via another protective pathway induced by HIF. However, our mRNA data show no induction of HIF-1α mRNA in untreated zebrafish 5 dpf exposed to 2h hypoxia which was the age of embryo and length of exposure to hypoxia in which we observed a cardioprotective effect of desferrioxamine. This leads us to conclude that desferrioxamine is most likely to have its protective effect in this model by an antioxidant effect, probably as a result of iron chelation.

The HIF-1α pathway inhibitor, α-ketoglutarate, had no effect on the proportion of embryos with normal HR and circulation, but increased the rate of recovery in normoxia. Although inhibiting HIF may be expected to detrimental to the potential of the embryos to maintain normal HR and circulation following acute hypoxic exposure (see Tekin *et al.*, 2010), α-ketoglutarate may be acting as a metabolic substrate in this model. Alpha-Ketoglutarate is an intermediate in the tricarboxylic acid cycle which is responsible for generation of adenosine trisphosphate (ATP), or cellular energy, during aerobic respiration. Therefore, in the presence of oxygen during recovery in normoxia, the incubation of embryos in α-ketoglutarate, may potentiate the tricarboxylic acid cycle thus generating more cellular energy and allowing the embryos to recover more quickly. Metabolic substrates such as α-

ketoglutarate have been shown to have antioxidant properties in some settings. In cyanide-induced oxidative stress in rat pheochromocytoma cells, α-ketoglutarate incubation diminished the effect of oxidative stress (Satpute *et al.*, 2010), while in rat brain homogenates α-ketoglutarate had a pro-oxidant effect (Puntel *et al.*, 2007). Therefore, the protective effect of α-ketoglutarate is likely to be due to its activity as an essential metabolite or by an antioxidant action.

In conclusion, we have developed a novel model of severe hypoxia-recovery in zebrafish embryos. We demonstrated, and quantified in terms of wall motion of the embryonic ventricle, an increase in susceptibility to hypoxia with increasing embryonic age. We demonstrated a small, convincing cardioprotective effect of exogenous pyr-apelin-13 in zebrafish 3dpf, but not in zebrafish 5 dpf. In zebrafish 5 dpf exposed to 4h hypoxia, apelin mRNA was markedly decreased with no associated increase in HIF-1α mRNA. Following apelin knockdown, the susceptibility of MO-apelin embryos to hypoxia at 3 dpf was not altered. The potassium channel modulators, nicorandil and glibenclamide, did not affect the cardiovascular response to hypoxia or the ability of the zebrafish embryos to recover. However, HIF modulators, desferrioxamine and α-ketoglutarate accelerated recovery from hypoxia. These data indicate, however, that the protective action of desferrioxamine is likely to be due to an antioxidant effect, while the protective action of α-ketoglutarate is likely to be metabolic or antioxidant in nature. The hypoxia-recovery model can be used for further drug screens for potentially cardioprotective drugs.

Chapter 7 Summary and Conclusions

7.1 The effect of apelin on the heart

7.1.1 Rat

The experimental work leading to this thesis aimed to investigate the cardiovascular effects of apelin. The primary aim was to confirm its inotropic effects and its vasoactive role. We then planned to further examine the cardioprotective role of apelin. It was therefore important to establish the effect of apelin on the heart in the normal rat before embarking on studies involving ischaemia. However, in the normal rat, apelin had no effect in isolated right ventricular papillary muscles or isolated right atrial strips. Apelin did not affect developed tension, time to peak or time to relaxation in our experiments. Furthermore, in the isolated, paced, perfused, rat heart (Langendorff) apelin had no inotropic or lusitropic effect.

Conversely, Szokodi *et al*. (2002) demonstrated a potent, sustained inotropic response to infusion of apelin-16 in the rat Langendorff heart. The authors reported a 40 - 50% increase in developed tension after 10 mins of infusion when measured by a transducer attached to the apex of the heart. This was the first report in the literature of apelin's inotropic action. Indeed, the literature since then suggests that apelin has a limited inotropic effect in the normal rat and that its inotropic effect is greater and faster in onset in animals with heart failure, whether induced by coronary artery ligation (Berry *et al.*, 2004) or by chronic isoproterenol treatment (Jia *et al.*, 2006). In isolated right ventricular rat trabeculae, Dai *et al*. (2006) identified a 36% increase in developed tension in trabeculae from animals with heart failure induced by chronic hypoxia, but found no significant change in developed tension in trabeculae from control animals. On contacting several other investigators in the

apelin field, we learned that others had also found little or no inotropic effect in the normal rat heart in these standard physiological preparations (Dr C Terracciano, Imperial College London, Personal Communication), although these negative findings have not been published. Studies assessing the effect of apelin in humans remain unclear. Japp *et al*. (2010) described a small increase in the rate of rise of left ventricular pressure in response to intracoronary bolus injection of apelin-36. However, these authors could not be certain if this increase in contractility was independent of loading conditions.

7.1.2 Zebrafish embryos

In the zebrafish embryo 3 dpf, we demonstrated that apelin had no effect on HR or more sensitive parameters of cardiac function: contraction velocity, relaxation velocity and wall motion amplitude of the ventricle wall. In isolated zebrafish hearts, from embryos with relatively high endogenous apelin mRNA (3 dpf), apelin increased relaxation velocity, but had no effect on HR, contraction velocity and wall motion amplitude of the ventricle wall. In isolated hearts from embryos with relatively low endogenous apelin mRNA (4 dpf), apelin had no effect on any of the measured contractility parameters. Apelin receptors were similarly expressed at both developmental time points (3 dpf and 4 dpf).

7.2 The vasoactive effect of apelin

We also investigated the potential vasoactive effect of apelin. *In vivo* in the normal rat, this study demonstrated a reduction in both MAP and HR in response to apelin-13. The reduction in MAP recovered spontaneously and rapidly, while the reduction in HR had not recovered 20 minutes post apelin administration. This suggests that the reduction in MAP and reduction in HR are mediated via different mechanisms. The reduction in MAP is likely to be a result of a vasodilatory response mediated via NO and is well described in the literature in an *in vivo* rat model (Tatemoto *et al.*, 2001) and in mouse, rat and human *in vitro* preparations (Jia *et al.*, 2007; Salcedo *et al.*, 2007; Zhong *et al.*, 2007a; Zhong *et al.*, 2007b). The decrease in HR has not been previously reported and we postulate that this may be due to a direct action of apelin on the sinoatrial node as vasodilation would have been expected to result in a reflex tachycardia as reported previously with nitrate infusions (Noll *et al.*, 1997) and dihydropyridine calcium antagonists (Erickson *et al.*, 2010). Apelin-16 also produced a decrease in HR, but had no effect on MAP. Yet, pyr-apelin-13 affected neither HR, nor MAP, when administered in an identical way via the jugular vein.

In isolated mesenteric artery, a vasodilator or vasoconstrictor effect with apelin-13 or apelin-36 could not be demonstrated. This was in contrast to human isolated mesenteric arteries which are reported to vasodilate in response to apelin (Salcedo *et al.*, 2007). However, we note that there has been only one published report of a vasoactive effect of apelin in a rat *in vitro* model to date, in the rat renal arterioles (Hus-Citharel *et al.*, 2008). In this preparation, apelin produced a vasodilator and

vasoconstrictor response in the presence and absence of a functional endothelium, respectively.

7.2.1 Activity of apelin isoforms

The twelve terminal amino acids at the C-terminus of the apelin peptide are thought to be responsible for ligand binding to the receptor as apelin fragments shorter than twelve amino acids have no biological activity (De Mota *et al.*, 2000; Reaux *et al.*, 2001). This suggests that all apelin isoforms bind with equal potency and efficacy. Maguire *et al.* (2009) demonstrated that pyr-apelin-13, apelin-13 and apelin-36 have comparable potency and efficacy both in terms of an inotropic action in isolated human trabeculae and a vasodilatory effect in isolated human internal mammary artery. However, the effect of apelin-16 has not been reported in these preparations.

The *in vivo* data presented in this thesis suggest that apelin isoforms may have different properties. Interestingly, the majority of publications describing an inotropic effect of apelin in the rat have studied apelin-16 (Berry *et al.*, 2004; Dai *et al.*, 2006; Farkasfalvi *et al.*, 2007; Szokodi *et al.*, 2002). *In vivo* in the rat, pyr-apelin-13 had no effect on HR or MAP. Apelin-16 consistently decreased HR, but had no effect on MAP. Apelin-13 reduced MAP and HR. The effect on MAP recovered rapidly, while the effect on HR had not recovered 20 minutes after apelin administration.

It is possible that although the apelin fragments bind equally to the receptor, that activation of the downstream signal transduction pathways is dependent upon the

bound apelin isoform, specific tissue type, distribution and accessibility of the receptor and temporal differences in activation of downstream pathways. There is some evidence to suggest that receptor internalisation is related to apelin isoform. Apelin-17 is a more potent inducer of APJ receptor internalisation than pyr-apelin-13 in Chinese hamster ovary cells (El Messari *et al.*, 2004). The authors also demonstrate that the rate of receptor internalisation appears to be related to the magnitude of decrease in MAP, with apelin-17 lowering MAP by 13 mmHg compared to a decrease of 6 mmHg with pyr-apelin-13 when administered intravenously. This provides an interesting avenue for further studies.

7.3 The cardioprotective effects of apelin

Despite the intention to focus on the cardioprotective effects of apelin using the isolated, perfused, rat heart (Langendorff) model which is a widely-used standard preparation for ischaemia-reperfusion studies (see Skrzypiec-Spring *et al.*, 2007), the lack of effect in rat tissues led us instead to pursue the cardioprotective effects of apelin in the zebrafish embryo. The zebrafish embryo was an attractive model as the apelin system had been described previously and developmental studies had suggested a specific cardiovascular role for the peptide in zebrafish. Zeng *et al.* (2007) demonstrate that knockdown of apelin results in reduction of the myocardial marker cardiac myosin light chain 2 and that knockdown of the apelin receptor, agtrl1b, prevents the formation of a beating heart, while the embryos appeared otherwise grossly normal.

However, the possible functional role of apelin in the zebrafish at baseline or under conditions of hypoxia had not been determined. Although apelin had no dramatic effects at baseline on heart function *in vivo* or in isolated embryonic hearts, we demonstrated a modest cardioprotective effect of pyr-apelin-13 in zebrafish embryos 3 dpf. However, in zebrafish 5 dpf, using a more efficient semi-quantitative scoring assessment, pyr-apelin-13 did not produce a cardioprotective effect. The semi-quantitative approach proved to be more efficient as 10-20 embryos could be analysed per experimental group using this method compared with only 3-5 embryos per group in video edge detection experiments.

7.4 Relevance of findings

Since its discovery as the endogenous peptide ligand of the orphan APJ receptor; the physiological role of apelin has been investigated in a variety of settings. Unlike the discovery of other endogenous peptides such as endothelin-1 where the effect was known prior to the discovery of the ligand and the receptor (Itoh *et al.*, 1988); the discovery of apelin as a ligand of an orphan receptor meant that investigators had no clear starting point in elucidating its biological role. As apelin and its receptor are well conserved across vertebrate species, there is adequate reason to suspect that it has a key, essential physiological and possibly developmental role.

In the last twelve years, apelin has been reported to have effects in a large number of organ systems in rodent models and *in vitro* studies which are represented in Fig 7.1. The effects reported range from an inotropic action in isolated rat heart (Szokodi *et al.*, 2002) and vasodilation of human arteries (Maguire *et al.*, 2009) to effects on the

central control of fluid homeostasis (Roberts *et al.*, 2009) and protective effects on bone (Xie *et al.*, 2007). However, for each of these reported effects, there exist a limited number of publications (Fig 7.2).

The data presented in this thesis demonstrate the challenges of working with the apelin peptide. Our studies of the peptide in several standard and well-described preparations of normal rat tissue indicate that apelin has consistently no effect, particularly *in vitro*. There may be a variety of reasons for this. Apelin may be enzymatically degraded when added to isolated preparations or high levels of endogenous apelin activity in isolated tissues may block or inhibit the response to exogenous apelin.

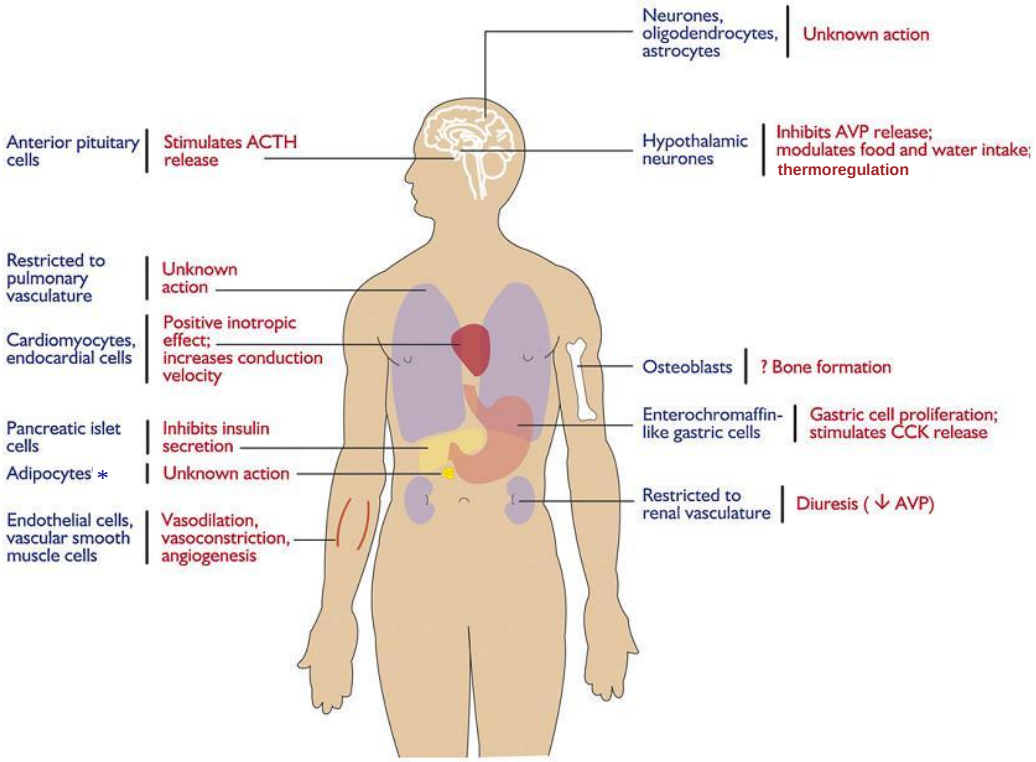

Figure 7.1: Expression and physiological functions of the apelin–APJ system. Most physiological effects not yet documented in humans. ACTH, adrenocorticotrophic hormone; AVP, arginine vasopressin; CCK, cholecystokinin. *Site of apelin but not APJ synthesis. Figure from Japp and Newby, 2008.

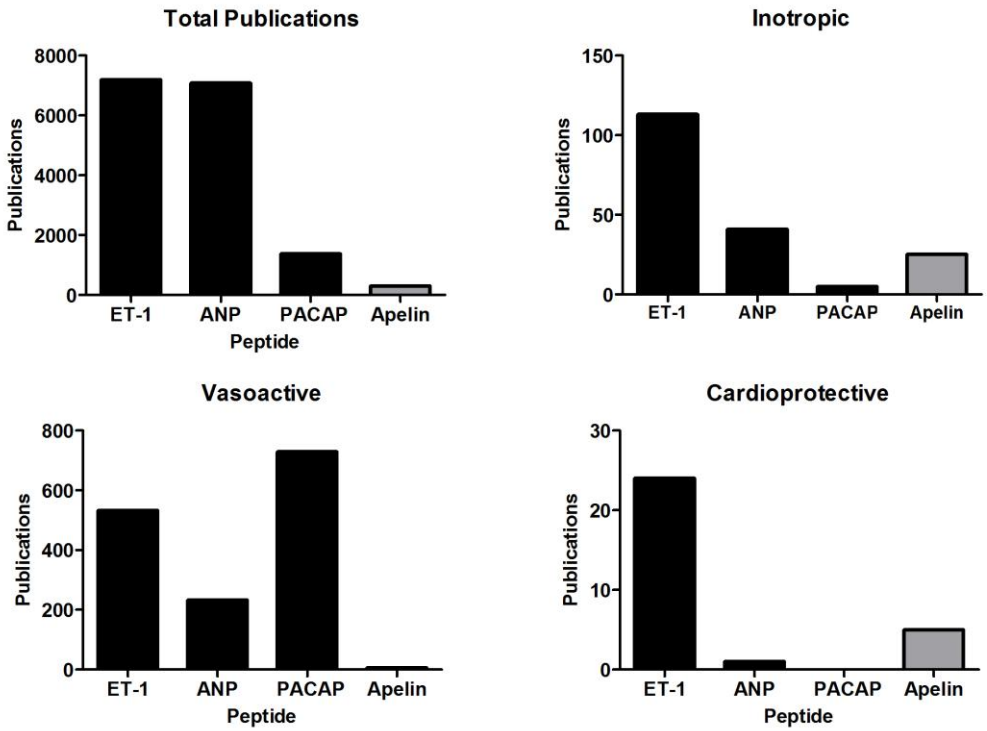

Figure 7.2: Comparison of apelin publication number to that of other named peptides.
Graphs display number of publications retrieved in PubMed for the search "named peptide" for the total publications and for the searches "named peptide and keyword eg. inotropic". Results are limited to publications within twelve years of the peptide's first report in the scientific literature and do not include review articles. ET-1 endothelin-1; ANP atrial natriuretic peptide; PACAP pituitary adenylate cyclase activating peptide.

From our knowledge of the literature, the apelin field and several personal communications with others investigating apelin, we speculate that others have either not published negative findings or failed to have work accepted for publication in spite of carrying out similar experiments in isolated cardiac tissue, isolated perfused rat heart and isolated rat vessel preparations. This idea of positive-outcome publication bias is widely discussed in the literature (Callaham *et al*., 1998, Timmer *et al*., 2002, Young *et al*., 2008). We also note that when compared to three other

peptides (endothelin-1, pituitary adenylate cyclase activating peptide (PACAP) and atrial natriuretic peptide (ANP)) in a twelve year period after their discovery apelin lags behind total publications and in the number of publications describing vasoactive effects (Figure 7.2). When compared to endothelin-1, apelin has limited numbers of papers describing an inotropic and cardioprotective effect; despite the claim of Szokodi *et al*. (2002) that apelin is an equally potent inotrope to endothelin-1 in the isolated, perfused, rat heart. Interestingly, this work was published eight years ago and has not been replicated in the literature since then.

7.5 Limitations and Future Directions

The data presented in this thesis illustrate that apelin has no inotropic, or lusitropic, effect in isolated cardiac tissue or the isolated, perfused heart (Langendorff) of the normal rat. *In vivo* in the normal rat, apelin has some influence on systemic blood pressure and HR. Yet, in isolated mesenteric arteries, we found no vasodilator or vasoconstrictor role of apelin. We had initially intended to pursue a cardioprotective effect of apelin using the Langendorff technique.

However, having been unable to demonstrate an effect of apelin in cardiac tissue of the rat, we felt that we should further develop our zebrafish model to investigate the potential cardioprotective effects of apelin. This decision was based upon the high cost of carrying on the model in the rat compared to the significantly lower cost of using the zebrafish. The rat Langendorff approach was a more high risk approach to pursue since we were uncertain of the baseline effect of the peptide in the rat heart.

In zebrafish 3 dpf, we demonstrated an apparent cardioprotective effect of apelin using video edge detection; however, in zebrafish 5 dpf we saw no cardioprotective effect of apelin using a semi-quantitative scoring assessment of global heart function and circulation. Interestingly, knockdown of apelin using a targeted morpholino resulted in severe developmental abnormalities. All MO-apelin embryos had died by 5 dpf suggesting a key role for apelin in development.

7.5.1 Is the cardioprotective effect of apelin dependent on developmental stage in zebrafish embryos?

We demonstrate a cardioprotective effect of apelin in zebrafish 3 dpf using video edge detection, but not in zebrafish 5 dpf using a semi-quantitative scoring assessment of HR and global circulation. The question remains as to whether: (a) apelin is cardioprotective in embryos 3 dpf and not in embryos 5 dpf or (b) apelin is equally cardioprotective in both settings yet the cardioprotective effect is too subtle to be detected by the semi-quantitative scoring assessment technique used in zebrafish 5 dpf. This study has also demonstrated that zebrafish 5 dpf are more susceptible to the cardiovascular effects of hypoxia than zebrafish 3 dpf. It is therefore possible that although apelin produced a modest cardioprotective effect in zebrafish 3 dpf, the peptide was unable to protect in zebrafish 5 dpf where the effect of hypoxia is more severe.

The question of whether apelin's cardioprotective effect is dependent on developmental stage would be answered by performing video edge detection on

zebrafish 5 dpf and using the semi-quantitative scoring assessment to measure global cardiovascular function in zebrafish 3 dpf following apelin incubation and hypoxia. However, the cardioprotective effect of desferrioxamine was demonstrated in zebrafish 5 dpf using both the global circulatory method and video edge detection. Therefore, we can infer that, as both methods are able to detect the same cardioprotective effect, it is likely that the findings are accurate and apelin is cardioprotective in zebrafish 3 dpf, but not zebrafish 5 dpf. Furthermore, plasma apelin has been shown to be increased in patients with mild heart failure compared to controls. However, in patients with end-stage heart failure, plasma apelin was reduced compared to controls (Sarzani *et al.*, 2007). The authors reason that it is therefore possible that apelin is protective in mild disease, but cannot protect in the face of more severe heart failure. This is in agreement with our data which suggest that apelin can protect zebrafish embryos from the mild cardiovascular effects of hypoxia at 3 dpf, but cannot protect against the severe cardiovascular effects of hypoxia at 5 dpf.

7.5.2 Mechanism of cardioprotection

Apelin has previously been reported to have cardioprotective properties in rodent models. In zebrafish, we demonstrate a small cardioprotective effect in zebrafish embryos exposed to acute hypoxia at 3 dpf. However, the mechanism of the cardioprotective effect remains unclear.

Cardioprotection is measured by a decrease in myocardial infarct size and/or by a measured improvement in heart function, for example, contraction velocity in the

zebrafish studies presented in this thesis. Necrosis, inflammation, hypertrophy and apoptosis of cardiac tissue contribute to injury in the face of an ischaemic or hypoxic insult. A reduction in one or more of these processes and an increase in beneficial processes such as angiogenesis will result in a cardioprotective effect (see Burger *et al.*, 2009) (Fig 7.3). The molecular and cellular mechanisms involved are complex and differ among cardioprotective agents.

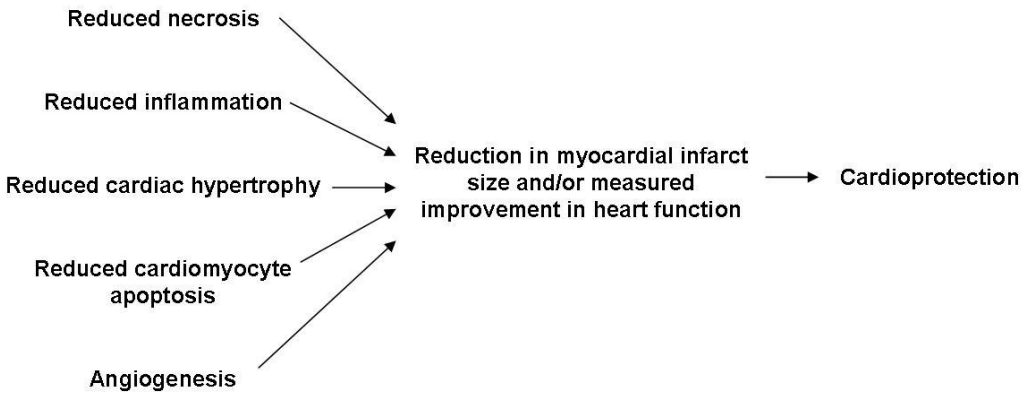

Figure 7.3: Summary of processes which may produce a cardioprotective outcome.
Figure summarises information gathered from Burger *et al*., 2009; Matsui *et al*., 2005; Schorlemmer *et al*., 2008.

Several cellular pathways have been implicated in the cardioprotective response (Matsui *et al.*, 2005; see Schorlemmer *et al.*, 2008) (Fig 7.4). There is a wealth of evidence supporting the role of the protein kinase B (Akt) and nitric oxide (NO) pathway in the cardioprotective effect of other endogenous cardioprotective agents including erythropoietin (see Burger *et al.*, 2009), ET-1 (Araki *et al.*, 2000) and bradykinin (Yang *et al.*, 2004). As the vasodilator action of apelin is mediated via the NO pathway, the cardioprotective action of apelin may also be mediated via NO. Further cardioprotective studies using the NO synthase inhibitor, L-NAME, would

allow us to test this hypothesis. However, the PI3K inhibitor, wortmannin, did not prevent the cardioprotective effect of apelin demonstrated in a model of ischaemia-reperfusion in the isolated rat heart, indicating that the cardioprotective effect of apelin is not via the Akt pathway (Kleinz *et al.*, 2008). Smith *et al*. (2007) did however show increased activity of Akt on reperfusion with apelin in a rat model of ischaemia-reperfusion. The role of the Akt pathway and the other cardioprotective mediators shown in Fig 7.4 in relation to apelin's cardioprotective effect clearly require further investigation.

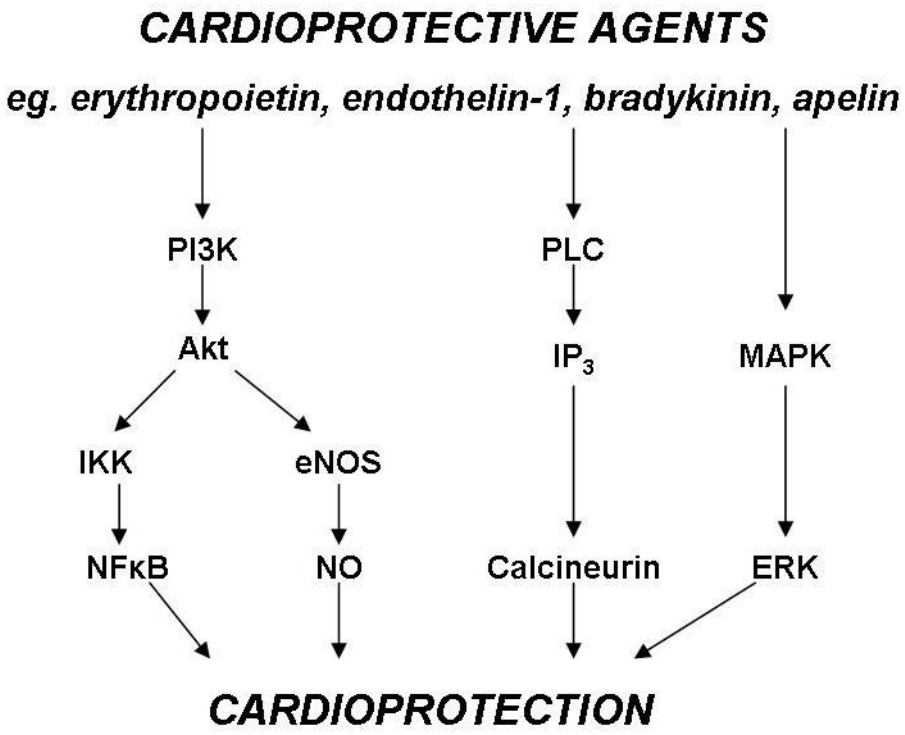

Figure 7.4: Cardioprotective mechanisms documented in the literature.
Many cardioprotective agents signal through more than one of these known cardioprotective pathways. The cardioprotective pathway(s) through which apelin signals is currently unclear. Figure summarises information gathered from the following publications: Burger *et al*., 2009; Matsui *et al*., 2005; Schorlemmer *et al*., 2008

7.5.3 Further investigation of the role of apelin in development

The apelin morpholino experiments presented in this thesis and genetic manipulation of the apelin system conducted by others (Nornes *et al.*, 2009; Scott *et al.*, 2007; Zeng *et al.*, 2007) identify a role for apelin in development. When apelin mRNA was knocked down by 92% in zebrafish embryos, severe total body developmental abnormalities were observed. Abnormal heart rate and circulation were also observed in MO-apelin embryos. However, no detrimental effect on baseline cardiac function or cardiac function in response to hypoxia was observed in MO-apelin embryos. More experiments are required to confirm or refute the findings of these experiments.

A splice blocking morpholino was used in these experiments as knockdown could be readily measured with a qPCR assay. A zebrafish apelin antibody could have been used to measure successful knockdown using a translation blocking morpholino (Bill *et al.*, 2009). However, a zebrafish apelin antibody was not commercially available and it would have been time-consuming and expensive to have the antibody custom made.

Further experiments are required to determine whether the severe developmental abnormalities observed following apelin knockdown are specific to the absence of functional apelin mRNA. The use of a translation blocking morpholino, or a non-overlapping splice blocking morpholino, would complement the data presented here. If the same phenotype was generated using a non-overlapping morpholino targeted to the apelin mRNA, then this would help define whether the phenotype is indeed specific to the knockdown of apelin mRNA (see Eisen and Smith *et al.*, 2008).

The final control for specificity of the phenotype is a "rescue" experiment (Corey *et al.*, 2001). The rescue experiment involves co-injection of apelin mRNA which does not contain the morpholino binding sequence. This is most commonly performed with a morpholino targeted to the 5'-untranslated region of the mRNA of interest, which sterically blocks translation of the mRNA without binding to the start codon, ATG (Fig 7.5). This means that, in this case, apelin mRNA could be co-injected to rescue apelin mRNA levels and phenotype, without the morpholino binding to the rescue sequence (see Ekker, 2000). The rescue experiment can also be performed with a splice blocking morpholino as the rescue mRNA does not contain the intron sequence to which the morpholino binds.

Figure 7.5: Morpholino rescue experiment involving coinjection of a rescue mRNA that does not contain the morpholino binding site.

However, rescue experiments are not always successful. In cases where the wild-type endogenous mRNA is low at the time of injection, overexpressing the mRNA of interest may also produce severe developmental abnormalities (see Eisen and Smith *et al.*, 2008). Our apelin mRNA expression profile suggests that this may be true in the case of apelin. Overexpression of apelin in the early zebrafish embryo has been previously reported to result in severe developmental abnormalities, including the

absence of a beating heart at 48 hpf (Zeng *et al.*, 2007). A rescue of the morpholino phenotype of around 60% is deeemed successful (Zeng *et al.*, 2007).

Further evidence for the difficulty in performing a successful rescue experiment is presented by Nornes *et al*. (2009). The authors report that the delay in epiboly they witness on agtrl1a knockdown can be rescued by injection of agtrl1a RNA at the 32-cell stage, but not at the single cell stage. The authors reason that this may be due to the RNA being specifically targeted to the phenotypically abnormal area of the embryo. Rescue RNA is injected specifically into the yolk cell at the 32-cell stage rather than into the total embryo at the single-cell stage, where in fact the RNA may not be as easily distributed throughout the embryo as a MO (Scholpp *et al.*, 2004).

7.5.4 Development of an apelin activity assay

As apelin had no effect in *in vitro* preparations, it was difficult to be convinced of the activity of the apelin peptide in all cases. Where possible, this resulted in the use of the same batch of apelin in *in vivo* experiments, where I did observe a response, as in *in vitro* experiments. The development of a cell-based system expressing the APJ receptor would be a more efficient and less costly way of assessing apelin activity routinely before performing other experiments. Application of apelin to the cells, for example CHO cells expressing the APJ receptor as used in the initial discovery of the peptide (Tatemoto *et al.*, 1998), and the subsequent measurement of a downstream second messenger would allow the activity of the apelin peptide to be confirmed. For example, measurement of cAMP (which would decrease following activation of the G-protein, G_i) or IL-1, a metabolite of IP_3 (which would increase following

activation of the G-protein, G_q) would be ideal candidates to measure in this approach.

7.6 Therapeutic potential of the apelin system in cardiovascular disease

The apelin system has effects on several organ systems (see Fig 7.1). Within the cardiovascular system, our data and the available published data suggest that apelin has limited inotropic (Berry *et al.*, 2004) and vasoactive effects (Tatemoto *et al.*, 2001) in the normal rat. The cardioprotective effect of apelin has been demonstrated in rodent models (Simpkin *et al.*, 2007) and we observe a modest cardioprotective effect in zebrafish 3 dpf. Importantly, in patients attending for diagnostic coronary angiography, apelin-36 increased rate of rise of left ventricular pressure towards the peak, but decreased maximum left ventricular pressure and left ventricular end diastolic pressure (Japp *et al.*, 2010). Furthermore, apelin-13, pyr-apelin-13 and apelin-36 elicited a positive inotropic effect in isolated atrial strips from atrial appendage of patients undergoing coronary artery bypass (Maguire *et al.*, 2009).

It is unclear whether apelin functions in an endocrine manner or has a paracrine action that is controlled locally. Apelin has been detected in human and rodent plasma (Foldes *et al.*, 2003; Kawamata *et al.*, 2001). However, Kleinz *et al*. (2005) postulate that apelin release is controlled locally and that low levels of apelin in plasma is due to overspill from tissues such as endothelial cells where apelin may be synthesised for local release. As the apelin receptor is widely expressed, a key

challenge of using an apelin agonist or antagonist therapeutically will be to influence the system in a target tissue, for example the heart, without influencing other organs.

Although we demonstrated that the inotropic and vasoactive effects are limited in the normal rat, apelin's reported inotropic and vasoactive effects appear to be enhanced in heart failure (Berry *et al.*, 2004; Dai *et al.*, 2006; Jia *et al.*, 2006). This would make the apelin system an attractive potential target for the treatment of heart failure. Endothelin-1 also has comparable positive inotropic actions, in addition to a potent vasoconstrictor action. Yet, modulation of the endothelin system is currently only approved for use in the treatment of pulmonary arterial hypertension by endothelin antagonists (Aubert *et al.*, 2009). An apelin agonist may therefore be suitable for use in some, but not other, cardiovascular conditions. The development of selective tools such as a non-peptidic apelin agonist, recently reported in the literature (Iturrioz *et al.*, 2009), or an apelin antagonist will allow for further characterisation of the effects of apelin in different tissues and species. Although the apelin system has clear therapeutic potential, only time will tell whether or not drugs targeting the apelin system will have benefit for patients with cardiovascular disease.

References

Andersen, CU, Markvardsen, LH, Hilberg, O, Simonsen, U (2009) Pulmonary apelin levels and effects in rats with hypoxic pulmonary hypertension. *Respir Med* **103**(11)**:** 1663-1671.

Araki, M, Hasegawa, K, Iwai-Kanai, E, Fujita, M, Sawamura, T, Kakita, T, Wada, H, Morimoto, T, Sasayama, S (2000) Endothelin-1 as a protective factor against beta-adrenergic agonist-induced apoptosis in cardiac myocytes. *J Am Coll Cardiol* **36**(4)**:** 1411-1418.

Ashley, EA, Powers, J, Chen, M, Kundu, R, Finsterbach, T, Caffarelli, A, Deng, A, Eichhorn, J, Mahajan, R, Agrawal, R, Greve, J, Robbins, R, Patterson, AJ, Bernstein, D, Quertermous, T (2005) The endogenous peptide apelin potently improves cardiac contractility and reduces cardiac loading in vivo. *Cardiovasc Res* **65**(1)**:** 73-82.

Aubert, JD, Juillerat-Jeanneret, L (2009) Therapeutic potential of endothelin receptor modulators: lessons from human clinical trials. *Expert Opin Ther Targets* **13**(9)**:** 1069-1084.

Bagatto, B (2005) Ontogeny of cardiovascular control in zebrafish (Danio rerio): effects of developmental environment. *Comp Biochem Physiol A Mol Integr Physiol* **141**(4)**:** 391-400.

Berghmans, S, Butler, P, Goldsmith, P, Waldron, G, Gardner, I, Golder, Z, Richards, FM, Kimber, G, Roach, A, Alderton, W, Fleming, A (2008) Zebrafish based assays for the assessment of cardiac, visual and gut function--potential safety screens for early drug discovery. *J Pharmacol Toxicol Methods* **58**(1)**:** 59-68.

Berry, MF, Pirolli, TJ, Jayasankar, V, Burdick, J, Morine, KJ, Gardner, TJ, Woo, YJ (2004) Apelin has in vivo inotropic effects on normal and failing hearts. *Circulation* **110**(11 Suppl 1)**:** II187-193.

Bill, BR, Petzold, AM, Clark, KJ, Schimmenti, LA, Ekker, SC (2009) A primer for morpholino use in zebrafish. *Zebrafish* **6**(1)**:** 69-77.

Boucher, J, Masri, B, Daviaud, D, Gesta, S, Guigne, C, Mazzucotelli, A, Castan-Laurell, I, Tack, I, Knibiehler, B, Carpene, C, Audigier, Y, Saulnier-Blache, JS, Valet, P (2005) Apelin, a newly identified adipokine up-regulated by insulin and obesity. *Endocrinology* **146**(4)**:** 1764-1771.

Brand, M, Granato, M, Nusslein-Volhard, C (2002) Keeping and raising zebrafish. *Zebrafish A Practical Approach***:** 12-18.

Burns, CG, Milan, DJ, Grande, EJ, Rottbauer, W, MacRae, CA, Fishman, MC (2005) High-throughput assay for small molecules that modulate zebrafish embryonic heart rate. *Nat Chem Biol* **1**(5)**:** 263-264.

Callaham, ML, Baxt, WG, Waeckerle, JF, Wears, RL (1998) Reliability of editors' subjective quality ratings of peer reviews of manuscripts. *JAMA* **280**(3)**:** 229-231.

Charles, CJ, Rademaker, MT, Richards, AM (2006) Apelin-13 induces a biphasic haemodynamic response and hormonal activation in normal conscious sheep. *J Endocrinol* **189**(3)**:** 701-710.

Chen, MM, Ashley, EA, Deng, DX, Tsalenko, A, Deng, A, Tabibiazar, R, Ben-Dor, A, Fenster, B, Yang, E, King, JY, Fowler, M, Robbins, R, Johnson, FL, Bruhn, L, McDonagh, T, Dargie, H, Yakhini, Z, Tsao, PS, Quertermous, T (2003) Novel role for the potent endogenous inotrope apelin in human cardiac dysfunction. *Circulation* **108**(12)**:** 1432-1439.

Cheng, X, Cheng, XS, Pang, CC (2003) Venous dilator effect of apelin, an endogenous peptide ligand for the orphan APJ receptor, in conscious rats. *Eur J Pharmacol* **470**(3)**:** 171-175.

Chun, HJ, Ali, ZA, Kojima, Y, Kundu, RK, Sheikh, AY, Agrawal, R, Zheng, L, Leeper, NJ, Pearl, NE, Patterson, AJ, Anderson, JP, Tsao, PS, Lenardo, MJ, Ashley, EA, Quertermous, T (2008) Apelin signaling antagonizes Ang II effects in mouse models of atherosclerosis. *J Clin Invest* **118**(10)**:** 3343-3354.

Clarke, KJ, Whitaker, KW, Reyes, TM (2009) Diminished metabolic responses to centrally-administered apelin-13 in diet-induced obese rats fed a high-fat diet. *J Neuroendocrinol* **21**(2)**:** 83-89.

Corey, DR, Abrams, JM (2001) Morpholino antisense oligonucleotides: tools for investigating vertebrate development. *Genome Biol* **2**(5)**:** REVIEWS1015.

Craig, MP, Gilday, SD, Hove, JR (2006) Dose-dependent effects of chemical immobilization on the heart rate of embryonic zebrafish. *Lab Anim (NY)* **35**(9)**:** 41-47.

Dai, T, Ramirez-Correa, G, Gao, WD (2006) Apelin increases contractility in failing cardiac muscle. *Eur J Pharmacol* **553**(1-3)**:** 222-228.

Davenport, A, Pitkin, S, Maguire, J, Macaluso, M, Glen, R (2009) Abstract 5787: Discovery and Characterisation of Linear and Cyclic Peptide Agonists of Apelins. *Circulation* **120:** S1148.

Davenport, AP, Pitkin, SL, Maguire, JJ, Macaluso, M, Glen, RC (2010) Abstract 5787: Discovery and Characterisation of Linear and Cyclic Peptide Agonists of Apelins. *Circulation* **120**(S1148).

De Mota, N, Lenkei, Z, Llorens-Cortes, C (2000) Cloning, pharmacological characterization and brain distribution of the rat apelin receptor. *Neuroendocrinology* **72**(6)**:** 400-407.

Denvir, MA, Tucker, CS, Mullins, JJ (2008) Systolic and diastolic ventricular function in zebrafish embryos: influence of norepenephrine, MS-222 and temperature. *BMC Biotechnol* **8:** 21.

Dray, C, Knauf, C, Daviaud, D, Waget, A, Boucher, J, Buleon, M, Cani, PD, Attane, C, Guigne, C, Carpene, C, Burcelin, R, Castan-Laurell, I, Valet, P (2008) Apelin stimulates glucose utilization in normal and obese insulin-resistant mice. *Cell Metab* **8**(5)**:** 437-445.

El Messari, S, Iturrioz, X, Fassot, C, De Mota, N, Roesch, D, Llorens-Cortes, C (2004) Functional dissociation of apelin receptor signaling and endocytosis: implications for the effects of apelin on arterial blood pressure. *J Neurochem* **90**(6)**:** 1290-1301.

Erdem, G, Dogru, T, Tasci, I, Sonmez, A, Tapan, S (2008) Low plasma apelin levels in newly diagnosed type 2 diabetes mellitus. *Exp Clin Endocrinol Diabetes* **116**(5)**:** 289-292.

Erickson, AL, DeGrado, JR, Fanikos, JR (2010) Clevidipine: a short-acting intravenous dihydropyridine calcium channel blocker for the management of hypertension. *Pharmacotherapy* **30**(5)**:** 515-528.

Eyries, M, Siegfried, G, Ciumas, M, Montagne, K, Agrapart, M, Lebrin, F, Soubrier, F (2008) Hypoxia-Induced Apelin Expression Regulates Endothelial Cell Proliferation and Regenerative Angiogenesis. *Circ Res* **103**(4)**:** 432-440.

Farkasfalvi, K, Stagg, MA, Coppen, SR, Siedlecka, U, Lee, J, Soppa, GK, Marczin, N, Szokodi, I, Yacoub, MH, Terracciano, CM (2007) Direct effects of apelin on cardiomyocyte contractility and electrophysiology. *Biochem Biophys Res Commun* **357**(4)**:** 889-895.

Foldes, G, Horkay, F, Szokodi, I, Vuolteenaho, O, Ilves, M, Lindstedt, KA, Mayranpaa, M, Sarman, B, Seres, L, Skoumal, R, Lako-Futo, Z, deChatel, R, Ruskoaho, H, Toth, M (2003) Circulating and cardiac levels of apelin, the novel ligand of the orphan receptor APJ, in patients with heart failure. *Biochem Biophys Res Commun* **308**(3)**:** 480-485.

Gitterman, DP, Evans, RJ (2000) Properties of P2X and P2Y receptors are dependent on artery diameter in the rat mesenteric bed. *Br J Pharmacol* **131**(8)**:** 1561-1568.

Glassford, AJ, Yue, P, Sheikh, AY, Chun, HJ, Zarafshar, S, Chan, DA, Reaven, GM, Quertermous, T, Tsao, PS (2007) HIF-1 regulates hypoxia- and insulin-induced expression of apelin in adipocytes. *Am J Physiol Endocrinol Metab* **293**(6)**:** E1590-1596.

Gray, C, Packham, IM, Wurmser, F, Eastley, NC, Hellewell, PG, Ingham, PW, Crossman, DC, Chico, TJ (2007) Ischemia is not required for arteriogenesis in zebrafish embryos. *Arterioscler Thromb Vasc Biol* **27**(10)**:** 2135-2141.

Gupta, A, Meng, X, Zhu, LJ, Lawson, ND, Wolfe, SA (2011) Zinc finger protein-dependent and -independent contributions to the in vivo off-target activity of zinc finger nucleases. *Nucleic Acids Res* **39**(1)**:** 381-392.

Gurzu, B, Petrescu, BC, Costuleanu, M, Petrescu, G (2006) Interactions between apelin and angiotensin II on rat portal vein. *J Renin Angiotensin Aldosterone Syst* **7**(4)**:** 212-216.

Han, S, Wang, G, Qi, X, Lee, HM, Englander, EW, Greeley, GH, Jr. (2008) A possible role for hypoxia-induced apelin expression in enteric cell proliferation. *Am J Physiol Regul Integr Comp Physiol* **294**(6)**:** R1832-1839.

Hashimoto, T, Kihara, M, Imai, N, Yoshida, S, Shimoyamada, H, Yasuzaki, H, Ishida, J, Toya, Y, Kiuchi, Y, Hirawa, N, Tamura, K, Yazawa, T, Kitamura, H, Fukamizu, A, Umemura, S (2007) Requirement of apelin-apelin receptor system for oxidative stress-linked atherosclerosis. *Am J Pathol* **171**(5)**:** 1705-1712.

Havranek, EP, Abrams, F, Stevens, E, Parker, K (1998) Determinants of mortality in elderly patients with heart failure: the role of angiotensin-converting enzyme inhibitors. *Arch Intern Med* **158**(18)**:** 2024-2028.

Hedrick, MS, Winmill, RE (2003) Excitatory and inhibitory effects of tricaine (MS-222) on fictive breathing in isolated bullfrog brain stem. *Am J Physiol Regul Integr Comp Physiol* **284**(2)**:** R405-412.

Heinonen, MV, Purhonen, AK, Miettinen, P, Paakkonen, M, Pirinen, E, Alhava, E, Akerman, K, Herzig, KH (2005) Apelin, orexin-A and leptin plasma levels in morbid obesity and effect of gastric banding. *Regul Pept* **130**(1-2)**:** 7-13.

Henriksson, M, Stenman, E, Edvinsson, L (2003) Intracellular pathways involved in upregulation of vascular endothelin type B receptors in cerebral arteries of the rat. *Stroke* **34**(6)**:** 1479-1483.

Herbomel, P, Thisse, B, Thisse, C (1999) Ontogeny and behaviour of early macrophages in the zebrafish embryo. *Development* **126**(17)**:** 3735-3745.

Higuchi, K, Masaki, T, Gotoh, K, Chiba, S, Katsuragi, I, Tanaka, K, Kakuma, T, Yoshimatsu, H (2007) Apelin, an APJ receptor ligand, regulates body adiposity and favors the messenger ribonucleic acid expression of uncoupling proteins in mice. *Endocrinology* **148**(6)**:** 2690-2697.

Hus-Citharel, A, Bouby, N, Frugiere, A, Bodineau, L, Gasc, JM, Llorens-Cortes, C (2008) Effect of apelin on glomerular hemodynamic function in the rat kidney. *Kidney Int* **74**(4)**:** 486-494.

Ishida, J, Hashimoto, T, Hashimoto, Y, Nishiwaki, S, Iguchi, T, Harada, S, Sugaya, T, Matsuzaki, H, Yamamoto, R, Shiota, N, Okunishi, H, Kihara, M, Umemura, S, Sugiyama, F, Yagami, K, Kasuya, Y, Mochizuki, N, Fukamizu, A (2004) Regulatory roles for APJ, a seven-transmembrane receptor related to angiotensin-type 1 receptor in blood pressure in vivo. *J Biol Chem* **279**(25)**:** 26274-26279.

Isogai, S, Horiguchi, M, Weinstein, BM (2001) The vascular anatomy of the developing zebrafish: an atlas of embryonic and early larval development. *Dev Biol* **230**(2)**:** 278-301.

Itoh, Y, Yanagisawa, M, Ohkubo, S, Kimura, C, Kosaka, T, Inoue, A, Ishida, N, Mitsui, Y, Onda, H, Fujino, M, et al. (1988) Cloning and sequence analysis of cDNA encoding the precursor of a human endothelium-derived vasoconstrictor peptide, endothelin: identity of human and porcine endothelin. *FEBS Lett* **231**(2)**:** 440-444.

Iturrioz, X, Alvear-Perez, R, De Mota, N, Franchet, C, Guillier, F, Leroux, V, Dabire, H, Le Jouan, M, Chabane, H, Gerbier, R, Bonnet, D, Berdeaux, A, Maigret, B, Galzi, JL, Hibert, M, Llorens-Cortes, C (2009) Identification and pharmacological properties of E339-3D6, the first nonpeptidic apelin receptor agonist. *FASEB J*.

Iwakura, K, Ito, H, Okamura, A, Koyama, Y, Date, M, Higuchi, Y, Inoue, K, Kimura, R, Nagai, H, Imai, M, Toyoshima, Y, Ozawa, M, Ito, N, Okazaki, Y, Shibuya, M, Suenaga, H, Kubota, A, Fujii, K (2009) Nicorandil treatment in patients with acute myocardial infarction: a meta-analysis. *Circ J* **73**(5)**:** 925-931.

Japp, AG, Cruden, NL, Amer, DA, Li, VK, Goudie, EB, Johnston, NR, Sharma, S, Neilson, I, Webb, DJ, Megson, IL, Flapan, AD, Newby, DE (2008) Vascular effects of apelin in vivo in man. *J Am Coll Cardiol* **52**(11)**:** 908-913.

Japp, AG, Cruden, NL, Barnes, G, van Gemeren, N, Mathews, J, Adamson, J, Johnston, NR, Denvir, MA, Megson, IL, Flapan, AD, Newby, DE (2010) Acute cardiovascular effects of apelin in humans: potential role in patients with chronic heart failure. *Circulation* **121**(16)**:** 1818-1827.

Jia, YX, Lu, ZF, Zhang, J, Pan, CS, Yang, JH, Zhao, J, Yu, F, Duan, XH, Tang, CS, Qi, YF (2007) Apelin activates L-arginine/nitric oxide synthase/nitric oxide pathway in rat aortas. *Peptides* **28**(10)**:** 2023-2029.

Jia, YX, Pan, CS, Zhang, J, Geng, B, Zhao, J, Gerns, H, Yang, J, Chang, JK, Tang, CS, Qi, YF (2006) Apelin protects myocardial injury induced by isoproterenol in rats. *Regul Pept* **133**(1-3)**:** 147-154.

Kagiyama, S, Fukuhara, M, Matsumura, K, Lin, Y, Fujii, K, Iida, M (2005) Central and peripheral cardiovascular actions of apelin in conscious rats. *Regul Pept* **125**(1-3)**:** 55-59.

Kane and Kimmel, DA (1993) The zebrafish midblastula transition. *Development* **119**(2)**:** 447-456.

Karmazyn, M, Gan, XT, Humphreys, RA, Yoshida, H, Kusumoto, K (1999) The myocardial Na(+)-H(+) exchange: structure, regulation, and its role in heart disease. *Circ Res* **85**(9)**:** 777-786.

Kasai, A, Shintani, N, Kato, H, Matsuda, S, Gomi, F, Haba, R, Hashimoto, H, Kakuda, M, Tano, Y, Baba, A (2008) Retardation of retinal vascular development in apelin-deficient mice. *Arterioscler Thromb Vasc Biol* **28**(10)**:** 1717-1722.

Katugampola, SD, Maguire, JJ, Matthewson, SR, Davenport, AP (2001) [(125)I]-(Pyr(1))Apelin-13 is a novel radioligand for localizing the APJ orphan receptor in human and rat tissues with evidence for a vasoconstrictor role in man. *Br J Pharmacol* **132**(6)**:** 1255-1260.

Kawamata, Y, Habata, Y, Fukusumi, S, Hosoya, M, Fujii, R, Hinuma, S, Nishizawa, N, Kitada, C, Onda, H, Nishimura, O, Fujino, M (2001) Molecular properties of apelin: tissue distribution and receptor binding. *Biochim Biophys Acta* **1538**(2-3)**:** 162-171.

Kearney, PM, Whelton, M, Reynolds, K, Muntner, P, Whelton, PK, He, J (2005) Global burden of hypertension: analysis of worldwide data. *Lancet* **365**(9455)**:** 217-223.

Khan, M, Meduru, S, Mostafa, M, Khan, S, Hideg, K, Kuppusamy, P (2010) Trimetazidine, administered at the onset of reperfusion, ameliorates myocardial dysfunction and injury by activation of p38 mitogen-activated protein kinase and Akt signaling. *J Pharmacol Exp Ther* **333**(2)**:** 421-429.

Kimmel, CB, Ballard, WW, Kimmel, SR, Ullmann, B, Schilling, TF (1995) Stages of embryonic development of the zebrafish. *Dev Dyn* **203**(3)**:** 253-310.

Kleinz, MJ, Baxter, GF (2008) Apelin reduces myocardial reperfusion injury independently of PI3K/Akt and P70S6 kinase. *Regul Pept* **146**(1-3)**:** 271-277.

Kleinz, MJ, Davenport, AP (2004) Immunocytochemical localization of the endogenous vasoactive peptide apelin to human vascular and endocardial endothelial cells. *Regul Pept* **118**(3)**:** 119-125.

Kleinz, MJ, Skepper, JN, Davenport, AP (2005) Immunocytochemical localisation of the apelin receptor, APJ, to human cardiomyocytes, vascular smooth muscle and endothelial cells. *Regul Pept* **126**(3)**:** 233-240.

Kotch, LE, Iyer, NV, Laughner, E, Semenza, GL (1999) Defective vascularization of HIF-1alpha-null embryos is not associated with VEGF deficiency but with mesenchymal cell death. *Dev Biol* **209**(2)**:** 254-267.

Kuba, K, Zhang, L, Imai, Y, Arab, S, Chen, M, Maekawa, Y, Leschnik, M, Leibbrandt, A, Markovic, M, Schwaighofer, J, Beetz, N, Musialek, R, Neely, GG, Komnenovic, V, Kolm, U, Metzler, B, Ricci, R, Hara, H, Meixner, A, Nghiem, M, Chen, X, Dawood, F, Wong, KM, Sarao, R, Cukerman, E, Kimura, A, Hein, L, Thalhammer, J, Liu, PP, Penninger, JM (2007) Impaired heart contractility in Apelin gene-deficient mice associated with aging and pressure overload. *Circ Res* **101**(4)**:** e32-42.

Lee, DK, Cheng, R, Nguyen, T, Fan, T, Kariyawasam, AP, Liu, Y, Osmond, DH, George, SR, O'Dowd, BF (2000) Characterization of apelin, the ligand for the APJ receptor. *J Neurochem* **74**(1)**:** 34-41.

Li, L, Yang, G, Li, Q, Tang, Y, Yang, M, Yang, H, Li, K (2006) Changes and relations of circulating visfatin, apelin, and resistin levels in normal, impaired glucose tolerance, and type 2 diabetic subjects. *Exp Clin Endocrinol Diabetes* **114**(10)**:** 544-548.

Loynes, CA, Martin, JS, Robertson, A, Trushell, DM, Ingham, PW, Whyte, MK, Renshaw, SA (2010) Pivotal Advance: Pharmacological manipulation of inflammation resolution during spontaneously resolving tissue neutrophilia in the zebrafish. *J Leukoc Biol* **87**(2)**:** 203-212.

Maguire, JJ, Kleinz, MJ, Pitkin, SL, Davenport, AP (2009) [Pyr1]apelin-13 identified as the predominant apelin isoform in the human heart: vasoactive mechanisms and inotropic action in disease. *Hypertension* **54**(3)**:** 598-604.

Manalo, DJ, Rowan, A, Lavoie, T, Natarajan, L, Kelly, BD, Ye, SQ, Garcia, JG, Semenza, GL (2005) Transcriptional regulation of vascular endothelial cell responses to hypoxia by HIF-1. *Blood* **105**(2)**:** 659-669.

Mao, SZ, Hong, L, Hu, LG, Fan, XF, Zhang, L, Guo, YM, Gong, YS (2009) [Effect of apelin on hypoxic pulmonary hypertension in rats: role of the NO pathway.]. *Sheng Li Xue Bao* **61**(5)**:** 480-484.

Masri, B, Lahlou, H, Mazarguil, H, Knibiehler, B, Audigier, Y (2002) Apelin (65-77) activates extracellular signal-regulated kinases via a PTX-sensitive G protein. *Biochem Biophys Res Commun* **290**(1)**:** 539-545.

Matsui, T, Rosenzweig, A (2005) Convergent signal transduction pathways controlling cardiomyocyte survival and function: the role of PI 3-kinase and Akt. *J Mol Cell Cardiol* **38**(1)**:** 63-71.

Matsumoto, K, Imagawa, S, Obara, N, Suzuki, N, Takahashi, S, Nagasawa, T, Yamamoto, M (2006) 2-Oxoglutarate downregulates expression of vascular endothelial growth factor and erythropoietin through decreasing hypoxia-inducible factor-1alpha and inhibits angiogenesis. *J Cell Physiol* **209**(2)**:** 333-340.

Meens, MJ, Fazzi, GE, van Zandvoort, MA, De Mey, JG (2009) Calcitonin gene-related peptide selectively relaxes contractile responses to endothelin-1 in rat mesenteric resistance arteries. *J Pharmacol Exp Ther* **331**(1)**:** 87-95.

Milan, DJ, Peterson, TA, Ruskin, JN, Peterson, RT, MacRae, CA (2003) Drugs that induce repolarization abnormalities cause bradycardia in zebrafish. *Circulation* **107**(10)**:** 1355-1358.

Morel, I, Cillard, J, Lescoat, G, Sergent, O, Pasdeloup, N, Ocaktan, AZ, Abdallah, MA, Brissot, P, Cillard, P (1992) Antioxidant and free radical scavenging activities of the iron chelators pyoverdin and hydroxypyrid-4-ones in iron-loaded hepatocyte cultures: comparison of their mechanism of protection with that of desferrioxamine. *Free Radic Biol Med* **13**(5)**:** 499-508.

Ngan, AK, Wang, YS (2009) Tissue-specific transcriptional regulation of monocarboxylate transporters (MCTs) during short-term hypoxia in zebrafish (Danio rerio). *Comp Biochem Physiol B Biochem Mol Biol* **154**(4)**:** 396-405.

Noll, G, Wenzel, RR, de Marchi, S, Shaw, S, Luscher, TF (1997) Differential effects of captopril and nitrates on muscle sympathetic nerve activity in volunteers. *Circulation* **95**(9)**:** 2286-2292.

Nornes, S, Tucker, B, Lardelli, M (2009) Zebrafish aplnra functions in epiboly. *BMC Res Notes* **2:** 231.

O'Dowd, BF, Heiber, M, Chan, A, Heng, HH, Tsui, LC, Kennedy, JL, Shi, X, Petronis, A, George, SR, Nguyen, T (1993) A human gene that shows identity with the gene encoding the angiotensin receptor is located on chromosome 11. *Gene* **136**(1-2)**:** 355-360.

Padilla, PA, Roth, MB (2001) Oxygen deprivation causes suspended animation in the zebrafish embryo. *Proc Natl Acad Sci U S A* **98**(13)**:** 7331-7335.

Panakova, D, Werdich, AA, Macrae, CA (2010) Wnt11 patterns a myocardial electrical gradient through regulation of the L-type Ca(2+) channel. *Nature* **466**(7308)**:** 874-878.

Parng, C, Ton, C, Lin, YX, Roy, NM, McGrath, P (2006) A zebrafish assay for identifying neuroprotectants in vivo. *Neurotoxicol Teratol* **28**(4)**:** 509-516.

Peterson, SM, Freeman, JL (2009) RNA isolation from embryonic zebrafish and cDNA synthesis for gene expression analysis. *J Vis Exp*(30).

Pitkin, SL, Maguire, JJ, Bonner, TI, Davenport, AP (2010) International Union of Basic and Clinical Pharmacology. LXXIV. Apelin receptor nomenclature, distribution, pharmacology, and function. *Pharmacol Rev* **62**(3)**:** 331-342.

Prus, E, Fibach, E (2009) Effect of iron chelators on labile iron and oxidative status of thalassaemic erythroid cells. *Acta Haematol* **123**(1)**:** 14-20.

Puntel, RL, Roos, DH, Grotto, D, Garcia, SC, Nogueira, CW, Rocha, JB (2007) Antioxidant properties of Krebs cycle intermediates against malonate pro-oxidant activity in vitro: a comparative study using the colorimetric method and HPLC analysis to determine malondialdehyde in rat brain homogenates. *Life Sci* **81**(1)**:** 51-62.

Qi, XL, Sia, YT, Stewart, DJ, Wei, G, Nguyen, QT, Cernacek, P, Picard, P, Sirois, M, Rouleau, JL (2001) Myocardial contractile responsiveness to endothelin-1 in the post-infarction rat model of heart failure: effects of chronic quinapril. *J Mol Cell Cardiol* **33**(11)**:** 2023-2035.

Qutub, AA, Popel, AS (2006) A computational model of intracellular oxygen sensing by hypoxia-inducible factor HIF1 alpha. *J Cell Sci* **119**(Pt 16)**:** 3467-3480.

Reaux, A, De Mota, N, Skultetyova, I, Lenkei, Z, El Messari, S, Gallatz, K, Corvol, P, Palkovits, M, Llorens-Cortes, C (2001) Physiological role of a novel neuropeptide, apelin, and its receptor in the rat brain. *J Neurochem* **77**(4)**:** 1085-1096.

Retailleau, K, Belin de Chantemele, EJ, Chanoine, S, Guihot, AL, Vessieres, E, Toutain, B, Faure, S, Bagi, Z, Loufrani, L, Henrion, D (2010) Reactive oxygen species and cyclooxygenase 2-derived thromboxane A2 reduce angiotensin II type 2 receptor vasorelaxation in diabetic rat resistance arteries. *Hypertension* **55**(2)**:** 339-344.

Roberts, EM, Newson, MJ, Pope, GR, Landgraf, R, Lolait, SJ, O'Carroll, AM (2009) Abnormal fluid homeostasis in apelin receptor knockout mice. *J Endocrinol* **202**(3)**:** 453-462.

Robu, ME, Larson, JD, Nasevicius, A, Beiraghi, S, Brenner, C, Farber, SA, Ekker, SC (2007) p53 activation by knockdown technologies. *PLoS Genet* **3**(5)**:** e78.

Ronkainen, VP, Ronkainen, JJ, Hanninen, SL, Leskinen, H, Ruas, JL, Pereira, T, Poellinger, L, Vuolteenaho, O, Tavi, P (2007) Hypoxia inducible factor regulates the cardiac expression and secretion of apelin. *FASEB J* **21**(8)**:** 1821-1830.

Russo, C, Violani, E, Salis, S, Venezia, V, Dolcini, V, Damonte, G, Benatti, U, D'Arrigo, C, Patrone, E, Carlo, P, Schettini, G (2002) Pyroglutamate-modified amyloid beta-peptides--AbetaN3(pE)--strongly affect cultured neuron and astrocyte survival. *J Neurochem* **82**(6)**:** 1480-1489.

Salcedo, A, Garijo, J, Monge, L, Fernandez, N, Luis Garcia-Villalon, A, Sanchez Turrion, V, Cuervas-Mons, V, Dieguez, G (2007) Apelin effects in human splanchnic arteries. Role of nitric oxide and prostanoids. *Regul Pept* **144**(1-3)**:** 50-55.

Sarzani, R, Forleo, C, Pietrucci, F, Capestro, A, Soura, E, Guida, P, Sorrentino, S, Iacoviello, M, Romito, R, Dessi-Fulgheri, P, Pitzalis, M, Rappelli, A (2007) The 212A variant of the APJ receptor gene for the endogenous inotrope apelin is associated with slower heart failure progression in idiopathic dilated cardiomyopathy. *J Card Fail* **13**(7)**:** 521-529.

Satpute, RM, Hariharakrishnan, J, Bhattacharya, R (2010) Effect of alpha-ketoglutarate and N-acetyl cysteine on cyanide-induced oxidative stress mediated cell death in PC12 cells. *Toxicol Ind Health* **26**(5)**:** 297-308.

Schafer, M, Frischkopf, K, Taimor, G, Piper, HM, Schluter, KD (2000) Hypertrophic effect of selective beta(1)-adrenoceptor stimulation on ventricular cardiomyocytes from adult rat. *Am J Physiol Cell Physiol* **279**(2)**:** C495-503.

Scholpp, S, Groth, C, Lohs, C, Lardelli, M, Brand, M (2004) Zebrafish fgfr1 is a member of the fgf8 synexpression group and is required for fgf8 signalling at the midbrain-hindbrain boundary. *Dev Genes Evol* **214**(6)**:** 285-295.

Schwerte, T, Uberbacher, D, Pelster, B (2003) Non-invasive imaging of blood cell concentration and blood distribution in zebrafish Danio rerio incubated in hypoxic conditions in vivo. *J Exp Biol* **206**(Pt 8)**:** 1299-1307.

Scott, IC, Masri, B, D'Amico, LA, Jin, SW, Jungblut, B, Wehman, AM, Baier, H, Audigier, Y, Stainier, DY (2007) The g protein-coupled receptor agtrl1b regulates early development of myocardial progenitors. *Dev Cell* **12**(3)**:** 403-413.

see Bendova, P, Mackova, E, Haskova, P, Vavrova, A, Jirkovsky, E, Sterba, M, Popelova, O, Kalinowski, DS, Kovarikova, P, Vavrova, K, Richardson, DR, Simunek, T (2010) Comparison of clinically used and experimental iron chelators for protection against oxidative stress-induced cellular injury. *Chem Res Toxicol* **23**(6)**:** 1105-1114.

see Bill, BR, Petzold, AM, Clark, KJ, Schimmenti, LA, Ekker, SC (2009) A primer for morpholino use in zebrafish. *Zebrafish* **6**(1)**:** 69-77.

see Burger, D, Xenocostas, A, Feng, QP (2009) Molecular basis of cardioprotection by erythropoietin. *Curr Mol Pharmacol* **2**(1)**:** 56-69.

see Eisen and Smith, JS, Smith, JC (2008) Controlling morpholino experiments: don't stop making antisense. *Development* **135**(10)**:** 1735-1743.

see Ekker, SC (2000) Morphants: a new systematic vertebrate functional genomics approach. *Yeast* **17**(4)**:** 302-306.

see Goldhaber and Hamilton, JI, Hamilton, MA (2010) Role of inotropic agents in the treatment of heart failure. *Circulation* **121**(14)**:** 1655-1660.

see Japp and Newby, AG, Newby, DE (2008) The apelin-APJ system in heart failure: pathophysiologic relevance and therapeutic potential. *Biochem Pharmacol* **75**(10)**:** 1882-1892.

see Moens, CB, Donn, TM, Wolf-Saxon, ER, Ma, TP (2008) Reverse genetics in zebrafish by TILLING. *Brief Funct Genomic Proteomic* **7**(6)**:** 454-459.

see Rocke, J, Lees, J, Packham, I, Chico, T (2009) The zebrafish as a novel tool for cardiovascular drug discovery. *Recent Pat Cardiovasc Drug Discov* **4**(1)**:** 1-5.

see Schorlemmer, A, Matter, ML, Shohet, RV (2008) Cardioprotective signaling by endothelin. *Trends Cardiovasc Med* **18**(7)**:** 233-239.

see Schwartz, A, Matlib, MA, Balwierczak, J, Lathrop, DA (1985) Pharmacology of calcium antagonists. *Am J Cardiol* **55**(7)**:** 3C-7C.

see Semenza, GL (2009) Regulation of oxygen homeostasis by hypoxia-inducible factor 1. *Physiology (Bethesda)* **24:** 97-106.

see Shiels and White, HA (2008) The Frank-Starling mechanism in vertebrate cardiac myocytes. *J Exp Biol* **211**(Pt 13)**:** 2005-2013.

see Skrzypiec-Spring, M, Grotthus, B, Szelag, A, Schulz, R (2007) Isolated heart perfusion according to Langendorff---still viable in the new millennium. *J Pharmacol Toxicol Methods* **55**(2)**:** 113-126.

see Sood, R, English, MA, Jones, M, Mullikin, J, Wang, DM, Anderson, M, Wu, D, Chandrasekharappa, SC, Yu, J, Zhang, J, Paul Liu, P (2006) Methods for reverse genetic screening in zebrafish by resequencing and TILLING. *Methods* **39**(3)**:** 220-227.

see Tekin, D, Dursun, AD, Xi, L (2010) Hypoxia inducible factor 1 (HIF-1) and cardioprotection. *Acta Pharmacol Sin* **31**(9)**:** 1085-1094.

see Urnov, FD, Rebar, EJ, Holmes, MC, Zhang, HS, Gregory, PD (2010) Genome editing with engineered zinc finger nucleases. *Nat Rev Genet* **11**(9)**:** 636-646.

Sheikh, AY, Chun, HJ, Glassford, AJ, Kundu, RK, Kutschka, I, Ardigo, D, Hendry, SL, Wagner, RA, Chen, MM, Ali, ZA, Yue, P, Huynh, DT, Connolly, AJ, Pelletier, MP, Tsao, PS, Robbins, RC, Quertermous, T (2008) In vivo genetic profiling and cellular localization of apelin reveals a hypoxia-sensitive, endothelial-centered pathway activated in ischemic heart failure. *Am J Physiol Heart Circ Physiol* **294**(1)**:** H88-98.

Simpkin, JC, Yellon, DM, Davidson, SM, Lim, SY, Wynne, AM, Smith, CC (2007) Apelin-13 and apelin-36 exhibit direct cardioprotective activity against ischemia-reperfusion injury. *Basic Res Cardiol* **102**(6)**:** 518-528.

Skuladottir, GV, Johannsson, M (1997) Inotropic response of rat heart papillary muscle to alpha 1- and beta-adrenoceptor stimulation in relation to dietary n-6 and n-3 polyunsaturated fatty acids (PUFA) and age. *Pharmacol Toxicol* **80**(2)**:** 85-90.

Smith, CC, Mocanu, MM, Bowen, J, Wynne, AM, Simpkin, JC, Dixon, RA, Cooper, MB, Yellon, DM (2007) Temporal changes in myocardial salvage kinases during reperfusion following ischemia: studies involving the cardioprotective adipocytokine apelin. *Cardiovasc Drugs Ther* **21**(6)**:** 409-414.

Spence, R, Gerlach, G, Lawrence, C, Smith, C (2008) The behaviour and ecology of the zebrafish, Danio rerio. *Biol Rev Camb Philos Soc* **83**(1)**:** 13-34.

Summerton, J (1999) Morpholino antisense oligomers: the case for an RNase H-independent structural type. *Biochim Biophys Acta* **1489**(1)**:** 141-158.

Sun, L, Lien, CL, Xu, X, Shung, KK (2008) In vivo cardiac imaging of adult zebrafish using high frequency ultrasound (45-75 MHz). *Ultrasound Med Biol* **34**(1)**:** 31-39.

Sviglerova, J, Kuncova, J, Stengl, M (2005) Negative inotropic effect of insulin in papillary muscles from control and diabetic rats. *Physiol Res* **54**(6)**:** 661-670.

Swedberg, K, Cleland, J, Dargie, H, Drexler, H, Follath, F, Komajda, M, Tavazzi, L, Smiseth, OA, Gavazzi, A, Haverich, A, Hoes, A, Jaarsma, T, Korewicki, J, Levy, S, Linde, C, Lopez-Sendon, JL, Nieminen, MS, Pierard, L, Remme, WJ (2005) Guidelines for the diagnosis and treatment of chronic heart failure: executive summary (update 2005): The Task Force for the Diagnosis and Treatment of Chronic Heart Failure of the European Society of Cardiology. *Eur Heart J* **26**(11)**:** 1115-1140.

Szokodi, I, Tavi, P, Foldes, G, Voutilainen-Myllyla, S, Ilves, M, Tokola, H, Pikkarainen, S, Piuhola, J, Rysa, J, Toth, M, Ruskoaho, H (2002) Apelin, the novel endogenous ligand of the orphan receptor APJ, regulates cardiac contractility. *Circ Res* **91**(5)**:** 434-440.

Taliyan, R, Singh, M, Sharma, PL, Yadav, HN, Sidhu, KS Possible involvement of alpha1-adrenergic receptor and K(ATP) channels in cardioprotective effect of remote aortic preconditioning in isolated rat heart. *J Cardiovasc Dis Res* **1**(3)**:** 145-151.

Tang, WH, Wu, S, Wong, TM, Chung, SK, Chung, SS (2008) Polyol pathway mediates iron-induced oxidative injury in ischemic-reperfused rat heart. *Free Radic Biol Med* **45**(5)**:** 602-610.

Tatemoto, K, Hosoya, M, Habata, Y, Fujii, R, Kakegawa, T, Zou, MX, Kawamata, Y, Fukusumi, S, Hinuma, S, Kitada, C, Kurokawa, T, Onda, H, Fujino, M (1998) Isolation and characterization of a novel endogenous peptide ligand for the human APJ receptor. *Biochem Biophys Res Commun* **251**(2)**:** 471-476.

Tatemoto, K, Takayama, K, Zou, MX, Kumaki, I, Zhang, W, Kumano, K, Fujimiya, M (2001) The novel peptide apelin lowers blood pressure via a nitric oxide-dependent mechanism. *Regul Pept* **99**(2-3)**:** 87-92.

Thirumalai, V, Cline, HT (2008) Endogenous dopamine suppresses initiation of swimming in prefeeding zebrafish larvae. *J Neurophysiol* **100**(3)**:** 1635-1648.

Thu, VT, Kim, HK, Ha, SH, Yoo, JY, Park, WS, Kim, N, Oh, GT, Han, J (2010) Glutathione peroxidase 1 protects mitochondria against hypoxia/reoxygenation damage in mouse hearts. *Pflugers Arch* **460**(1)**:** 55-68.

Timmer, A, Hilsden, RJ, Cole, J, Hailey, D, Sutherland, LR (2002) Publication bias in gastroenterological research - a retrospective cohort study based on abstracts submitted to a scientific meeting. *BMC Med Res Methodol* **2:** 7.

Ton, C, Stamatiou, D, Liew, CC (2003) Gene expression profile of zebrafish exposed to hypoxia during development. *Physiol Genomics* **13**(2)**:** 97-106.

Tucker, B, Hepperle, C, Kortschak, D, Rainbird, B, Wells, S, Oates, AC, Lardelli, M (2007) Zebrafish Angiotensin II Receptor-like 1a (agtrl1a) is expressed in migrating hypoblast, vasculature, and in multiple embryonic epithelia. *Gene Expr Patterns* **7**(3)**:** 258-265.

Vickers, C, Hales, P, Kaushik, V, Dick, L, Gavin, J, Tang, J, Godbout, K, Parsons, T, Baronas, E, Hsieh, F, Acton, S, Patane, M, Nichols, A, Tummino, P (2002) Hydrolysis of biological peptides by human angiotensin-converting enzyme-related carboxypeptidase. *J Biol Chem* **277**(17)**:** 14838-14843.

Wenger, RH (2000) Mammalian oxygen sensing, signalling and gene regulation. *J Exp Biol* **203**(Pt 8)**:** 1253-1263.

Werno, C, Schmid, T, Schnitzer, SE, Peters, K, Milke, L, Brune, B (2010) A combination of hypoxia and lipopolysaccharide activates tristetraprolin to destabilize proinflammatory mRNAs such as tumor necrosis factor-alpha. *Am J Pathol* **177**(3)**:** 1104-1112.

Wong, YY, Handoko, ML, Mouchaers, KT, de Man, FS, Vonk-Noordegraaf, A, van der Laarse, WJ (2010) Reduced mechanical efficiency of rat papillary muscle related to degree of hypertrophy of cardiomyocytes. *Am J Physiol Heart Circ Physiol* **298**(4)**:** H1190-1197.

Xie, H, Yuan, LQ, Luo, XH, Huang, J, Cui, RR, Guo, LJ, Zhou, HD, Wu, XP, Liao, EY (2007) Apelin suppresses apoptosis of human osteoblasts. *Apoptosis* **12**(1)**:** 247-254.

Yamamoto, S, Matsumoto, N, Kanazawa, M, Fujita, M, Takaoka, M, Matsumura, Y (2004) Effects of ET(A) and ET(B) receptor blockade on post-ischemic cardiac dysfunction and norepinephrine overflow in isolated rat hearts. *J Cardiovasc Pharmacol* **44 Suppl 1:** S394-397.

Yang, XM, Krieg, T, Cui, L, Downey, JM, Cohen, MV (2004) NECA and bradykinin at reperfusion reduce infarction in rabbit hearts by signaling through PI3K, ERK, and NO. *J Mol Cell Cardiol* **36**(3)**:** 411-421.

Young, NS, Ioannidis, JP, Al-Ubaydli, O (2008) Why current publication practices may distort science. *PLoS Med* **5**(10)**:** e201.

Zeng, XX, Wilm, TP, Sepich, DS, Solnica-Krezel, L (2007) Apelin and its receptor control heart field formation during zebrafish gastrulation. *Dev Cell* **12**(3)**:** 391-402.

Zhang, J, Chen, L, Raina, H, Blaustein, MP, Wier, WG (2010) In vivo assessment of artery smooth muscle [Ca2+]i and MLCK activation in FRET-based biosensor mice. *Am J Physiol Heart Circ Physiol* **299**(3)**:** H946-956.

Zhong, JC, Huang, Y, Yung, LM, Lau, CW, Leung, FP, Wong, WT, Lin, SG, Yu, XY (2007a) The novel peptide apelin regulates intrarenal artery tone in diabetic mice. *Regul Pept* **144**(1-3)**:** 109-114.

Zhong, JC, Yu, XY, Huang, Y, Yung, LM, Lau, CW, Lin, SG (2007b) Apelin modulates aortic vascular tone via endothelial nitric oxide synthase phosphorylation pathway in diabetic mice. *Cardiovasc Res* **74**(3)**:** 388-395.